ISTANBUL TECHNICAL UNIVERSITY ★ GRADUATE SCHOOL OF SCIENCE ENGINEERING AND TECHNOLOGY

ANALYSIS OF HEAT TRANSFER IN CRUDE OIL TANKER'S CARGO TANKS AND CARGO HEATING SYSTEM

M.Sc. THESIS

Koray ŞAHİN

Department of Naval Architecture and Marine Engineering

Naval Architecture and Marine Engineering Programme

AUGUST 2015

ISTANBUL TECHNICAL UNIVERSITY ★ GRADUATE SCHOOL OF SCIENCE ENGINEERING AND TECHNOLOGY

ANALYSIS OF HEAT TRANSFER IN CRUDE OIL TANKER’S CARGO TANKS AND CARGO HEATING SYSTEM

M.Sc. THESIS

Koray ŞAHİN
(508131012)

Department of Naval Architecture and Marine Engineering

Naval Architecture and Marine Engineering Programme

Thesis Advisor: Prof.Dr.Selma ERGİN

AUGUST 2015

İSTANBUL TEKNİK ÜNİVERSİTESİ ★ FEN BİLİMLERİ ENSTİTÜSÜ

HAM PETROL TANKERİ KARGO TANKLARI ISI TRANSFERİ VE KARGO ISITMA SİSTEMİ ANALİZİ

YÜKSEK LİSANS TEZİ

Koray ŞAHİN
(508131012)

Gemi İnşaatı ve Gemi Makineleri Mühendisliği Anabilim Dalı

Gemi İnşaatı ve Gemi Makineleri Programı

Tez Danışmanı: Prof.Dr.Selma ERGİN

AĞUSTOS 2015

Koray Şahin, a **M.Sc.** student of ITU **Graduate School of Science Engineering and Technology** student ID 508131012, successfully defended the **thesis/dissertation** entitled "ANALYSIS OF HEAT TRANSFER IN CRUDE OIL TANKER'S CARGO TANKS AND CARGO HEATING SYSTEM", which he prepared after fulfilling the requirements specified in the associated legislations, before the jury whose signatures are below.

Thesis Advisor : **Prof.Dr.Selma ERGİN** ....
Istanbul Technical University

Jury Members : **Prof. Dr. Oğuz Salim SÖĞÜT** ....
Istanbul Technical University

Prof. Dr. Nurten VARDAR ....
Yıldız Technical University

Date of Submission : 15 June 2015
Date of Defense : 3 August 2015

To my family, my love and niece

FOREWORD

I would like to express my sincere gratitude to Dr.Roman Liberacki and Prof.Dr.Selma Ergin for their support, continuous guidance, endless understanding, encouragement and supervision of throughout this study.
My special thanks go to my life, love Aylin Çapkın for being with me all the time, cuteness, endless supports and encouragement.
I am also endless grateful to my family for their love, faith in me.
Lastly, my very very precious and special thanks go to my dad for his vision foresight, faith in me which provide to brought me to this point.

June 2015

Koray Şahin
Naval Architect

x

TABLE OF CONTENTS

Page

ABBREVIATIONS

IEA	**:** International Energy Agency
DWT	**:** Dead Weight Ton
DNV	**:** Det Norske Veritas
AFRA	**:** Average Freight Rate Assessment
LTBP	**:** London Tanker Broker's Panel
VLCC	**:** Very Large Crude Carrier
ULCC	**:** Ultra Large Crude Carrier
ISO	**:** International Standardization Organisation
BSFC	**:** Break Specific Fuel Consumption
Nu	**:** Nusselt Number
Gr	**:** Grashof Number
Pr	**:** Prandtl Number
Ra	**:** Rayleigh Number
Re	**:** Reynolds Number

LIST OF TABLES

LIST OF FIGURES

ANALYSIS OF HEAT TRANSFER IN CRUDE OIL TANKER'S CARGO TANKS AND CARGO HEATING SYSTEM

SUMMARY

Crude oil is one of the most actively traded commodities in the world. Oil transportation has become a complex and highly technical operation. One of the major difficulties in the transportation is the high viscous fluids that require efficient and economical ways to transfer the heavy crude. Heavy crude oils have a density approaching or even exceeding that of water. They are usually extremely viscous, with a consistency ranging from that of heavy molasses to a solid at room temperature. Heavy crude oils are not pumped easily through the pipelines because of the high concentrations of sulfur and several metals, particularly nickel and vanadium. Crude oils are complex fluids that can cause a variety of difficulties during the production, separation, transportation and refining of oil.

One of the most prominent challenges is transportation of heavy and extra heavy crude oil from ship to the station. The transportation of heavy and extra-heavy oil presents many operational difficulties that limit their economical viability. Therefore, solving this operational difficulties is very essential due to the economical aspects in terms of increasing use of heavy and extra heavy crude oil in the future.

The most widely and efficient enhanced oil recovery technologies are the thermal techniques. Thermal methods reduce the viscosity of heavy crude oil by several orders of magnitude rapidly, in contrast to non-thermal methods in which the mode of viscosity reduction is quite slow. Heating is a common method utilized to overcome the above noted problems of transporting heavy oil from ship to the station. The basis for this method lies in the fact that as heavy oil is heated, the viscosity of the heavy oil is reduced and thus made easier to pump. Therefore it is important to heat the oil to a point where the oil has a substantially reduced viscosity. This method is aimed at reducing viscosity as well as the energy required for pumping, to enhance flowability of the oil.

However, heating to increase the temperature of the fluid involves a considerable amount of energy and cost as well. Thus, identifying correctly the heating system requirements, development of appropriate heating system, calculating correctly the factors that affect heat transfer rate is important in terms of energy conservation ,environment effectiveness and cost.

This thesis aims to develop appropriate cargo heating system, to determine correctly the heating system requirements, calculating correctly the factors that affect heat transfer rate, to determine the optimal cargo heating management plan,in terms of energy conservation, saving cost depend on fuel consumption and environment effectiveness. Furthermore, this thesis is aimed to find optimal methods scientifically to determine the cargo oil heating time in order to save energy during oil transportation.

In this thesis, in the first section presents general information, purpose and scope and literature review about development of cargo oil heating system and plan in oil tankers.

In order to accomplish our purpose which was mentioned above, initially 100,000 dwt crude oil tanker (aframax) preliminary design is performed in the second section. In addition to this part, aframax tanker`s main dimensions and its cargo tanks capacities which are necessary to calculate heat transfer rate and coefficients are determined in this chapter. Additionally, crude oil tanker main engine and generating sets are identified and selected.

In the third section, general theories of conduction and convection heat transfer are described. Natural and forced convection correlations for vertical and horizontal plates are explained in briefly.

In the next chapter, Shell and Spirax Sarco cargo heating systems solutions are analyzed and examined with the values which are written in their literature. In this examination, quantity of heat requirements for Shell and Spirax Sarco are calculated and then these heat requirements for both solutions are compared with each other. Finally, steam consumptions for this cargo heating solutions are determined and compared.

In the fifth section, heat transfer coefficients for each section of cargo tanks are calculated under different conditions independently. Spirax Sarco and Shell heat transfer coefficients which are written their literature for double side, deck and double bottom are compared with independent solution of heat transfer coefficients for double side, deck and double bottom.

Heat requirements differences occured due to the heat transfer coefficients differences between Shell, Spirax Sarco and our independent solutions and heat requirements for each solutions are compared. Additionally, these two solutions and our independent solution’s boiler fuel consumption onboard crude oil tanker is compared with each other.

In the sixth section, solution of heat transfer from heat equipment to the cargo is performed. Cargo heating methods are explained and appropriate one which is called submerged heating coil is implemented to proposed design ship.

Finally, discussions and reviews of the obtained numerical results are discussed in the last section of the thesis. Suggestions for any academic studies, research and development in the future are mentioned in final part.

HAM PETROL TANKERİ KARGO TANKLARI ISI TRANSFERİ VE KARGO ISITMA SİSTEMİ ANALİZİ

ÖZET

Ham petrol dünyanın en aktif işlem gören ürünlerinden biridir. Petrol taşımacılığı karmaşık ve son derece teknik bir operasyon haline gelmiştir. Yüksek vizkoziteye sahip akışkanların verimli ve ekonomik olarak transferi petrol taşımacılığının ana zorluklarından biridir. Ağır ham petrolün yoğunluğu suyun yoğunluğa yaklaşmakta hatta çoğu durumda suyun yoğunluğunu aşmaktadır. Ağır ham petroller oda sıcaklığında pekmez ile bir katı maddenin arasında bir kıvama sahip ve genellikle viskozitesi yüksektir. Ağır ham petroller içerisindeki çeşitli metallerin, özellikle nikel ve vanadyumun, sülfürün yüksek konsantrasyonlarından dolayı boru hatları üzerinden kolayca pompalanamazlar. Ham petroller; çıkarılması, ayrılması, taşınması ve rafinesi boyunca çeşitli zorluklara neden olan karmaşık sıvılardır.

Ağır ve aşırı ağır ham petrolün gemiden istasyona taşınması bu zorlukların önde gelenlerindendir. Ağır ve aşırı ham petrollerin taşınması onların ekonomik canlılığını sınırlayan birçok operasyonel zorluk sunuyor. Bundan dolayı, ağır ve aşırı ağır ham petrollerin gelecekte kullanımının artmasına bağlı olarak bu operasyonel zorlukları çözmek ekonomik açıdan çok önemlidir.

En yaygın ve verimli ham petrol iyileştirme teknolojileri termal teknikleridir. Termal metodlar ağır ham petrolün viskozitesini, vizkozite düşümü oldukça yavaş olan termal olmayan metodlara göre hızlı bir şekilde düşürmektedir. Isıtma, ağır petrolün gemiden istasyona taşınması ile ilgili yukarıda bahsedilen problemlerin üstesinden gelmek için kullanılan yaygın bir yöntemdir. Bu yöntemin temelinde, ağır ham petrolün ısıtılması, ağır petrolün vizkozitesinin azaltılması ve böylece kolay bir şekilde pompalanabilmesi yatmaktadır. Bu nedenle, ham petrolün büyük ölçüde viskozitesinin düşük olduğu bir noktaya kadar ısıtılması önemlidir. Bu yöntem petrolün viskozitesinin azaltılmasının yanında ham petrolü pompalamak için gerekli enerjinin azaltılması ve petrolün akışkanlığını arttırmayı amaçlamaktadır. Fakat, akışkanın sıcaklığını arttırmak için ısıtmak önemli miktarda enerji ve maliyet gerektirmektedir.

Bundan dolayı, doğru ısıtma sistemi gereksinimlerinin belirlenmesi, uygun ısıtma sisteminin geliştirilmesi, ısı transfer oranını etkileyen faktörlerin doğru bir şekilde hesaplanması enerji tasarrufu, çevre etkinliği ve maliyet açışından önemlidir.

Bu tez enerji tasarrufu, yakıt tüketimine bağlı maliyet ve çevre etkinliği açısından uygun kargo ısıtma sisteminin geliştirilmesini, doğru ısıtma sistemi gereksinimlerinin belirlenmesini, ısı transfer oranını etkileyen faktörlerin doğru olarak hesaplanmasını, optimum kargo ısıtma yönetim planının belirlenmesini amaçlamaktadır. Bununla birlikte, bu tez ham petrolün taşınması esnasında enerji tasarrufu açısından ham petrolün ısıtılma süresini belirlemek için bilimsel optimum metodların bulunmasını amaçlamaktadır.

Bu tezin ilk bölümünde genel bilgiler, tezin amacı ve kapsamı ,ham petrol tankerlerindeki kargo ısıtma sistemi ve planının gelişimi hakkında literatür çalışması sunulmuştur.

İkinci bölümde, yukarıda değindiğimiz amacımızı başarmak için ilk olarak 100.000 (dwt) dead weight tonluk ham petrol (aframax) tankerinin ön dizaynını gerçekleştirdik. Bu kısma ek olarak, bu bölümde ısı transfer oranını ve katsayılarını belirlemek için gerekli olan aframax tankerin ana boyutları ve kargo tanklarının kapasiteleri belirlendi. Ayrıca ham petrol tankerinin ana makine ve jeneratör setleri tespit edildi ve seçildi.
Üçüncü kısımda, iletim ve konveksiyon ısı transferi genel teorisi tarif edildi. Yatay ve dikey plakalardaki doğal ve zorlanmış konveksiyon bağıntıları kısaca açıklandı.
Sonraki bölümde, Shell ve Spirax Sarco kargo ısıtma sistemlerinin çözümleri literatürlerinde yazan değerlerle analiz edildi ve incelendi. Bu incelemede, Shell ve Spirax Sarco ısı gereksinim miktarları hesaplandı ve daha sonra bu ısı gereksinim değerleri birbiriyle karşılaştırıldı. Bu iki ısıtma sisteminin buhar tüketimleri belirlendi ve karşılaştırıldı. Son olarak, Aframax tankerlerin dünya üzerinde kullanıldığı rotalar belirlendi ve bu rotalara ait mesafeler bulundu. Bu mesafelerden yola çıkarak uygun gemi seyir hızında bu rotalardaki gemi yolculuk süreleri faz 2 ve faz 3 durumları için Shell ve Spirax Sarco yöntemleri için ayrı ayrı hesaplandı. Geminin bir yolculuğu boyunca faz 2 ve faz 3 durumları için gemi kazan toplam yakıt tüketimleri hesaplandı ve karşılaştırıldı. Bunun sonucu olarak hangi yöntemin toplam yakıt tüketimi açısından veya saatlik buhar tüketimi açısından uygun olup olmadığı belirlendi. Toplam yakıt tüketimi açısından hangi yöntemin çevresel olduğu da doğal bir sonuç olarak verildi.
Beşinci bölümde, kargo tankındaki ısı transfer katsayıları tanımlandı ve kargo tankın her bir bölümü için ısı transfer katsayıları farkı şartlar altında bağımsız olarak hesaplandı. Bu ısı transfer katsayıları hesaplanırken kargo tankının içindeki ve dışındaki şartlar ayrı ayrı belirlendi . Akışkanların fiziksel özellikleri bulundukları ortama göre belirlendi. Bu şartlar altında levha sıcaklık dağılımları belli sayıda iterasyon yapılarak bulundu. Daha sonra boyutsuz sayıların yardımı ile levhanın yatay ve dikey olması durumuna göre farklı Nu korelasyonlarıyla ısı transfer katsayıları hesaplandı ve ısı transfer eşitliği kullanılarak plakalardaki ısı transfer katsayılarında düzeltme yapıldı. Bu düzeltmeler yapıldıktan sonra son olarak güverte, çift dip ve borda çift sacı ısı transfer katsayıları belirlendi. Spirax Sarco ve Shell ısıtma sistemi çözümlerinin güverte, çift dip ve borda çift sacı için literatürlerinde yazan değerlerle; güverte,çift dip ve borda çift sacı için bağımsız çözümümüzden elde ettiğimiz değerler karşılaştırıldı. Aynı zamanda; güverte, çift dip ve borda çift sacı için elde ettiğimiz ısı transfer katsayıları literatürde sonlu elemanlar yöntemiyle hesaplanmış ısı transfer katsayıları ile karşılaştırıldı. Literatürdeki yazan değerler ile bağımsız çözümümüzden elde ettiğimiz değerlerin birbirine yakın olduğu tespit edildi. Shell ve Spirax Sarco yöntemlerinde kullanılan ısı transfer katsayılarının literatürde ve bağımsız çözümümüzden elde ettiğimiz değerler arasında önemli farklılıklar olduğu tespit edildi. Doğal olarak bu yöntemlerle hazırlanan sistemlerde ısı kayıplarının daha fazla hesaplandığı tespit edildi. Buna bağlı olarak Shell ve Spirax Sarco yöntemleri ile hazırlanan sistemlerde daha büyük kapasiteli kazanların kullanılması gerektiğini ve bunun fazla yakıt tüketmeyi beraberinde getirdiği nedenleriyle açıklandı. Bu amaçla doğru ısı transfer katsayıların hesaplanması ısı kayıplarının doğru hesaplanmasını sağlamaktadır ve bu sistemden hiçbir şey eksiltmeden otomatik olarak bize önemli miktarda yakıt tasarrufu sağlamakta olduğu gösterildi.
Shell, Spirax Sarco ve bizim bağımsız çözümümüz arasında ısı transfer katsayıları farklılığına bağlı olarak ısı gereksinim farklılığı ortaya çıktı ve her çözüm için ısı gereksinimleri karşılaştırıldı. Ayrıca, ham petrol tankerindeki Shell, Spirax Sarco ve bizim bağımsız çözümümüzdeki kazan yakıt tüketimleri birbirleriyle karşılaştırıldı.

Altıncı bölümde, ısı ekipmanlarından kargoya ısı transferi çözümü gerçekleştirildi. Kargo ısıtma metodları açıklandı ve uygun ısıtma metodu olan ısıtma kangalları metodu önerilen gemi dizaynına uygulandı.
Son olarak; elde edilen sayısal bulguların tartışma ve yorumları tezin son bölümünde ele alındı. Gelecekteki akademik calışmalar, incelemeler ve gelişmeler için öneriler son bölümde verildi.

1. INTRODUCTION

The US Department of Energy, the International Energy Agency (IEA) and World Energy Council have projected that energy demand would increase year in year out as the world population is ever-growing. The world demand for crude oil has increased from 60 million barrels per day to 84 million barrels per day, in the past 20 years [1]. Serious international studies still foresee that in the next 20 years, at least 80 % of the world's energy requirements will come from petroleum, natural gas and coal (IEA, 2008). Consequently, oil will remain the dominant source of energy for the next half century. According to some estimates from the International Energy Agency (IEA), heavy oil represents at least half of the recoverable oil resources of the world [2].

In the past, demand for heavy and extra-heavy oil was low because of their high viscosity and composition complexity. That make them difficult and expensive to transport, refine and produce. Nowadays, there has been a remarkable increase in the number of heavy and extra heavy oil production places in the world. They will replace the decreasing production of conventional middle and light oil. Therefore, there is a growing interest in the use of non-conventional heavy and extra heavy oil resources to produce fuels and petrochemicals. The incorporation of heavy oil to energy markets presents important challenges that require significant technological developments in the production, transportation and refining chain. Especially transportation of heavy and extra heavy crude oil reveals operational challenges. That restricts their economic viability. So, solving these challenges is very important because of their economical aspects in terms of increasing use of these oils in the future [2].

One of the most leading operational challenge is decreasing viscosity of the heavy crude oil which exhibits a high viscosity at moderate and low temperature and highly sensitive to the oil temperature. This make heavy crude oils virtually impossible to transport from one place to another using pumping system. Several methods were developed to reduce viscosity of the heavy crude oil for the transportation easily. These methods were examined in the following :

Methodologies For The Easy Transport of Heavy Crude Oil

Methods for enhancing transport of heavy oils include the following possibilities:

Thermal

- Preheat oil and transport hot

  * Uninsulated Line

  * Insulated Line

- Heat oil by hot fluid tracing

Mechanical

- Pump oil at temperature below pour point

Chemical

- Dilute oil with solvent

Preheat Oil and Transport Hot: Uninsulated Line

This technique is the standard treatment. Heat is transferred to the oils by exchange with hot oil in shell or tube exchanger at the pipeline main pump station and some booster pump stations. Fired heaters warmed heat transfer fluid to heat the crude oil to 130-160 ^{0}F (54.4-71.1 ^{0}C) at each location.

Preheat Oil and Transport Hot: Insulated Line

In this technique, pipelines thermally insulated and generally somewhat short in length. Mostly, polyurethane foam use to insulate pipelines.

Heat Oil By Hot Fluid Tracing

The use of heat tracing by a small pipe attached to the line pipe is well-known. Either a hot glycol-water solution, hot oil, or steam is flowed through the heat trace pipe.

Pump Oil At Temperature Below Pour Point

The pour point of a liquid is the temperature at which becomes semi solid and loses its flow characteristics. In crude oil a high pour point is generally associated with a high paraffin content.

Dilute Oil With Solvent

Dilution of oil with a light-hydrocarbon solvent lowers the viscosity to an acceptable value and allows pumping at reasonable flow rates [3].

The most widely enhanced oil recovery technologies are the thermal techniques. Thermal methods reduce the viscosity of heavy crude oil by several orders of magnitude rapidly, in contrast to non-thermal methods (chemical, mechanical) in which the mode of viscosity reduction is quite slow. Heating is a common method utilized to overcome the above noted problems of transporting heavy oil from ship to the station. The basis for this method lies in the fact that as heavy oil is heated, the viscosity of the heavy oil is reduced and thus made easier to pump. Viscosity change with temperature is shown in Figure 1.1.

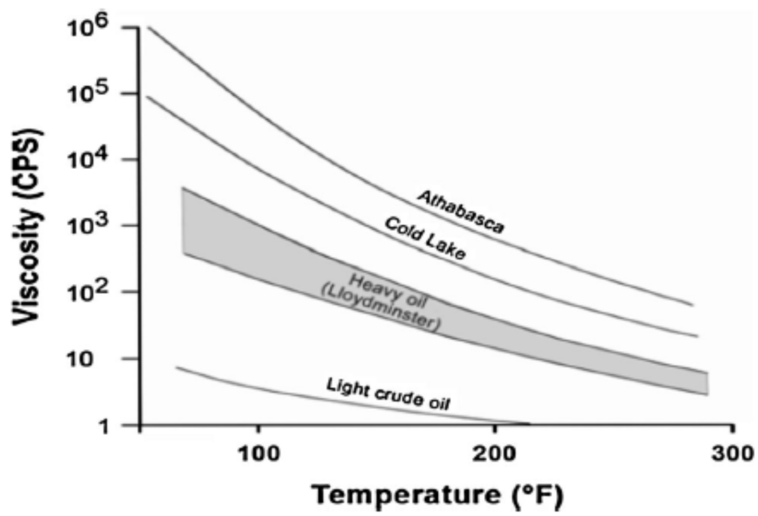

Figure 1. 1: Response of viscosity to increase in temperature[1].

At this point, how to pump viscous liquids and pump constraints are explained in the following.

Pumping Viscous Liquids

The motive force required to transport the oil is almost generally provided by centrifugal pumps. They have many favorable properties such as little pulsation, no safety valve needed as with positive displacement pumps and simple flow control. Centrifugal pumps are often being used in high-viscous media (up to 1000.10^{-6} m^2/s-1000 cSt) but efficiency loss should be taken into account and should compare the positive displacement pumps with the same service data.

The economical application limit for centrifugal pumps is about (150 to 500) 10^{-6} m^2/s; this limit very much depends on the pump size and application. The use of a centrifugal pump is possible up to about $1500x10^{-6}$ m^2/s and even above [4].

1.1 Purpose of Thesis

Fuel economy and its associated environmental impact, is the most important challenge facing ship owners, operators and shipbuilders today .Today's maritime industry is very competitive and it is going to be more competitive in the near future. New maritime rules related with the environmental regulations become effective in the near future. Therefore, it is important to improve suitable ship systems according to the these new rules, regulations and restrictions. Inspired by this opinion, this thesis aims to develop appropriate cargo heating system, to determine correctly heating system requirements, calculating correctly the factors that effect heat transfer rate, determine the optimal cargo heating management plan in terms of energy conservation, saving cost depend on fuel consumption and environment effectiveness. Furthermore, this thesis is aimed to find optimal methods scientifically to determine the cargo oil heating time in order to save energy during oil transportation. The final objective is a precise prediction of heating strategy with the aim of fuel and energy savings during periods of intensive cargo heating before unloading.

1.2 Literature Review

Crude oil tanker cargo heating system has been investigated in literature extensively. Limited number of studies, research and informations are reached due to the small numbers of researchers are studying this field.

One of the article about this topic is Chinese researchers Danting Yue, Hui Xing, Zhanhua Wu and Yanwu Xu. These researchers studied about development of cargo oil heating system on oil tanker. They wrote an article about this subject in 2010. According to their articles, they analyzed the heating and thermal insulation process of 300 kinds of cargo oil onboard and 7 types of double-hull oil tanker of Dalian Ocean Shipping Company. They used non-steady-state lumped parameter method and taking into account five variables such as loaded capacity, ballast water, ship voyage record, hydrographic-meteorology and heating steam parameters. They mentioned in their article that they developed optimized cargo oil heating system and their system is used in 60000 DWT, 65000 DWT, 72000 DWT, 75000 DWT, 75000 DWT, 110000 DWT and 159000 DWT oil tankers in Dalian Ocean Shipping Company. They save 4500 tons of oil fuel for one year’s application of these ships [5].

2. PRELIMINARY DESIGN OF POWER PLANT FOR AFRAMAX TANKER

2.1 General Characteristic of Crude Oil Tankers

Crude oil tankers are constructed with the specific purpose of transporting crude oil from the oil field to the oil refinery. Crude oil tankers would portrayed by not having coated tanks, because crude oil doesn't result in erosion of the tanks. Also oil refineries don't force very stringent caliber necessities for the crude oil. For example, it will be not necessary to clean the tank totally preceding stacking new crude oil. Crude oil tankers depend on the on-shore facilities when their tanks are refilled, but they use their pumps to discharging the tanks. Consequently, this crude oil tanker vessel must be equipped with large capacity pumps. Oil tanker side view is shown in Figure 2.1[Url-1].

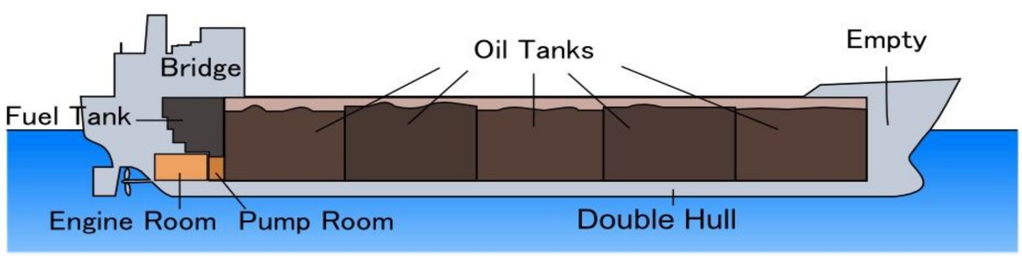

Figure 2. 1: Oil tanker side view [Url-1].

2.1.1 Size categories of crude oil tanker

In 1954 Shell Oil developed the average freight rate assessment (AFRA) system which classifies tankers of different sizes. To make it an independent instrument, Shell consulted the London Tanker Brokers' Panel (LTBP). At first, they divided the groups as General Purpose for tankers under 25,000 tons deadweight(DWT); Medium Range for ships between 25,000 and 45,000 DWT and Large Range for the enormous ships that were larger than 45,000 DWT. The ships became larger during the 1970s, which prompted rescaling. Oil tanker size categories are shown in Table 2.1[Url-2] and AFRA scales are shown in Figure 2.2.

Table 2. 1: Oil tanker size categories [Url-2].

AFRA SCALES	
Class	**Size in DWT**
General Purpose Tanker	10,000-24,999
Medium Range Tanker	25,000-44,999
LR1(Large Range 1)	45,000-79,999
LR2(Large Range 2)	80,000-159,999
VLCC(Very Large Crude Carrier)	160,000-319,999
ULCC(Ultra Large Crude Carrier)	320,000-549,999

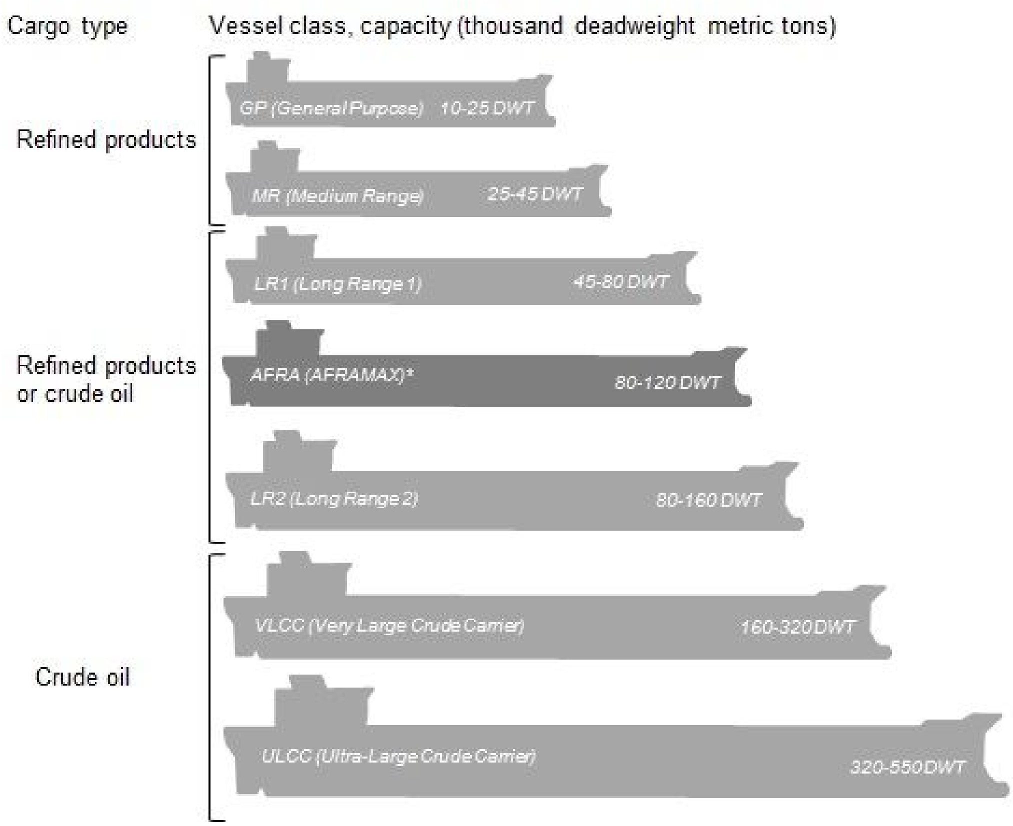

Figure 2. 2: Average freight rate assessment scaled-fixed [Url-3].

2.1.2 Segments of the crude oil tanker

Crude oil tankers are classified according to vessel size. The size of a tanker is usually measured in DWT. The four most common crude oil segments are ULCC/VLCC (Ultra Large Crude Containers/Very Large Crude Containers), Suezmax, Aframax and

Panamax. These most common crude oil tankers are explained seperately in the following :

Very Large Crude Carriers (VLCC)/Ultra Large Crude Carriers (ULCC)

VLCC and ULCC are the largest operating cargo vessels in the world. These enormous ships are capable of carrying huge amount of crude oil in a single trip. They are known as supertankers and these vessels are primarily used for long-haul crude transportation from the Persian Gulf to countries in Europe, Asia and North America [Url-4].

On short distances, with relatively weak oil demand at the destination point, using VLCC or ULCC is not efficient due to the long mooring periods for loading and unloading. Using smaller tankers instead of VLCC and ULCC is profitable on short distances [Url-1].

VLCC have a size ranging between 180,000 to 320,000 DWT. They are capable of passing through the Suez Canal in Egypt, and as a result are used extensively around the North Sea, Mediterranean and West Africa. VLCC are very large shipping vessels with dimensions of up to 470 m in length, beam of up to 60 m and draught of up to 20 m. But the standard dimensions of these ships range between 300 to 330 meters in length, 58 meters breath and 31 meters in depth. They can operate in ports with some depth limitations due to the their enormous dimensions.

ULCC are the largest shipping vessels in the world with a size ranging between 320,000 to 550,000 DWT. Due to their enormous size, they need custom built terminals. As a result they serve a limited number of ports with adequate facilities to accommodate them. They are primarily used for very long distance crude oil transportation from the Persian Gulf to Europe, Asia and North America. ULCC are the largest shipping vessels being built in the world with standard dimensions of 415 meters length, 63 meters width and 35 meters draught [Url-4].

Suezmax

Suezmax are midsized tankers with displacement between 120,000 and 200,000 DWT. They are the largest marine vessels that meet the restrictions of the Suez, and are capable of transiting the canal in a laden condition. Prior to 1967, the size of suezmax vessels was restricted to 80,000 DWT, but the maximum was increased to 150,000 DWT in 1975. After the further deepening of the Suez Canal from 18 m to 20.1 m in 2009, a Suezmax of up to 200,000 DWT or even more can easily pass through it. Future plans of further deepening the canal's draft to 21.3 m may lead to redefining of Suezmax vessels' specifications in the coming years.

As the Suez Canal has no locks, the major limiting factors for suezmax vessels are the beam, draught, and length**.** The current depth of the canal allows for a maximum of 20.1 m of draught and 50 m of beam for ships. This means some of fully laden supertankers can't pass through the Suez channel, and they must discharge part of their cargo to other tankers or to a pipeline terminal in order to traverse the canal. A typical Suezmax vessel would be 275 m in length, 48 m in width, and 16.2 m in draught corresponding to about 150,000 DWT [Url-4].

Suezmax tankers offer the relative economies of scale that can be achieved with VLCCs; however their slightly smaller size offers increased versatility and access to a majority of the world's ports. Suezmax tankers primarily operate in the Atlantic Basin delivering cargoes from West Africa, the North Sea and the Former Soviet Union (FSU) [Url-5].

Panamax

Panamax tankers are primarily used for both the transportation of crude oil and petroleum products. Panamax tankers have displacement betweeen 50,000 and 80,000 dwt and trade in short haul. Panamax are the mid-sized cargo ships that are capable of passing through the lock chambers of the Panama Canal which are 320.04 m in length, 33.53 m in width, and 12.56 m in depth. A Panamax shouldn't exceed the dimensional limit of 294,13 m in length, 32,31 m in width and 12,04 m draught wise in order to easily and safely fit to the lock chambers and the height of the Bridge of Americas at Balboa.

In 2009, the Panama Canal Authority published the dimensions for New Panamax**.** The authority has initiated the construction of the third lane of locks having bigger dimension of 427 m in length, 55m in width and 18.3 m in depth, in order to accommodate larger ships called New Panamax. The new locks are expected to be operational from 2014. With this the Panama Canal will be equipped to handle large-sized New Panamax vessels with a cargo capacity of up to 13,000 TEU. Currently, Panamax vessels have a cargo capacity of up to 5,000 TEU only. The new bigger locks will also help in reducing the locking time and thus significantly reducing the traffic congestion and the travelling time for ships crossing the Atlantic into the

Pacific Ocean and vice versa. The completion of new locks in 2014 is expected to double the tonnage capacity of the Panama Canal.

New Panamax ships will have a dimension of 366 m in length, 49 m in width and 15.2 m in depth. They have been designed strictly in accordance with the dimensions of new locks at the Panama Canal. Several ship manufacturing companies across the world are already following the new parameters for container ships to match the dimensions of New Panamax**.** They are also getting large orders for the New Panamax vessels from shipping companies [Url-4].

Aframax

Aframax vessels are mid-size tankers with displacement between 80,000 and 120,000 metric tons. Aframax vessels typically engage in medium to short haul oil trades in nearly all operating regions and can carry cargoes of 80,000 to 120,000 dwt [Url-5]. The tanker derives its name from AFRA which stands for Average Freight Rate Assessment. AFRA system was created by Shell Oil to standardize contract terms.

Due to their favorable size, Aframax tankers can serve most ports in the world. These vessels serve regions which do not have very large ports or offshore oil terminals to accommodate very large crude carriers and ultra large crude carriers. Aframax tankers are just perfect for short to medium haul crude oil transportation.

Aframax **t**ankers are extensively used in areas of lower crude oil production such as in Non-OPEC countries which lack large harbors and canals to accommodate VLCC and ULCC class of tankers. Their main areas of operations include South American oil cargo exports to the US Gulf region through the Caribbean, North African exports to Southern Europe through Mediterranean, exports from former Soviet Union Republics to Northern Europe through the Black Sea and the North Sea, and South East Asian exports to the Far East. As Aframax vessels are mainly used in transporting crude oil, they are sometimes called ‘dirty tankers’[Url-4]

Crude oil tanker size compares are shown in Table 2.2.

Table 2. 2: Crude oil tanker size compares [Url-6].

Class	Length Overall (m)	Breadth (m)	Draft (m)	Speed(nautical miles/hour)	Typical Min DWT	Typical Max DWT
Seawaymax	226	24	7.92		10,000 DWT	60,000 DWT
Panamax	228.6	32.3	12.6	14 knots	60,000 DWT	80,000 DWT
Aframax	253	44.2	11.6	14 knots	80,000 DWT	120,000 DWT
Suexmax	273	47	16	14 knots	120,000 DWT	200,000 DWT
VLCC	330	60	20	15 knots	200,000 DWT	315,000 DWT
ULCC					320,000 DWT	550,000 DWT

2.2 List of Similar Ships

Preliminary design of Aframax tanker with a cargo capacity of 100.000 dwt will be performed. Similar Aframax tankers were examined to make the preliminary assessment of aframax tanker main dimensions, main engine power and speed, generator power and speed, and steam boiler capacity. Then, these values will be used to analyze of cargo heating systems and to calculate heat transfer coefficients independently defined for specific parts of the ship structure surfaces correctly. In addition to this, these values are necessary to determine cargo heating model properly in the following chapters.

The main dimensions of similar Aframax tankers are shown in the following Table 2.3, main engine and generator properties are shown in following Table 2.4 and steam boiler capacity and properties are shown in following Table 2.5.

Table 2. 3: Similar Aframax tanker main dimensions.

NBR	Name of the Ship	Year of Building	Length Overall(L_{OA}) [m]	Length Between Perpendiculars(L_{BP}) [m]	Beam(B) [m]	Draft(T) [m]	Hight(H) [m]	DWT [t]	References
1	KAIMON MARU	2013	246.80	238.40	44.40	15.44	22.00	120015	[6]
2	FS DILIGENCE	2012	249.97	241.00	44.00	14.80	21.20	115656	[7]
3	NIKOLAY ZUYEV	2012	249.90	243.00	46.00	14.90	21.20	120600	[7]
4	ESER K	2010	250.00	239.00	44.00	14.97	21.35	115800	[8]
5	MOSKOVSKY PROSPECT	2010	249.99	239.00	44.00	15.00	21.00	113900	[8]
6	ZENOVIA LADY	2009	247.90	237.00	44.00	14.80	21.00	112090	[9]
7	FAIR SEAS	2008	250.00	239.00	44,00	14.90	21.00	115406	[10]
8	PROMITHEAS	2006	250.00	239.00	44,00	15,40	22.70	117050	[11]
9	BRITISH CORMORANT	2005	251.51	239.00	43.80	15.00	21.30	113782	[12]
10	VIKTOR TITOV	2005	247.00	234.00	42.00	14.50	21.60	100800	[12]
11	MINERVA LISA	2004	243.57	233.00	42.00	14.75	21.30	103755	[13]
12	NEVSKIY PROSPECT	2003	249.90	239.00	44.00	14.80	21.00	133280	[14]
13	KRONVIKEN	2006	249.00	239.00	43.80	14.90	21.00	114500	[11]
14	ARAMON	2010	229.11	219.00	32.24	14.25	20.65	74059	[8]

Table 2. 4: Similar Aframax tanker main engine and generator properties.

NBR	Name of the Ship	Number of Main Engines	Engine Power [kW]	Speed of Engine/Propeller [rpm]	Ship Speed [knot]	Number of Generators	Power of Generators [kW]	Reference
1	KAIMON MARU	1	12210	94.5	14.50	3	3x680kW/900rpm	[6]
2	FS DILIGENCE	1	13560	105	15.20	3	3x660kW/ 900 rpm	[7]
3	NIKOLAY ZUYEV	1	13250	98.4	14.60	1	1x1000kW/900rpm	[7]
4	ESER K	1	13560	105	15.00	3	3x800kW/720 rpm	[8]
5	MOSKOVSKY PROSPECT	1	14280	105	15.00	3	3x1000kWX920rpm	[8]
6	ZENOVIA LADY	1	14310	105	14.70	3	3x880kW/900 rpm	[9]
7	FAIR SEAS	1	14235	109	15.00	3	3x900kW/900rpm	[10]
8	PROMITHEAS	1	16625	105	15.10	3	3x1050kW	[11]
9	BRITISH CORMORANT	1	15820	105	15.42	3	3x960kW/900rpm	[12]
10	VIKTOR TITOV	1	16397	105	15.20	3	3x980kW/720rpm	[12]
11	MINERVA LISA	1	14280	105	15.45	3	3x1054kW	[13]
12	NEVSKIY PROSPECT	1	15570	91	15.10	3	3x780kW/720 rpm	[14]
13	KRONVIKEN	1	14520	105	14.60	3	3x1050kW/720rpm	[11]
14	ARAMON	1	13500	105	16.00	3	3x1120kW/900rpm	[8]

Table 2. 5: Similar Aframax tanker steam boiler properties.

NBR	Name of the Ship	Number of Steam Boilers	Type of Steam Boilers	Capacity of Steam Boilers [t/h]	Reference
1	KAIMON MARU	1	MHI: Two drum type	1x45 t/h	[6]
2	FS DILIGENCE	1	1xMAC-45B(Mitsubishi)	1x45 t/h	[7]
3	NIKOLAY ZUYEV	2	Vertical,water tube(Kangrim)	2x20 t/h	[7]
4	ESER K	2	Aux boiler Exh.gas economiser	1x30 t/h 1x1.2 t/h	[8]
5	MOSKOVSKY PROSPECT	2	Automatic,forced draft H.F.O burning	2x25 t/h	[8]
6	ZENOVIA LADY	2	Make:Aalborg	2x30 t/h	[9]
7	FAIR SEAS	2	Water tube(Kangrim)	2x30 t/h	[10]
8	PROMITHEAS	/	/	/	[11]
9	BRITISH CORMORANT	2	Mission OL(Aalborg)	2x25 t/h	[12]
10	VIKTOR TITOV	2	Automatic marine(Aalborg)	2x35 t/h	[13]
11	MINERVA LISA	2	MAC-30B oil fired	2x26 t/h	[13]
12	NEVSKIY PROSPECT	2	Mission OL(Aalborg)	2x25 t/h	[14]
13	KRONVIKEN	2	MAC-35B(Mitsubushi)	2x35 t/h	[11]
14	ARAMON	2	Large Oil fired boiler+ Forced circulation type	1x25 t/h 1x1.4 t/h	[8]

2.3 Determining Ship Class Notation

Det Norske Veritas (DNV) is used as a ship class notation. Especially, DNV's common structural rules for double hull oil tankers [15] are used to obtain information about structure of double hull oil tankers, constraints on dimensions of the ship structure components in the hull.

2.4 Estimation Main Dimensions of the Proposed Design Ship and Cargo Tanks

The main dimensions are estimated according to list of similar vessels. Based on a similar ships, determined the suitable ship for proposed design criterias and is used it's main dimensions.

Total Length	L_{OA}=247 m
Length Between Perpendicular	L_{BP}=234 m
Breadth,moulded	B=42 m
Draught scantling/design	T=14.5 m
Depth,moulded	H=21.6 m

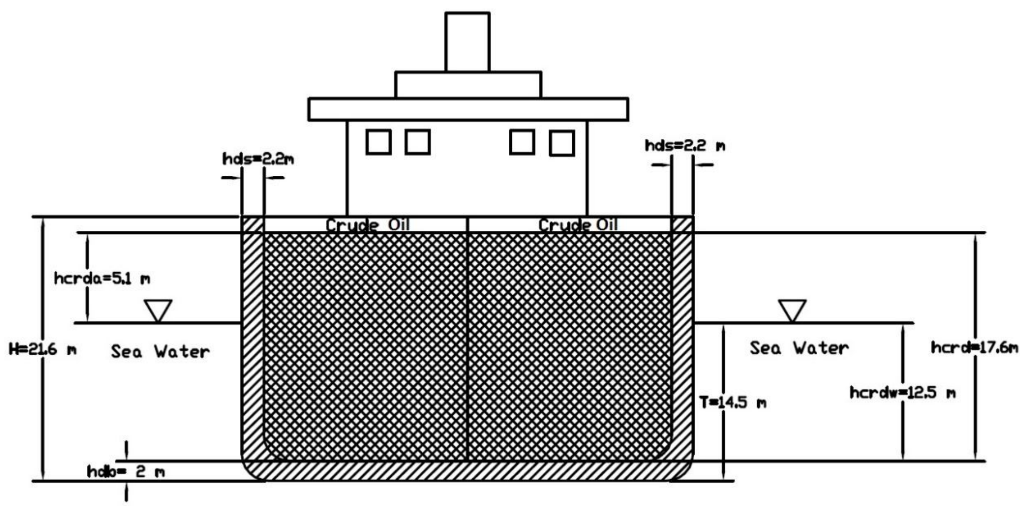

Figure 2. 3: Aframax tanker cross section view.

Double bottom depth and double side width are determined according to DNV's double hull oil tankers structure rules [15]. Aframax tanker cross section view is shown in Figure 2.3.

The minimum double bottom depth (2.1), d_{db}, is to be taken as the lesser of :

$$d_{db} = \frac{B}{15} \text{ m , but not less than 1 m} \quad \textbf{(2.1)}$$

B=moulded breadth [m]

d_{db}= 2 m [minimum double bottom depth]

According to these equations double bottom depth was determined as 2 m.

The minimum double side width (2.2), w_{ds} is to be taken as the lesser of :

$$w_{ds} = 0.5 + \frac{DWT}{20000} \text{ , but not less than 1 m} \quad \textbf{(2.2)}$$

w_{ds}=2 m [minumum double side width]

According to these equations double side width was determined as 2.2 m

h_{db}=double bottom depth=2 m

w_{ds}=double side width=2.2 m

h_{crdw}=crude oil depth from double bottom plate until the sea water level=12.5 m

h_{crd}=crude oil depth in tank=17.6 m

h_{crda}=crude oil depth above the level of sea water = 5.1 m

Tanks dimensions were obtained from scale drawings of optimal ship and dimension values were used to calculate of the proposed ship's tanks capacities (Table 2.6).

Table 2. 6: Cargo tank dimensions and capacities.

NBR	TANK NAMES	LENGTH[m]	BREADTH[m]	DEPT[m]	TANK CAPACITY[m^3]
1	SLOP TANK(P)	4.13	18.80	17.60	1366.5344
2	SLOPTANK(STRB)	4.13	18.80	17.60	1366.5344
3	TANK 1(P)	28.96	18.80	17.60	9582.2848
4	TANK1(STRB)	28.96	18.80	17.60	9582.2848
5	TANK 2(P)	28.96	18.80	17.60	9582.2848
6	TANK2(STRB)	28.96	18.80	17.60	9582.2848
7	TANK 3(P)	30.30	18.80	17.60	10025.6640
8	TANK3(STRB)	30.30	18.80	17.60	10025.6640
9	TANK 4(P)	29.64	18.80	17.60	9807.2832
10	TANK4(STRB)	29.64	18.80	17.60	9807.2832
11	TANK 5(P)	30.30	18.80	17.60	10025.6640
12	TANK5(STRB)	30.30	18.80	17.60	10025.6640
13	TANK 6(P)	24.51	18.80	17.60	8110.2848
14	TANK 6(STRB)	24.51	18.80	17.60	8110.2848
				Total Cargo Capacity[m^3]	117000

V=LxBxD m^3 (Tank Capacity)

V_{cargo}= V_1+V_2+..............V_{14} m^3 (Total Cargo Volume)

As shown in the Table 2.6,total capacities of the cargo was calculated as 117000 m^3.

2.5 Prognosis of Main Engine Systems

Based on a list of similar ships, the Admiralty formula is useful. These method use at the initial stage of the ship design.

The Admiralty formula is still used today and shown as follow equation (2.3) :

$$P_B = \frac{\Delta^{\frac{2}{3}} V^3}{C} \tag{2.3}$$

Where

P_B=Main engine power (kW)

V=Ship speed (knot)

Δ=Displacement (t)

C=Admiralty constant ($t^{2/3}.kn^3/kW$)

Formally it should be the displacement but the information about the displacement is mostly not available for civil ships in the reference. So, the DWT is used in the place of displacement.

The Admiralty constant C is assumed to be constant for similar ships with similar Froude numbers ,ships that have almost the same C_B, C_P, Δ/L, F_n, Δ typical values for C ($t^{2/3}\cdot kn^3/kW$) are shown in Table 2.7 [16] :

Table 2. 7: Admiralty constant.

Type of Ship	C
General Cargo Ships	400-600
Bulker and Tanker	600-750
Reefer	550-700
Feedership	350-500
Warship	150

These valus give an order of magnitude only. The constant C should be determined individually for basis ships used in design.

As shown in Table 2.8, admiralty constants for all similar vessels were calculated and average value of Admiralty factor ($c_{average}$) determined as 550.83. At the same time, similar aframax tankers engine/propeller speeds was averaged and estimated proposed design engine/propeller speed as 103 rpm.

The load capacity and speed of the proposed ship design criterias are considered as 100,000 dwt and 15 knot, respectively. Based on equations 2.3, main engine power was determined as 13200 kW.

Table 2. 8: Calculation of Admiralty factor and speed of the engine.

NBR	Name of the Ship	DWT(Δ) [t]	Engine Power(N) [kW]	Ship Speed(V) [knot]	Admiralty Factor(c)	Speed of Engine/ Propeller(n) [rpm]
1	KAIMON MARU	120015	12210	14.50	607.50	94.5
2	FS DILIGENCE	115656	13560	15.20	614.78	105
3	NIKOLAY ZUYEV	120600	13250	14.60	573.33	98.4
4	ESER K	115800	13560	15.00	591.32	105
5	MOSKOVSKY PROSPECT	113900	14280	15.00	555.34	105
6	ZENOVIA LADY	112090	14310	14.70	516.05	105
7	FAIR SEAS	115406	14235	15.00	562.00	109
8	PROMITHEAS	117050	16625	15.10	495.55	105
9	BRITISH CORMORANT	113782	15820	15.42	544.20	105
10	VIKTOR TITOV	100800	16397	15.20	463.88	105
11	MINERVA LISA	103755	14280	15.45	570.25	105
12	NEVSKIY PROSPECT	133280	15570	15.10	576.97	91
13	KRONVIKEN	114500	14520	14.60	505.39	105
14	ARAMON	74059	13500	16.00	535.07	105
				$C_{average}$ =	550.83	
					$n_{average}$ =	103

2.5.1 Selection of Main Engine

Proposed design tanker contractual parameters are in the following :

Main Engine Power (N_X) : 13200 kW

Engine/Propeller Speed (n_x) : 103 rpm

Pre-Selection Criterias

$n_{L4} \leq n_x \leq n_{L1}$

$N_{L4} \leq N_X \leq N_{L1}$

Initially, engines has to satisfy these criterias.

The most popular engine producer firms which are MAN B&W and WÄRTSILÄ in marine and energy markets are examined to find suitable solutions for proposed aframax tanker design.

MAN B&W ENGINES

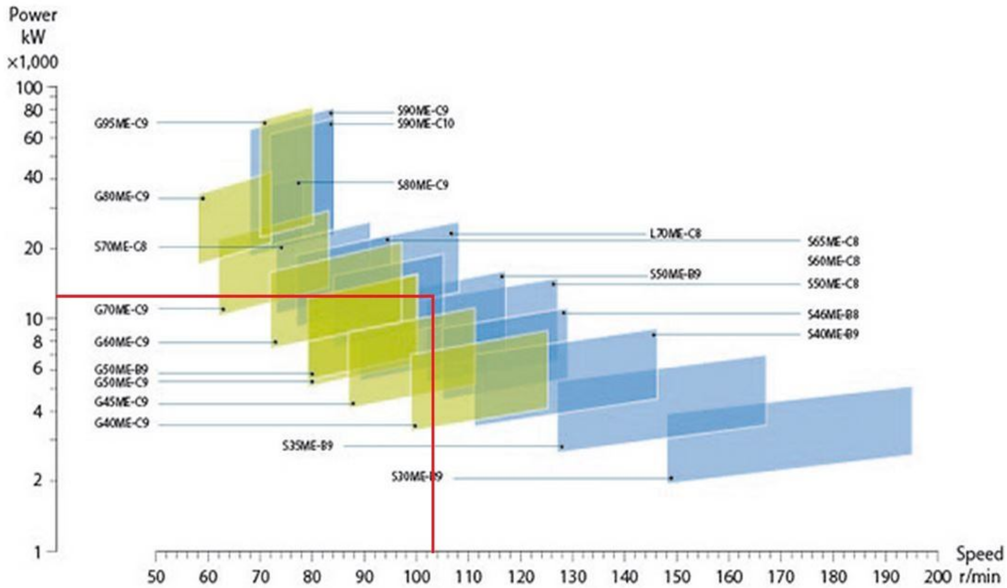

Figure 2. 4: Man B&W two stroke engines power and speed range [Url-7].

Figure 2.4 demonstrate Man B&W two stroke engines power and speed range and also the red lines shows engine design power and speed. According to Figure 2.4 , S50ME-B9, S60ME-C8,L70ME-C8 these 3 engines types are suitable for proposed ship design.

- S50ME-B9-TII
  9S50ME-B9.5-TII (9 cylinders)
- S60ME-C8-TII
  -6S60ME-C8.5-TII (6 cylinders)
  -7S60ME-C8.5-TII (7 cylinders)
- L70ME-C8-TII
  5L70ME-C8.5-TII (5 cylinders)

The company has many cylinder options for each engines. So, it is really important to find right engine which satisfy our criterias of engine power and engine speed. 9 cylinders of S50ME-B9-TII ,6 and 7 cylinders of S60ME-C8-TII and 5 cylinders of L70ME-C8-TII these engines satisfy the design parameters and it is shown in the following Table 2.9 to Table 2.17. Figure 2.5, 2.6, 2.7, 2.8 show engine layout diagrams with contract points.

Table 2. 9: Boundary points of contractual engines parameters field [Url-7].

		MAN			
		9S50ME-B9.5-TII	6S60ME-C8.5-TII	7S60ME-C8.5-TII	5L70ME-C8.5-TII
n[rpm]	n_{L1}	89	84	84	91
	n_{L2}	89	84	84	91
	n_{L3}	117	105	105	108
	n_{L4}	117	105	105	108
N[kW]	L_1	9600	9100	10600	11000
	L_2	12200	11400	13300	13800
	L_3	12700	11200	13200	13100
	L_4	16000	14200	16600	16300

- S50ME-B9.5-TII ENGINE

Table 2. 10: 9S50ME-B9.5-TII engine boundary points.

	N/N_{L4}[%]		n/n_{L4}[%]
N_{L1}/N_{L4}	60	n_{L1}/n_{L4}	76
N_{L2}/N_{L4}	76.25	n_{L2}/n_{L4}	76
N_{L4}/N_{L4}	100	n_{L4}/n_{L4}	100
N_{L3}/N_{L4}	79.35	n_{L3}/n_{L4}	100
N_{L1}/N_{L4}	60	n_{L1}/n_{L4}	76

Table 2. 11: 9S50ME-B9.5-TII design engine parameters points.

N[Kw]	n[rpm]	N_{L4}	n_{L4}[rpm]	N/N_{L4}	n/n_{L4}
13200	103	16000	117	82.5	88.03419

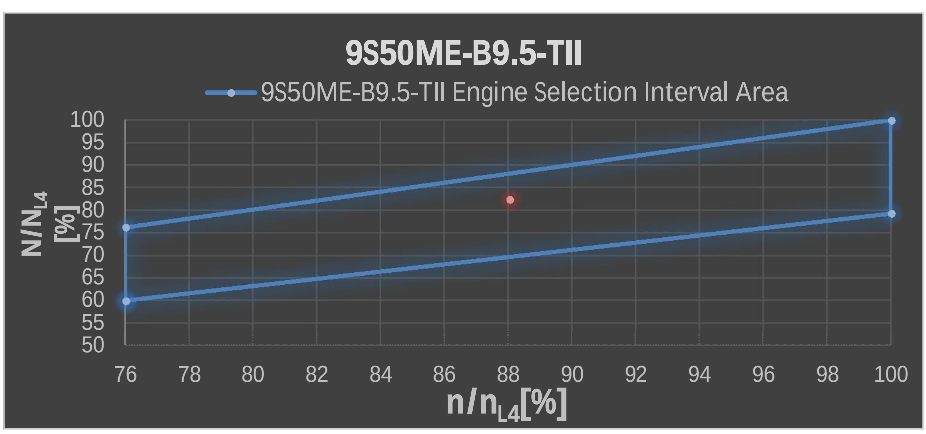

Figure 2. 5: 9S50ME-B9.5-TII engine layout diagram with the contract point.

- **6S60ME-C8.5-TII**

Table 2. 12: 6S60ME-C8.5-TII engine boundary points.

	N/N_{L4}[%]		n/n_{L4}[%]
N_{L1}/N_{L4}	64	n_{L1}/n_{L4}	80
N_{L2}/N_{L4}	80.28	n_{L2}/n_{L4}	80
N_{L4}/N_{L4}	100	n_{L4}/n_{L4}	100
N_{L3}/N_{L4}	78.87	n_{L3}/n_{L4}	100
N_{L1}/N_{L4}	64	n_{L1}/n_{L4}	80

Table 2. 13: 6S60ME-C8.5-TII design engine parameters points.

N[kW]	n[rpm]	N_{L4}	n_{L4}[rpm]	N/N_{L4}	n/N_{L4}
13200	103	14200	105	92.95775	98.09524

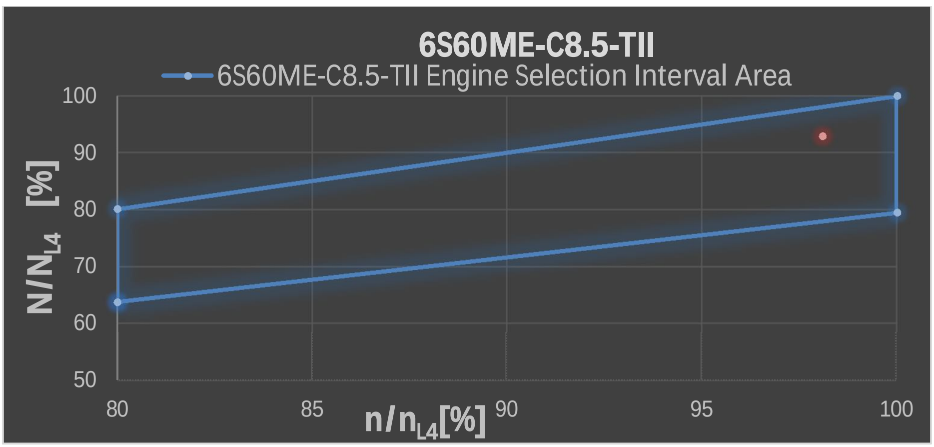

Figure 2. 6: 6S50ME-C8.5-TII engine layout diagram with the contract point.

- **7S60ME-C8.5-TII**

Table 2. 14: 7S60ME-C8.5-TII engine boundary points.

	N/N_{L4}[%]		n/n_{L4}[%]
N_{L1}/N_{L4}	63.8	n_{L1}/n_{L4}	80
N_{L2}/N_{L4}	80.12	n_{L2}/n_{L4}	80
N_{L4}/N_{L4}	100	n_{L4}/n_{L4}	100
N_{L3}/N_{L4}	79.5	n_{L3}/n_{L4}	100
N_{L1}/N_{L4}	63.8	n_{L1}/n_{L4}	80

Table 2. 15: 7S60ME-C8.5-TII design engine parameters points.

N[kW]	n[rpm]	N_{L4}	n_{L4}[rpm]	N/N_{L4}	n/N_{L4}
13200	103	16600	105	79.51807	98.09524

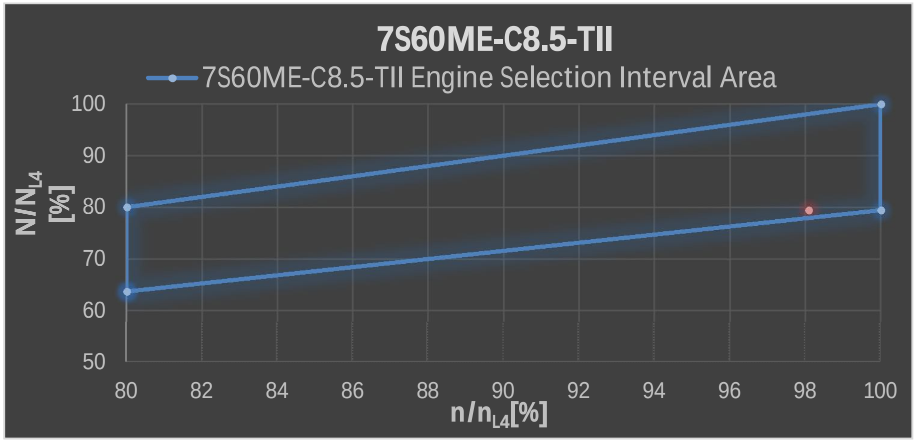

Figure 2. 7: 7S60ME-C8.5-TII engine layout diagram with the contract point.

- **5L70ME-C8.5-TII**

Table 2. 16: 5L70ME-C8.5-TII engine design parameters.

	N/N_{L4}[%]		n/n_{L4}[%]
N_{L1}/N_{L4}	67.48	n_{L1}/n_{L4}	84.25
N_{L2}/N_{L4}	84.66	n_{L2}/n_{L4}	84.25
N_{L4}/N_{L4}	100	n_{L4}/n_{L4}	100
N_{L3}/N_{L4}	80.36	n_{L3}/n_{L4}	100
N_{L1}/N_{L4}	67.48	n_{L1}/n_{L4}	84.25

Table 2. 17: 5L70ME-C8.5-TII design engine parameters points.

N[Kw]	n[rpm]	N_{L4}	n_{L4}[rpm]	N/N_{L4}	n/N_{L4}
13200	103	16300	108	80.9816	95.37037

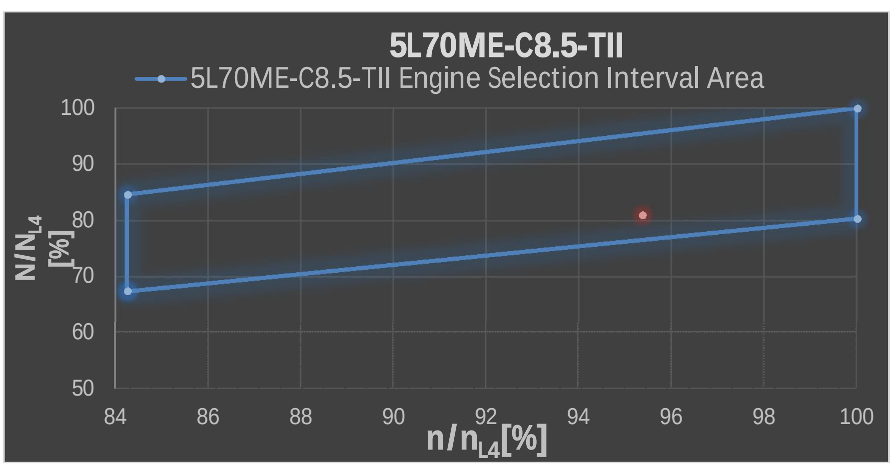

Figure 2. 8: 5L70ME-C8.5-TII engine layout diagram with the contract point.

WÄRTSILÄ MARINE LOW SPEED ENGINE

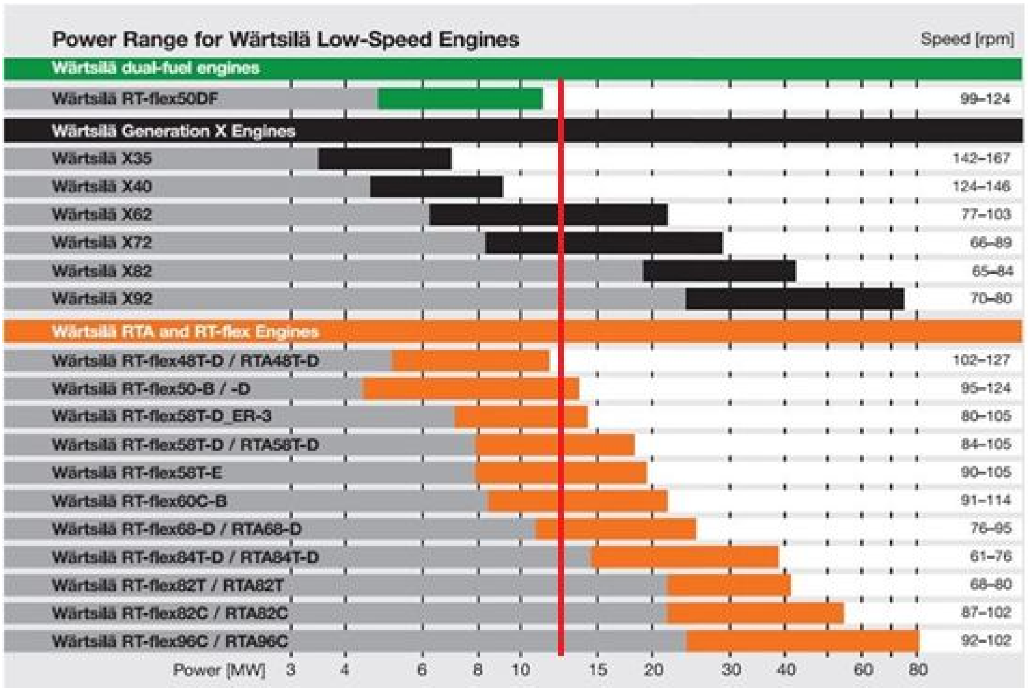

Figure 2. 9: Wärtsilä low-speed engines power range [Url-8].

Figure 2.9 demonstrate Wärtsilä two stroke low-speed engines power and speed range. According to Figure 2.9 , Wärtsilä X62, Wärtsilä RT-flex58T-D_ER-3 , Wärtsilä RT-flex58T-D, Wärtsilä RT-flex58T-E, Wärtsilä RT-flex60C-B these 5 engines types are suitable for proposed ship design .

- **Wärtsilä X62**
  Wärtsilä 5X62 (5 cylinders)
  Wärtsilä 6X62 (6 cylinders)
- **Wärtsilä RT-flex58T-D ER-3**
  Wärtsilä 7RT-flex58T-D ER-3 (7 cylinders)
- **Wärtsilä RT-flex58T-D**
  Wärtsilä 6RT-flex58T-D (6 cylinders)
  Wärtsilä 7RT-flex58T-D (7 cylinders)
  Wärtsilä 8RT-flex58T-D (8 cylinders)
- **Wärtsilä RT-flex58T-E**
  Wärtsilä 6RT-flex58T-E (6 cylinders)
  Wärtsilä 7RT-flex58T-E (7 cylinders)
  Wärtsilä 8RT-flex58T-E (8 cylinders)

- **Wärtsilä RT-flex60C-B**
  Wärtsilä 7RT-flex60C-B (7 cylinders)

The company has many cylinder options for each engines. So, it is really important to find right engine which satisfy our criterias of engine power and engine speed. 5 and 4 cylinders of Wärtsilä X62 , 7 cylinders of Wärtsilä RT-flex58T-D ER-3; 6,7 and 8 cylinders of Wärtsilä RT-flex58T-D and Wärtsilä RT-flex58T-E ,7 cylinders of Wärtsilä RT-flex60C-B these engines satisfy the design parameters and this is shown in the following Figures (2.10 to 2.19) :

Wärtsilä X62

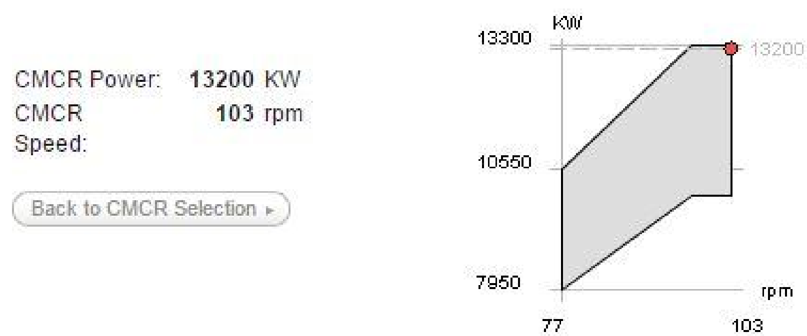

Figure 2. 10: Wärtsilä 5 cylinders engine layout diagram with the contract point (5X62) [Url-8].

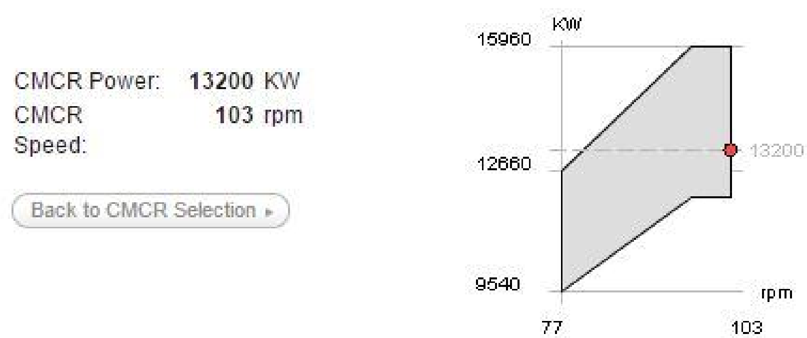

Figure 2. 11: Wärtsilä 6 cylinders engine layout diagram with the contract point (6X62) [Url-8].

Wärtsilä RT-flex58T-D ER-3

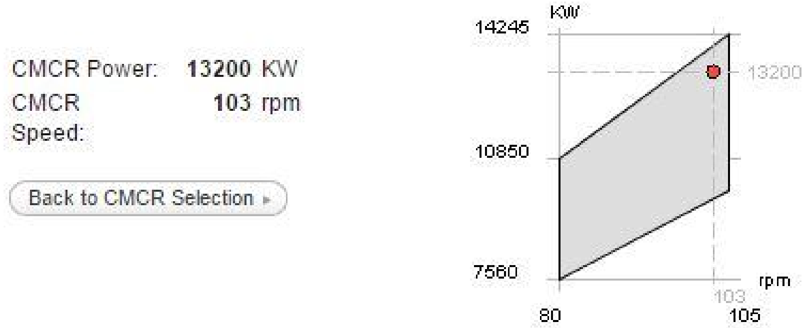

Figure 2. 12: Wärtsilä 7 cylinders engine layout diagram with the contract point (7RT-flex58T-D ER-3).

Wärtsilä RT-flex58T-D

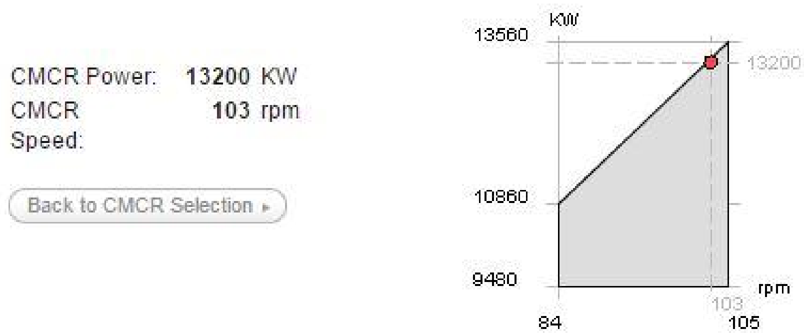

Figure 2. 13: Wärtsilä 6 cylinders engine layout diagram with the contract point (6RT-flex58T-D).

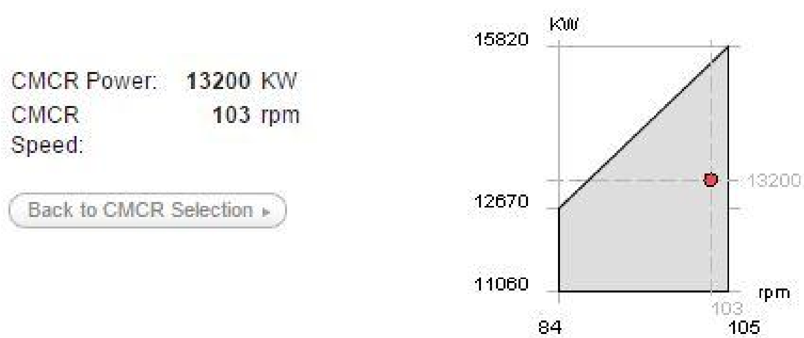

Figure 2. 14: Wärtsilä 7 cylinders engine layout diagram with the contract point (7RT-flex58T-D).

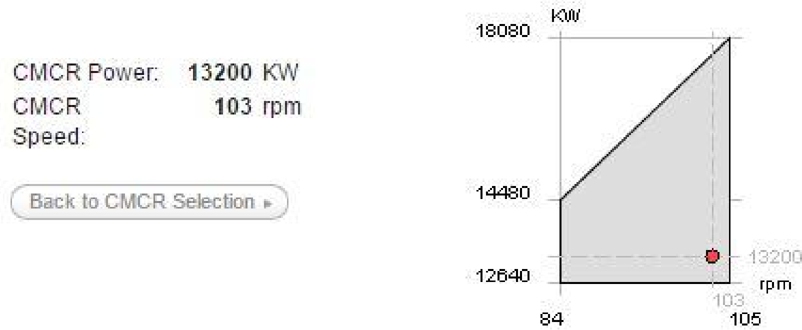

Figure 2. 15: Wärtsilä 8 cylinders engine layout diagram with the contract point (8RT-flex58T-D).

Wärtsilä RT-flex58T-E

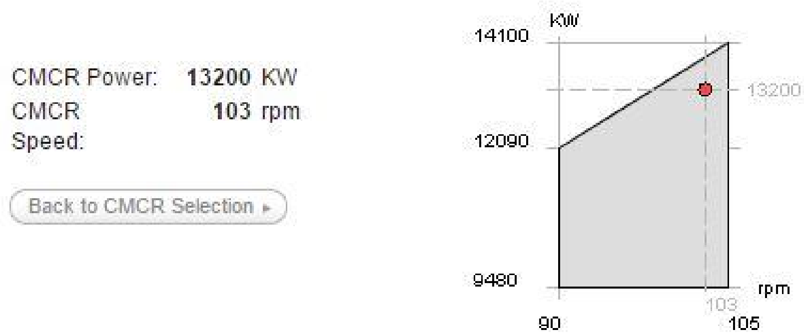

Figure 2. 16: Wärtsilä 6 cylinders engine layout diagram with the contract point (6RT-flex58T-E).

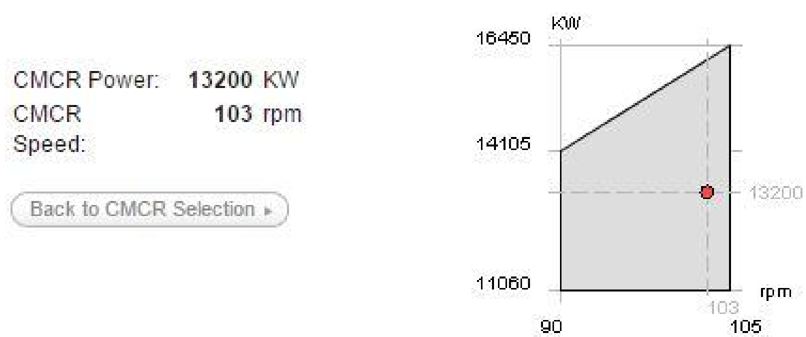

Figure 2. 17: Wärtsilä 7 cylinders engine layout diagram with the contract point (7RT-flex58T-E).

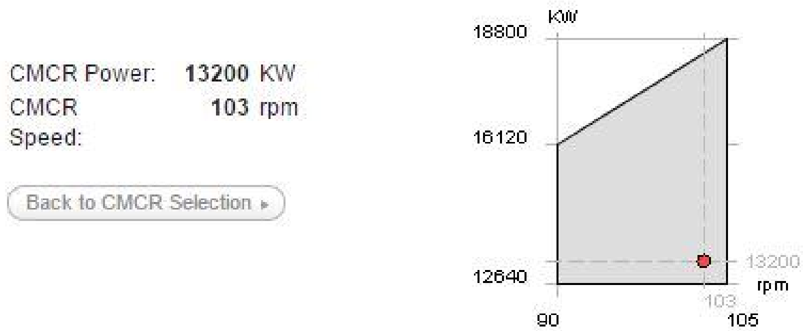

Figure 2. 18: Wärtsilä 8 cylinders engine layout diagram with the contract point (8RT-flex58T-E).

Wärtsilä RT-flex58T-60C-B

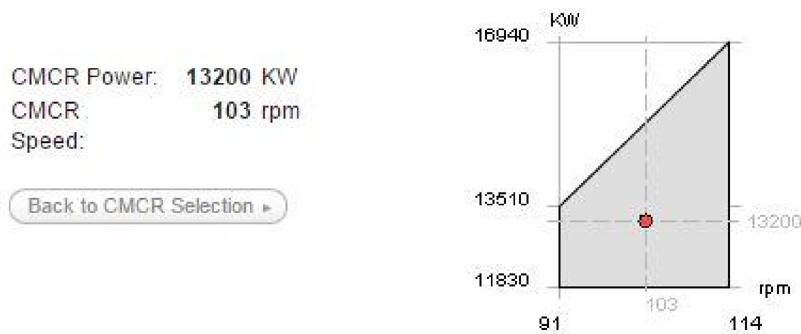

Figure 2. 19: Wärtsilä 7 cylinders engine layout diagram with the contract point (7RT-flex60C-B).

Engine brake specific fuel consumption values are taken in ISO conditions which showed in Table 2.18 for both companies engines.

Table 2. 18: ISO conditions [Url-7].

CONDITIONS	Reference Conditions(ISO)
Air temperature before blower	25.0 °C
Engine room ambient air temp	25.0 °C
Coolant temp. before SAC	29.0 °C
Air relative humidity	30.00%
Barometric pressure	1000 mbar
Cylinder water outlet temperature	90.0 °C
Oil temperature before engine	45.0 °C
Exhaust gas back pressure	300 mmWG

In order to select best engine for proposed ship design, Man B&W and WÄRTSILÄ company engines's size (V), weight (W) and brake specific fuel consumption (bsfc) are compared. Lowest value of engine size, weight and brake specific fuel consumption are determined and these values are :

$BSFC_{(lowest)}$=161.1 g/kW·h

$Weight_{(lowest)}$=321 t

$Volume_{(lowest)}$=311.434 m^3

Brake specific fuel consumption is more worthy than mass and volume for more efficiency and economic design . Brake specific fuel consumption's weighting factor is chosen higher values comparing the other criterias.

W_1= Brake specific fuel consumption weighting factor = 0.6

W_2=Mass weighting factor=0.2

W_3=Volume weighting factor=0.2

Dimensionless

The brake specific fuel consumption (bsfc(i)), weight(m(i)) and volume(v(i)) dimensionless values are generated as below.

$$bsfc(i) = \frac{Bsfc(i)}{Bsfc(lowest)}$$

$$m(i) = \frac{W(i)}{W(lowest)}$$

$$v(i) = \frac{V(i)}{V(lowest)}$$

I=indeks factor

$I=W_1 \times bsfc(i)+W_2 \times m(i)+ W_3 \times v(i)$

Engine comparisions in terms of engine size, weight and brake specific fuel consumption are shown in Table 2.19.

Lowest indeks factor (I) is chosen due to providing the best solution for efficiency and economical design. Considering the criterion of minimum fuel consumption as more important than the mass and size criterias in terms of economic, it was decided that the proposed drive unit motor is selected **9S50ME-B9-5-TII MAN B & W** as shown in Table 2.20.

Table 2. 19: Comparisions in terms of engine size, weight and brake specific fuel consumption.

FIRM	MODEL	WEIGHT [t]	LENGTH [m]	WIDTH [m]	HEIGHT [m]	*BSFC [g/kW.h]	Volume[m^3]
MAN B&W	9S50ME-B9.5-TII	321	9.573	3.290	10.090	166.1	317.786
MAN B&W	6S60ME-C8.5-TII	350	7.459	3.770	11.075	167.3	311.434
MAN B&W	7S60ME-C8.5-TII	393	8.479	3.770	11.075	163.3	354.022
MAN B&W	5L70ME-C8.5-TII	437	7.639	3.980	11.887	165.4	361.403
WÄRTSILÄ	5X62	325	7.000	4.200	11.690	165.7	343.686
WÄRTSILÄ	6X62	377	8.110	4.200	11.690	161.1	398.185
WÄRTSILÄ	7RT-flex58T-D ER-3	377	8.997	3.820	10.810	165.3	371.524
WÄRTSILÄ	6RT-flex58T-D	322	7.991	3.820	10.810	168.8	329.982
WÄRTSILÄ	7RT-flex58T-D	377	8.997	3.820	10.810	164.5	371.524
WÄRTSILÄ	8RT-flex58T-D	418	10.003	3.820	10.810	163.0	413.066
WÄRTSILÄ	6RT-flex58T-E	322	7.991	3.820	10.810	166.6	329.982
WÄRTSILÄ	7RT-flex58T-E	377	8.997	3.820	10.810	162.5	371.524
WÄRTSILÄ	8RT-flex58T-E	418	10.003	3.820	10.810	162.0	413.066
WÄRTSILÄ	7RT-flex60C-B	377	9.291	3.700	10.525	166.9	361.815

*BSFC : Break Specific Fuel Consumption[g/kW.h]

Yellow points show the lowest values for weight,BSFC and Volume

Table 2. 20: Determination of engine according to the indeks factor.

NBR(i)	FIRM	MODEL	BSFC [g/kW·h]	$bsfc_{(i)}$	WEIGHT [t]	m(i)	Volume[m^3]	v(i)	I
1	MAN B&W	9S50ME-B9.5-TII	166.1	103.10	321	100.00	317.786	102.04	102.270
2	MAN B&W	6S60ME-C8.5-TII	167.3	103.85	350	109.03	311.434	100.00	104.116
3	MAN B&W	7S60ME-C8.5-TII	163.3	101.37	393	122.43	354.022	113.67	108.040
4	MAN B&W	5L70ME-C8.5-TII	165.4	102.67	437	136.14	361.403	116.04	112.038
5	WÄRTSILÄ	5X62	165.7	102.86	325	101.25	343.686	110.36	104.034
6	WÄRTSILÄ	6X62	161.1	100.00	377	117.45	398.185	127.86	109.060
7	WÄRTSILÄ	7RT-flex58T-D ER-3	165.3	102.61	377	117.45	371.524	119.29	108.912
8	WÄRTSILÄ	6RT-flex58T-D	168.8	104.78	322	100.31	329.982	105.96	104.121
9	WÄRTSILÄ	7RT-flex58T-D	164.5	102.11	377	117.45	371.524	119.29	108.614
10	WÄRTSILÄ	8RT-flex58T-D	163.0	101.18	418	130.22	413.066	132.63	113.278
11	WÄRTSILÄ	6RT-flex58T-E	166.6	103.41	322	100.31	329.982	105.96	103.302
12	WÄRTSILÄ	7RT-flex58T-E	162.5	100.87	377	117.45	371.524	119.29	107.869
13	WÄRTSILÄ	8RT-flex58T-E	162.0	100.56	418	130.22	413.066	132.63	112.906
14	WÄRTSILÄ	7RT-flex60C-B	166.9	103.60	377	117.45	361.815	116.18	108.885

2.6 Determination of Electrical Power and Selection Of Generating Sets

It is always better to delve deep into power generation requirements before making a choice. Before selection of generating sets, it is better to do these statements to determine exact generator power requirements for design.

-Making a list of the items that need to be powered by the generator

-Making a note of the of starting and running wattage the respective items

-Calculating the total power requirements in kVA or kW

Table 2.21 is demonstrated some examples as how starting and running wattage varies between various electrical devices . As in Table 2.21 ,in ship design it is necessary to know each electrical devices starting and running wattage and to accumulate them separately to get total electrical power consumption. Generator power and numbers for proposed ship design are selected depending on similar ships genarators power and numbers due to lack of information about electrical devices. Generators total powers are averaged and the power requirements is obtained for proposed ship design.

Table 2. 21: Some examples as how starting and running wattage varies between various electrical devices [Url-9].

ITEM	Starting Wattage(W)	Running Wattage(W)
Circular Saw	2400	1200
Central Air Conditioner(10,000 BTU)	2200	1500
Central Air Conditioner(20,000 BTU)	3300	2500
Air Compressor(Average)	4000	2000
Winch	5400	1800
Water Pump	3000	1000

Based on the data contained in the list of similar ships, it is determined that a proposed design ship will consist of the same rated power three generating units. One of the generating sets is designed to cover demand for electric power while driving in the sea. The second will be in the hot reserve, and the third possibly supported.

On average capacity of generating sets :

Generator Power(kW)=Similar Ships Sum of Genarator Power(kW)/ Number of Ships

According to this equation, one of the requisite generator power is calculated that is showed in Table 2.22.

Table 2. 22: Obtaining generator power.

NBR	Name of the Ship	Number of Generators	Power of Generators[kW]	One of the Generators Power[kW]
1	KAIMON MARU	3	3x680kW/900rpm	680
2	FS DILIGENCE	3	3X660kW/ 900 rpm	660
3	ESER K	3	3X800kW/720 rpm	800
4	MOSKOVSKYPROSPECT	3	3X1000kWX920rpm	1000
5	ZENOVIA LADY	3	3x880kW/900 rpm	880
6	FAIR SEAS	3	3x900kW/900rpm	900
7	PROMITHEAS	3	3x1050Kw	1050
8	BRITISH CORMORANT	3	3x960kW/900rpm	960
9	VIKTOR TITOV	3	3x980kW/720rpm	980
10	MINERVA LISA	3	3x1054 kW	1054
11	NEVSKIY PROSPECT	3	3x780kW/720 rpm	780
12	KRONVIKEN	3	3x1050kW/720rpm	1050
13	ARAMON	3	3x1120kW/900rpm	1120
			Mean of the total generators power [kW]	916

Table 2. 23: Selection of suitable generator [Url-7,Url-8].

FIRM	MODEL	SPEED[rpm]	FREQUENCY [Hz]	GENERATOR[kW]	SFC[g/kWh]
MANB&W	5L28/32H	720	60	1000	190
MANB&W	5L28/32H	750	50	1045	191
MANB&W	6L23/30H	900	60	998	193
MANB&W	7L23/30H	720	60	944	191
MANB&W	7L23/30H	750	50	984	192
MANB&W	5L21/31	900	60	950	192
MANB&W	5L21/31	1000	50	950	193
MANB&W	9L16/24	1200	60	941	191
WÄRTSILÄ	975W6L20	900	60	975	182
WÄRTSILÄ	1000W6L20	1000	50	1000	182

When selecting independent generator sets, it is taken into account reliability, fuel consumption, dimensions, operating costs and the purchase. Due to the lack of opportunity to get knowledge about the price of an independent team generator, it is not taken into account. Frequency of the gensets is determined as 60 Hz in accordance with using commonly in new ship designs. Specific fuel consumption is more worthy than other parameters for our gensets selection . The other parameters like dimensions and mass are nearly same for both companies models. MAN and WÄRTSILÄ's generators were compared according to their specific fuel consumptions which is shown in Table 2.23 and generator (WÄRTSILÄ 975W6L20) which has the lowest specific fuel consumption values was chosen for proposed ship design.

2.7 Preliminary Selection of Boilers

It is important to select suitable boilers according to the total steam requirements. According to the similar vessels, steam boiler capacity varies between 20 t/h and 70 t/h. One of the reason for this difference is physical properties of the crude oil. Some crude oils have bigger viscosity than the others, thereby it requires more steam to heat crude oil until the crude oil reach sufficient viscosity to pump out of the tank. At the same time, number of steam boilers differ according to the usage. In some vessels, small capacity boilers (2 t/h) were used due to the resolve only small requirements but some vessels resolve this small requirements using large capacity boilers. 2 units of steam boilers with the capacity of 35 tons steam per hour (Mitsubishi MAC-35B series) are selected for proposed design ship. Boilers total capacity of 70 tons is the biggest value on similar vessels. The final selection of boilers capacity will be provided after more accurate calculations which is shown in page number 72.

3. GENERAL THEORY OF HEAT TRANSFER

3.1 Conduction

Conduction physical mechanism involves concepts of atomic and molecular activity, which sustains the transfer of energy from the more energetic to the less energetic particles of a substance due to interactions between the particles [17].

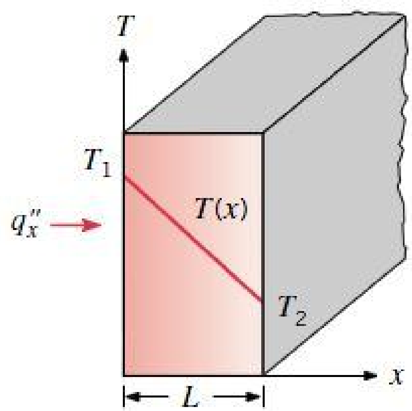

Figure 3. 1: One dimensional heat transfer by conduction [18].

It is possible to quantify heat transfer processes in terms of appropriate rate equations. These equations can be used to compute the amount of energy being transferred per unit time. For heat conduction, the rate equation is known as Fourier's law. For the one-dimensional plane wall shown in Figure 3.1, having a temperature distribution T(x), the rate equation is expressed as equation (3.1) [18] :

$$q'' = -k\frac{\partial T}{\partial x} \quad \text{Fourier's Law Equation} \qquad \textbf{(3.1)}$$

q''= The heat flux is the heat transfer rate in the x direction per unit area perpendicular to the direction of transfer (W/m^2)

$\frac{\partial T}{\partial x}$ = is the temperature gradient in this direction

k= is the thermal conductivity and is characteristic of the material (W/m·K)

Under the steady-state conditions shown in Figure 3.1, where the temperature distribution is linear, the temperature gradient and heat flux, respectively, may be expressed as equations (3.2) and (3.3).

$$\frac{\partial T}{\partial x} = \frac{T_2 - T_1}{L} \quad \textbf{(3.2)}$$

$$q_x'' = -k\frac{T_2 - T_1}{L} \quad \textbf{(3.3)}$$

Note that this equation provides a heat flux, that is, the rate of heat transfer per unit area. The heat rate by conduction, q_x (W), through a plane wall of area A, is then the product of the flux and area, $q_x = q'' \cdot A$.

3.1.1 One dimensional steady-state conduction

The temperature at each point is independent of time in steady-state conditions. In a one-dimensional system, temperature gradients exist along only a single coordinate direction, and heat transfer occurs exclusively in that direction. We will determine expressions for temperature distribution and heat transfer rate for plane wall which are interested. Concept of thermal resistance will introduce and also how thermal circuits may be used to model heat flow [17].

Steady State Conduction For Plane Wall

For one-dimensional conduction in a plane wall, temperature is a function of the *x*-coordinate only and heat is transferred exclusively in this direction. In Figure 3.2, a plane wall separates two fluids of different temperatures. Heat transfer occurs by convection from the hot fluid at $T_{\infty,1}$ to one surface of the wall at $T_{s,1}$, by conduction through the wall, and by convection from the other surface of the wall at $T_{s,2}$ to the cold fluid at $T_{\infty,2}$ [18].

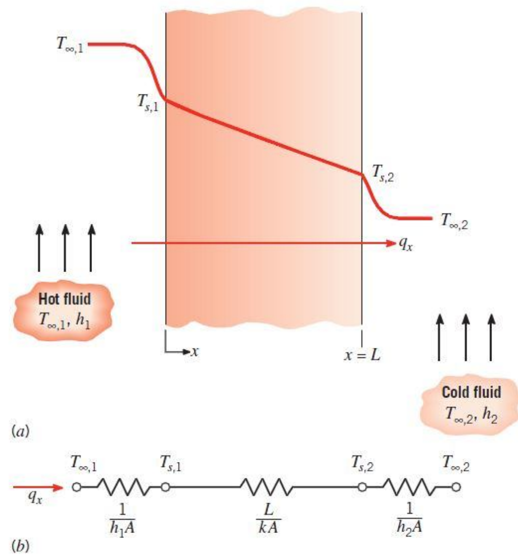

Figure 3. 2: Heat transfer through a plane wall [18].

(*a*) Temperature distribution.
(*b*) Equivalent thermal circuit.

Temperature Distribution

The temperature distribution in the wall can be determined by solving the heat equation with the proper boundary conditions. For steady-state conditions with no distributed source or sink of energy within the wall, the appropriate form of the heat equation is shown in equation (3.4) [17] :

$$\frac{\partial}{\partial x}\left(\frac{\partial T}{\partial x}\right) = 0 \tag{3.4}$$

We assumed that thermal conductivity of the wall and heat flux is constant and it is independent of x. If we integrate this equation twice ,we will obtain this general solution

$T(x)=C_1 . x+C_2$

We should determine our boundary conditions to obtain these constants (C_1 and C_2).

x =0 and x=L are our boundary conditions for these system.

$T(0)=T_{s,1}$ and $T(L)=T_{s,2}$

Applying for these equations to the general solution, we will get

For x =0 $T(0)=C_2= T_{s,1}$

For x=L $T(L)=C_1L+C_2= T_{s,2}$

We will obtain constants values (C_1 and C_2) from these equations and consequently temperature distribution is shown in equation (3.5) :

$$T(x) = (T_{s,2} - T_{s,1})\frac{x}{L} + T_{s,1} \tag{3.5}$$

As a result of this equation, we can observe that temperature varies linearly with x. Combination of Fourier's law and temperature distribution we will get equations (3.6) and (3.7) as shown below :

$$q_x = -kA\frac{\partial T}{\partial x} = \frac{kA}{L}\left(T_{S,1} - T_{S,2}\right) \quad \textbf{(3.6)}$$

q_x = conduction heat transfer rate (W)
A=is the area of the wall normal to the direction of heat transfer and plane wall (m^2)

$$q_x^{"} = \frac{q_x}{A} = \frac{k}{L}\left(T_{S,1} - T_{S,2}\right) \quad \textbf{(3.7)}$$

Heat flux ($q_x^{"}$) and heat rate (q_x) both are constants independent of x .

3.1.2 Thermal resistance

There is an analogy exists between the diffusion of heat and electrical charge. Just as an electrical resistance is associated with the conduction of electricity, a thermal resistance may be associated with the conduction of heat. Defining resistance as the ratio of a driving potential to the corresponding transfer rate, it follows from and thermal resistance for conduction in a plane wall is expressed in the following formula (3.8) [18]:

$$R_{t,cond} = \frac{(T_{S,1} - T_{S,2})}{q_x} = \frac{L}{kA} \quad \textbf{(3.8)}$$

Similarly, for electrical conduction in the same system, Ohm's law provides an electrical resistance of the form which is shown in equation (3.9).

$$R_e = \frac{(E_{S,1} - E_{S,2})}{I} = \frac{L}{\sigma A} \quad \textbf{(3.9)}$$

A thermal resistance may also be associated with heat transfer by convection at a surface. From Newton's law of cooling which is shown in equation (3.10).

$$q = h \cdot A \cdot (T_S - T_\infty) \quad \textbf{(3.10)}$$

The thermal resistance for convection can be written as equation (3.11) :

$$R_{t,conv} = \frac{(T_S - T_\infty)}{q_x} = \frac{1}{hA} \quad \textbf{(3.11)}$$

The heat transfer rate may be determined from separate consideration of each element in the network. Since q_x is constant throughout the network, it follows that equation (3.12) :

$$q_x = \frac{T_{\infty,1} - T_{S,1}}{1/h_1 A} = \frac{T_{S,1} - T_{S,2}}{L/kA} = \frac{T_{s,2} - T_{\infty,2}}{1/h_2 A} \quad \textbf{(3.12)}$$

In terms of the overall temperature difference, $T_{\infty,1}$-$T_{\infty,2}$ and the total thermal resistance R_{tot}, the heat transfer rate may also be expressed as equation (3.13) :

$$q_x = \frac{T_{\infty,1} - T_{\infty,2}}{R_{tot}} \quad \textbf{(3.13)}$$

Because the conduction and convection resistances are in series and may be summed and overall heat transfer coefficients (R_{tot}) is expressed in the following formula (3.14)

$$R_{tot} = \frac{1}{h_1 A} + \frac{L}{kA} + \frac{1}{h_2 A} \quad \textbf{(3.14)}$$

3.2 Theory of Similarity

Similarity of heat transfer on the surface of the body is dependent on the geometric similarity of the bodies, physical property similarities, temperature field similarity and heat transfer coefficient similarity.

Equation of motion for x component can be written in the following equation (3.15) :

$$\frac{\partial w_x}{\partial t} + w_x \frac{\partial w_x}{\partial x} + w_y \frac{\partial w_x}{\partial y} + w_z \frac{\partial w_x}{\partial z} = g - \frac{1}{\rho}\frac{\partial P}{\partial x} + \nu \left(\frac{\partial^2 w_x}{\partial x^2} + \frac{\partial^2 w_x}{\partial y^2} + \frac{\partial^2 w_x}{\partial z^2} \right) \quad \textbf{(3.15)}$$

In this equation , w is a vector describing the fluid velocity, g is acceleration of gravity, ρ is the fluid density, P is the specific pressure of the fluid on the volume element surface and ν is referred to as the kinematical viscosity. Dimensionless parameters that govern momentum equation are shown in equation (3.16) and (3.17) :

$$w^+ = \frac{w'_x}{w_x} = \frac{w'_y}{w_y} = \frac{w'_z}{w_z}, \quad t^+ = \frac{t'}{t} \quad , \quad l^+ = \frac{x'}{x} = \frac{y'}{y} = \frac{z'}{z} \quad \textbf{(3.16)}$$

$$g^+ = \frac{g'}{g} \quad , \quad \rho^+ = \frac{\rho'}{\rho} \quad , \quad P^+ = \frac{P'}{P} \quad , \quad \nu^+ = \frac{\nu'}{\nu} \quad \textbf{(3.17)}$$

Equation of motion for model is shown in equation (3.18) and equation (3.19) is obtained from solution of equation (3.18) with certain assumptions for convection.

$$\frac{\partial w'_x}{\partial t'} + w'_x \frac{\partial w'_x}{\partial x'} + w'_y \frac{\partial w'_x}{\partial y'} + w'_z \frac{\partial w'_x}{\partial z'} = g' - \frac{1}{\rho'} \frac{\partial P'}{\partial x'} + \nu' \left(\frac{\partial^2 w'_x}{\partial x'^2} + \frac{\partial^2 w'_x}{\partial y'^2} + \frac{\partial^2 w'_x}{\partial z'^2} \right) \quad \textbf{(3.18)}$$

$$\frac{w^+}{t^+} = \frac{(w^+)^2}{l^+} = g^+ = \frac{P^+}{\rho^+ l^+} = \frac{\nu^+ w^+}{(l^+)^2} \quad \textbf{(3.19)}$$

The following dimensionless numbers which are shown in equation (3.20) and (3.21) are defined according to the equation (3.19) result.

$$\frac{w^+ l^+}{\nu^+} = 1, \quad Re = \frac{wl}{\nu} = \frac{w'l'}{\nu'} = \text{const.} \quad \textbf{(3.20)}$$

$$Ga = FrRe^2 = \frac{gl^3}{\nu^2} \qquad Gr = Ga\frac{\rho - \rho_0}{\rho} = \frac{gl^3 \beta \Delta T}{\nu^2} \quad \textbf{(3.21)}$$

Energy equation can be written in the following equation (3.22) :

$$\frac{\partial T}{\partial t} + w_x \frac{\partial T}{\partial x} + w_y \frac{\partial T}{\partial y} + w_z \frac{\partial T}{\partial z} = \alpha \left(\frac{\partial^2 T}{\partial x^2} + \frac{\partial^2 T}{\partial y^2} + \frac{\partial^2 T}{\partial z^2} \right) \quad \textbf{(3.22)}$$

In this equation, w is vector describing the fluid velocity, T is temperature and α is referred to as thermal diffusivity. Dimensionless parameters that govern energy equation are shown in equation (3.23) :

$$t^+ = \frac{t'}{t}, T^+ = \frac{T'}{T}, \quad w^+ = \frac{w'_x}{w_x} = \frac{w'_y}{w_y} = \frac{w'_z}{w_z}, \ \alpha^+ = \frac{\alpha'}{\alpha}, \quad l^+ = \frac{x'}{x} = \frac{y'}{y} = \frac{z'}{z} \quad \textbf{(3.23)}$$

Equation of energy for model is shown in equation (3.24) and equation (3.25) is obtained from solution of equation (3.24) with certain assumptions for convection.

$$\frac{\partial T'}{\partial t'} + w'_x \frac{\partial T'}{\partial x'} + w'_y \frac{\partial T'}{\partial y'} + w'_z \frac{\partial T'}{\partial z'} = \alpha' \left(\frac{\partial^2 T'}{\partial x'^2} + \frac{\partial^2 T'}{\partial y'^2} + \frac{\partial^2 T'}{\partial z'^2} \right) \quad \textbf{(3.24)}$$

$$\frac{T^+}{t^+} = \frac{w^+ T^+}{l^+} = \frac{\alpha^+ T^+}{(l^+)^2} \quad \textbf{(3.25)}$$

The following dimensionless numbers which are shown in equation (3.26), (3.27) and (3.28) are defined according to the equation (3.25) result.

$$\frac{w^+ l^+}{\alpha^+} = 1, \quad Pe = \frac{wl}{\alpha} = \frac{w'l'}{\alpha'} = \text{const.} \quad \textbf{(3.26)}$$

$$Pr = \frac{Pe}{Re} = \frac{\nu}{\alpha} \quad \textbf{(3.27)}$$

$$St = \frac{Nu}{RePr} = \frac{\alpha}{\rho c_p w} \quad \textbf{(3.28)}$$

3.2.1 Heat transfer coefficient similarity

Convection boundary layer is necessary to understanding convective heat transfer rate between a surface and a fluid flowing past it.
Heat transfer rate can be written as equation (3.29) :

$$Q_y = h \cdot A \cdot (T_S - T_\infty) \tag{3.29}$$

Heat transfer at the surface by conduction is shown in equation (3.30) :

$$Q_y = -k \cdot A \cdot \frac{\partial(T - T_S)}{\partial y} \tag{3.30}$$

These two terms are equal which is showned in equation (3.31) and dimensionless parameters for this situation are shown in equation (3.32).

$$h \cdot (T_S - T_\infty) = -k \cdot \frac{\partial(T - T_S)}{\partial y} \tag{3.31}$$

$$h^+ = \frac{h'}{h},\ \ T^+ = \frac{T_S'}{T_S} = \frac{T_\infty'}{T_\infty},\ \ k^+ = \frac{k'}{k},\ \ l^+ = \frac{y'}{y} \tag{3.32}$$

Using equation (3.32) into the equation (3.31) , equation (3.33) and (3.34) and are derived and finally get Nusselt number which is shown in equation (3.35) .

$$h' \cdot (T'_S - T'_\infty) = -k' \cdot \frac{\partial(T' - T'_S)}{\partial y'} \tag{3.33}$$

$$h' \cdot T^+ \cdot h \cdot (T_S - T_\infty) = -\frac{k' \cdot T^+}{l^+} \cdot \frac{\partial(T - T_S)}{\partial y} \tag{3.34}$$

$$\frac{h^+ \cdot l^+}{k^+} = 1\,,\quad Nu = \frac{h \cdot l}{k} = \frac{h'l'}{k'} = \text{Const.} \tag{3.35}$$

The process of convection is described by a very complex set of differential equations that a large number of variables and whose analytical solution run into many difficulties. The theory of similarity helps to resolve some of them. In that theory, the terms present in the convection equations can be united in dimensionless groups, for which one selects scales of reduction. The so-called dimensionless numbers are used to characterize and classify convection heat transfer problems enabling us to take our knowledge from experimenting with one scale system to learning about another system with different dimensions. They allow us to experiment with models and predict the behavior of large bodies under actual conditions. All that one has to establish is to make sure that there is similarity between the model and the actual thing.

3.3 Convection

Convection refers to heat transfer that will occur between a surface and a moving or stationary fluid when they are at different temperatures. When heat is to be transferred from one fluid to another through a barrier convection is involved on both sides of the barrier. In most cases the main resistance to heat flow is by convection [17].

Regardless of the particular nature of the convection heat transfer process, the appropriate rate equation, known as Newton's law of cooling is shown in equation (3.36) :

$$q''=h\cdot(T_S-T_\infty) \quad \textbf{(3.36)}$$

Where

q''= is the convective heat flux (W/m^2)

T_S and T_∞ =is proportional to the difference between the surface and fluid temperatures, respectively.(K)

h=is the the proportionality constant term convection heat transfer coefficients (W/m^2K)

Convection heat flux is presumed to be positive if the heat transfer is from the surface $T_S > T_\infty$

and negative if the heat transfer is to the surface $T_S < T_\infty$. There is nothing to keep from us to expressing Newton`s law of cooling as

$q''=h\cdot(T_\infty-T_S)$

which case heat transfer is positive to the surface.

The convection coefficient depends on conditions in the boundary layer, which is influenced by surface geometry, the nature of fluid motion, and an assortment of fluid thermodynamic and transport properties.

Convection heat transfer may be classified according to the nature of the flow. Forced convection is occurred when the flow is caused by external means, such as by a fan, a pump, or atmospheric winds. In contrast, for free (or natural) convection**,** the flow is induced by buoyancy forces, which arise from density differences caused by temperature variations in the fluid [18].

3.3.1 Natural convection

Natural convection is a type of heat transport. In this heat transport type, fluid motion is not generated by any external sources like a pump or fan. Convection currents which is induced by buoyancy forces caused of heat transfer in natural convection . These buoyancy forces occurs differences of density caused by temperature variations in the fluid.

Free convection flow velocities are generally much smaller than forced convection flow velocities, corresponding heat transfer rates are much also smaller but in many thermal systems free convection may provide the largest resistance to heat transfer and therefore plays an important roles in the design or performance of the system [17].

The dimensionless parameters that play the role of the characterizing free convection. Important dimensionless numbers in natural convection are explained below :

Nusselt Number (Nu_L)= Nusselt number (3.37) represents dimensionless temperature gradient at the surface and provide to measure of the convection heat transfer coefficients.

$$Nu_L = \frac{h \cdot L_C}{k} \tag{3.37}$$

Where

L_C = is the characteristic length of the surface of interest (m)

k= is the thermal conductivity of the fluid (W/m·K)

h= is the heat transfer coefficients. (W/m^2·K)

Grashof Number (Gr)= The ratio of the buoyancy force to the viscous force.This dimensionless parameter (3.38) that plays the role of the characterizing free convection flows.

$$Gr = \frac{g \cdot \beta \cdot L_C^3 \cdot \Delta T}{\nu^2} \tag{3.38}$$

The key buoyancy-related parameters are temperature difference, $\Delta T \cdot (T_s - T_\infty)$, or if a heating process , $\Delta T \cdot (T_\infty - T_s)$ and the volumetric thermal expansion coefficient which is shown in equation (3.39).

$$\beta = -\frac{1}{\rho}\left(\frac{\partial \rho}{\partial T}\right)_p \tag{3.39}$$

Volumetric thermal expansion coefficient is a thermodynamic property relating the variation of density with temperature .Volumetric thermal coefficients for ideal gas, ρ=p/R·T ,and it follows that equation (3.40).

$$\beta = -\frac{1}{\rho}\left(\frac{\partial \rho}{\partial T}\right)_p = \frac{1}{\rho}\frac{p}{RT^2} = \frac{1}{T} \quad \mathbf{(3.40)}$$

where T is absolute temperature. For liquids and non-ideal gases, β must be obtained from appropriate tables.

g =is the gravitational acceleration (m/s^2)

L_c= is the characteristic length of the surface of interest (m)

ν =is the kinematic viscosity of the fluid (m^2/s)

Prandtl number(Pr)=Prandtl number (3.41) is a transport property of the fluid and provides a measure of the relative effectiveness of the momentum and energy transport in the hydrodynamic and thermal boundary layers. Ratio of the momentum and thermal diffusivities.

$$Pr = \frac{c_p \cdot \mu}{k} = \frac{\nu}{\alpha} \quad \mathbf{(3.41)}$$

where

c_p=is specific heat capacity of fluid (J/kg·K)

μ=is dynamic viscosity (Pa.s(kg/s.m))

α=is the thermal diffusivity of the fluid (m^2/s)

For free convection flows convection coefficients can be functionally expressed by equations of the form which is shown in equation (3.42).

$$\overline{Nu_L} = f(Gr_L, Pr) \quad \mathbf{(3.42)}$$

The overbar indicates an average over the surface of the immersed geometry of characteristic length L. The most common empirical correlations suitable for engineering calculations have the form which is shown in equation (3.43).

$$\overline{Nu_L} = \frac{\bar{h} \cdot L_c}{k} = c(Ra_L)^n \quad \mathbf{(3.43)}$$

Where the Rayleigh number which is shown in equation (3.44).

$$Ra_L = Gr_L \, Pr = \frac{g \cdot \beta \cdot \Delta T \cdot L_C^3}{\nu \cdot \alpha} \quad \mathbf{(3.44)}$$

Is based on the characteristic length L of the geometry. Typically , n=1/4 and 1/3 for laminar and turbulent flows, respectively.

3.3.1.1 Correlations for vertical plate

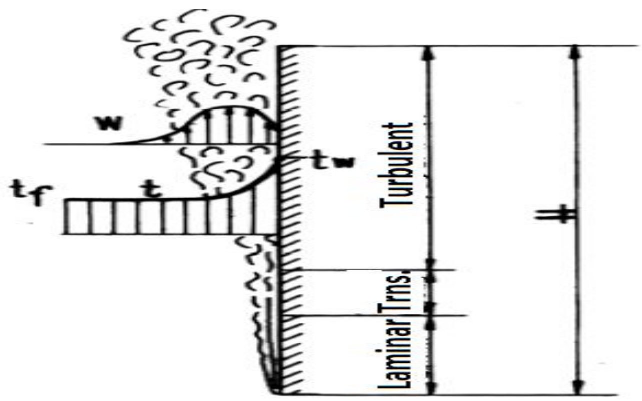

Figure 3. 3: Convection currents on vertical plate [19].

$Nu=C.(Gr.Pr)^n$

C=0.5	and	n=0	$(Gr.Pr)<0.001$	
C=1.8	and	n=1/8	$0.001< (Gr.Pr) < 500$	**$Pr \geq 0.7$**
C=0.54	and	n=1/4	$500< (Gr.Pr) < 20.10^6$	
C=0.135	and	n=1/3	$20.10^6< (Gr.Pr) <10^{13}$	

For shown in Figure 3.3 convection currents on the vertical plate. Nusselt number is calculated from Mihejev formula. The only condition using this formula that Prandtl number has to be higher than 0.7 [19].

3.3.1.2 Correlations for horizantal plate

The buoyancy force is normal to the surface for horizontal plate. The flow patterns and heat transfer rate depend strongly on whether the surface is hot or cold and on whether it is facing upward or downward.

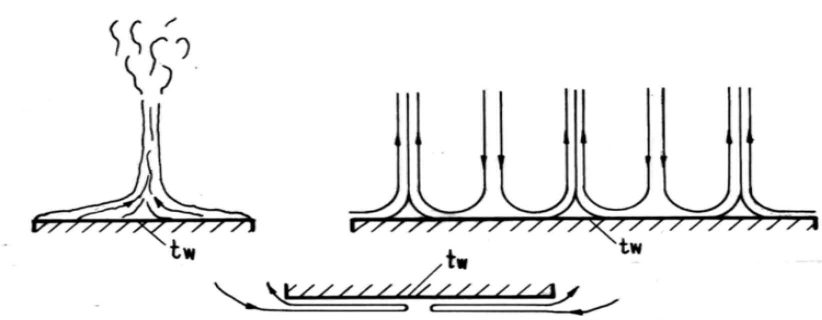

Figure 3. 4: Convection currents on horizontal plates [19].

For horizontal walls may also be used the Mihejev formula. Characteristic length for finding Grashoff number (Gr) and Nusselt Number (Nu) should be taken maximum 0.6 m [19].

The result of Nusselt number has to increase 30 % percent for walls facing hot surface upward and reduced by 30 % for walls facing hot surface downward in this solution [19]. Convection currents on horizontal plates are shown in Figure 3.4.

3.3.2 Forced convection

Forced convection is a type of transport in which fluid motion is generated by an external force (like a pump, fan, suction device, etc). Significant amounts of heat energy can be transported very efficiently.

External Flow

Flow around bodies completely surrounded by a fluid are considered to be external flows. Examples of external flows include flow of air around airplanes, automobiles and buildings or the low of water around submarines and fish. In these situations the object, is completely surrounded by the fluid and the flows are termed external flows.

The Flat Plate in Parallel Flow

Parallel flow over a flat plate occurs in numerous engineering applications. Boundary layer flow conditions are characterized by the Reynolds number. Laminar boundary layer development begins at the leading edge (x=0). Transition to turbulence may occur at a downstream location (x_c) for which the critical Reynolds number is $Re_{xc}=5x10^5$ [17].

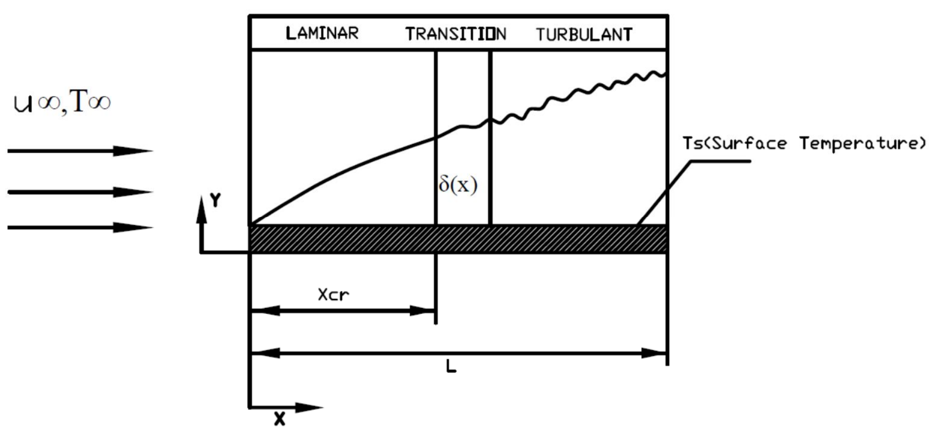

Figure 3. 5: Boundary layers appearance at parallel flow over a flat plate.

Laminar Flow

Motions of the particles of the fluid is very orderly and all particles moving in straight lines in laminar flow.

Reynolds number (3.45) is the ratio of the inertia to viscous forces and is used to determine the boundary layer flow conditions.

$$Re_L = \frac{\text{inertia forces}}{\text{viscous forces}} = \frac{\rho VL}{\mu} = \frac{VL}{\nu} \qquad \mathbf{(3.45)}$$

Where

V=is the mean velocity of the object relative to the fluid (m/s)

L=is a characteristic linear dimension (m)

μ = is the dynamic viscosity of the fluid (Pa·s or N·s/m² or kg/(m·s))

ν =is the kinematic viscosity of the fluid (m^2/s)

ρ= is the density of the fluid (kg/m^3).

According to the Figure 3.5 , Reynolds number can be written in the following formula:

$Re_x = \frac{u_\infty \cdot x}{\nu}$

where

x= is distance from the leading edge and the characteristic length and in the Reynolds number (m)

u_∞=free stream velocity (m/s^2)

The local Nusselt number is of the form which is shown in equation (3.46) :

$$Nu_x = \frac{h_x \cdot x}{k} = 0.332 Re_x^{1/2} Pr^{1/3} \qquad \mathbf{(3.46)}$$

$$[0.6 \le Pr \le 50]$$

h_x=local heat transfer coefficients ($W/m^2 \cdot K$)

In this equation local heat transfer coefficient is used to determine the local Nusselt number. Between average heat transfer coefficients and local heat transfer coefficients is correlated by performing the integration. Hence, the average heat transfer coefficient was calculated to be twice the local heat transfer coefficient [18].

In laminar flow, the average Nusselt number over the entire surfaces is the form which is shown in equation (3.47) :

$$\overline{Nu_x} = \frac{\overline{h_x} \cdot x}{k} = 0.664 Re_x^{1/2} Pr^{1/3} \qquad \mathbf{(3.47)}$$

$$[0.6 \leq Pr \leq 50]$$

$\overline{h_x}$=average heat transfer coefficients [$W/m^2 \cdot K$]

Mixed Flow

In the mixed boundary layer situation average Nusselt number over the entire surfaces is the form which is shown in equation (3.48) and this equation is derived from equation (3.49) using equation (3.50) :

$$\overline{Nu_L} = (0.664Re_{x,c}^{\frac{1}{2}} + 0.037(Re_L^{\frac{4}{5}} - Re_{x,c}^{\frac{4}{5}}))Pr^{\frac{1}{3}} \quad \mathbf{(3.48)}$$

$$\overline{Nu_L} = (0.037\,Re_L^{\frac{4}{5}} - A)Pr^{\frac{1}{3}} \quad \mathbf{(3.49)}$$

Constant A (3.50) is determined by the value of the critical Reynolds number $Re_{x,c}$ and that is:

$$A = 0.037Re_{x,c}^{\frac{4}{5}} - 0.664Re_{x,c}^{\frac{1}{2}} \quad \mathbf{(3.50)}$$

Turbulent Flow

The local Nusselt number is of the form in turbulent flow which is shown in equation (3.51) :

$$Nu_x = \frac{h_x \cdot x}{k} = 0.0296Re_x^{4/5}Pr^{1/3} \quad \mathbf{(3.51)}$$

$$[\, Re_x \leq 10^8 \,,\, 0.6 \leq Pr \leq 60 \,]$$

In turbulent flow, the average Nusselt number over the entire surfaces (3.52) is the form :

$$\overline{Nu_L} = 0.037Re_L^{4/5}Pr^{1/3} \quad \mathbf{(3.52)}$$

$$[\, Re_{x,c}=0 \,,\, 0.6 \leq Pr \leq 50 \,]$$

This equation for turbulent flow is obtained from mixed boundary layer equations. Boundary layer is assumed to be fully turbulent from the leading edge over the entire plate. Hence, critic Reynolds number was put in the place as zero in the mixed boundary layer equation which is showed above and this equation was obtained [17].

4. ANALYSIS OF POSSIBLE SOLUTIONS OF THE CARGO HEATING SYSTEMS

Assumptions of some calculation values are required before progress to cargo heating solutions methods. It has been assumed that heated cargo is from Wenezuela “BACHEQUERO”crude oil that properties are as follows [20]:

Mass density = 965 (kg/m^3)

Viscosity at temperature 20 ^{0}C = 7x10^{-3} (m^2/s)

Specific heat of crude oil = 1.9678 (kJ /kg ^{0}C)

Steam boiler leading companies Alfa Laval and Mitsubishi’s actual boiler characteristics are examined. Considering the similar vessels steam consumptions and actual steam boilers properties, saturated steam of 1.6 MPa [Url-10] will be used for heating.

4.1 Cargo Heating System Shell Solutions

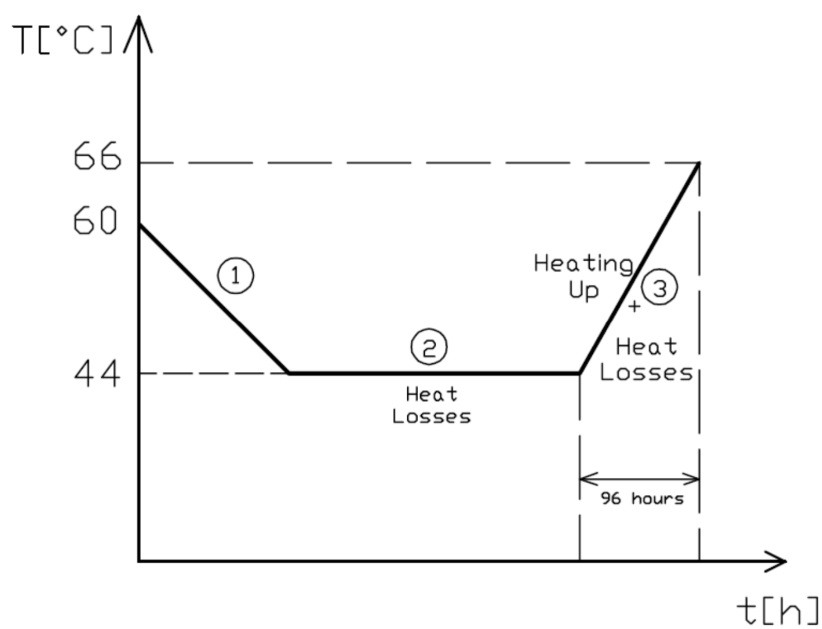

Figure 4. 1: Cargo temperature changes in Shell solutions.

One of the tanker cargo heating system solution is Shell. In this solution's crude oil temperature changes which is showed in Figure 4.1. Shell separate the crude oil temperature changes in three parts as shown in Figure 4.1. Number 1 shows that crude oil is loaded in Aframax tanker at 60 ^{0}C and is waiting until the temperature of the crude oil reach 44 ^{0}C. In number 2, heat losses occur according to heat exchanges from crude oil to environment. This heat losses replace same quantity of heat generation giving to the system for keeping the crude oil temperature at 44 ^{0}C. In number 3,heat losses occur also in this part according to heat transfer from crude oil to the ambient and the cargo is heated from 44 ^{0}C to 66 ^{0}C in the period of 96 hours [20] at the following ambient temperatures :

Winter conditions

Sea Water Temperature = +5 ^{0}C

Air Temperature= +2 ^{0}C

Summer conditions

Sea Water Temperature = +32 ^{0}C

Air Temperature= +40 ^{0}C

Steam consumption for a permanent cargo temperature 44 ^{0}C in tanks is also calculated for the above ambient temperature values.

4.1.1 Shell calculation procedure

4.1.1.1 Calculation of cargo tanks heat losses (Q_s)

- The calculation of heat losses of the heated cargo carried out according to the following formula (4.1) :

$$Q_S = \Sigma_i = k_i \cdot A_i \cdot (T_{ti} - T) \qquad \textbf{(4.1)}$$

Where :

Q_S= Heat losses to surroundings through wall (W)

k= Heat transfer coefficient (W/m^2 ^{0}C)

A_i= Heat transfer area (m^2)

T_{ti}= Temperature outside wall (^{0}C)

T= Temperature inside tank (^{0}C)

Calculation assumption for heat transfer coefficients

Heat transfer coefficients (k) defined for specific parts of the tanker structure surfaces are obtained from a project performed analogously. The calculation of heat losses of the heated cargo carried out according to the following k values [20]:

Double side k=5.9 $W/m^2\ {}^0C$

Double bottom k=5.31 $W/m^2\ {}^0C$

Deck k=8.72 $W/m^2\ {}^0C$

Shell winter condition heat losses for double side

As shown in Figure 4.1, there are two parts which occur heat losses according to the heat exchanges from crude oil to environment. In number 2 heat losses occur while keeping the temperature of crude oil at 44 ${}^0C$. In number 3, heat losses occur while preheating of the crude oil from 44 ${}^0C$ to 66 ${}^0C$. This two heat losses can be defined as follows :

Q_{T1}=Heat losses which is showed as number 2 in figure 4.1(W)-at 44 ${}^0C$

Q_{T2}=Heat losses which is showed as number 3 in figure 4.1(W)-between 44 ${}^0C$ to 66${}^0C$

h_{crda}= crude oil depth in contact with air= 5.1 m

h_{crdw}=crude oil depth from double bottom until the sea water level= 12.5 m

k= heat transfer coefficients for double side wall= 5.9 $W/m^2\ {}^0C$

T_c=Crude oil temperature= 44 ${}^0C$

T_a=Ambient air temperature= 2 ${}^0C$

T_w=Sea water temperature= 5 ${}^0C$

A_1= Double side wall surface area above the sea water=1803.36 m^2

A_2= Double side wall surface area under the sea water= 4420 m^2

Q_1= Double side total heat transfer losses above the sea water= -446873 W

Q_2= Double side total heat transfer losses under the sea water= -1017042 W

Q_{T1}=Heat transfer losses for double side at 44 ${}^0C$ =Q_1+Q_2= -1463915 W

Q_{T2}= Heat transfer losses for double side between 44 ${}^0C$ to 66 ${}^0C$=-1867810 W

Q_T= Total heat transfer losses for double side=Q_{T1}+Q_{T2}=-3331725 W

Double side steel wall contact with air and sea water .Therefore, there will be two different heat transfer losses for double side wall because of the sea water and ambient air temperature differences. Crude oil depth from double bottom until the sea water level and crude oil depth in contact with air values are used to calculate double side surface area. As shown in Table 4.1, heat transfer losses for both parts calculated by using fundamental equation of heat transfer rate. Consequently, the temperature of the crude oil is 44 ^{0}C in number 2 and heat transfer losses in this part is 1463915 W (1464 kW) for double side wall. In addition to this, Q_{T2} was calculated by the same procodure which is illustrated in Table 4.1. Heat transfer losses was calculated for each ^{0}C increment between 44 ^{0}C to 66 ^{0}C and heat transfer losses in this interval (number 3) is calculated by averaging these values. Finally, total heat transfer losses for double side calculated by accumulating Q_{T1} and Q_{T2} and these value is 3331725 W (3332 kW).

Shell winter condition heat losses for deck

A_3= Deck surface area =6647.68 m^2

k= Heat transfer coefficients for deck= 8.72 (W/m^2 ^{0}C)

T_a= Ambient air temperature=2 ^{0}C

Q_{T1}=Heat transfer losses for deck at 44 ^{0}C= -2434646 W (-2435 kW)

Q_{T2}=Heat transfer losses for deck between 44 ^{0}C to 66 ^{0}C=-3072291W (-3072 kW)

Q_T=Total heat transfer losses for deck=Q_{T1}+Q_{T2}= -5506940 W

It is neglected the effect of sea water collecting on the deck. Assumed that the only air contact with the deck. So, there is only air temperature on Table 4.2. As shown in Table 4.2, heat transfer losses for deck calculated by using fundamental equation of heat transfer rate. Consequently, the temperature of the crude oil is 44 ^{0}C in number 2 and heat transfer losses in this part is 2434646 W (2435 kW) for deck. In addition to this, Q_{T2} was calculated by the same procedure which is illustrated in Table 4.2. Heat transfer losses was calculated for each ^{0}C increment between 44 ^{0}C to 66 ^{0}C and heat transfer losses in this interval (number 3) is calculated by averaging these values. Finally, total heat transfer losses for deck are determined by accumulating Q_{T1} and Q_{T2} and these value is 5506937 W (5507 kW).

Shell winter condition heat losses for double bottom

A_4=Double bottom surface area =6647.68 m^2

k=Heat transfer coefficients for double bottom=5.31 (W/m^2 ^{0}C)

T_w=Sea water temperature=5 ^{0}C

Q_{T1}=Heat transfer losses for double bottom= -1376668 W (-1377 kW)

Q_{T2}=Heat transfer losses for double bottom between 44 ^{0}C to 66 ^{0}C= -1764960W (-1765 kW)

Q_T=Total heat transfer losses for double bottom=Q_{T1}+Q_{T2}= -3141628 W (-3142 kW)

Table 4. 1: Shell winter conditions heat transfer losses at 44 ^{0}C for double side wall.

NBR	TANK NAMES	LENGHT [m]	hcrda [m]	hcrdw [m]	A1 [m^2]	A2 [m^2]	k [$W/m^{2\,0}C$]	Tc [^{0}C]	Ta [^{0}C]	Tw [^{0}C]	Q1 [W]	Q2 [W]	QT1 [W]
1	SLOP TANK(P)	4.1	5.1	12.5	21.1	51.6	5.9	44	2	5	-5219.4	-11878.9	-17098
2	SLOP TANK(STRB)	4.1	5.1	12.5	21.1	51.6	5.9	44	2	5	-5219.4	-11878.9	-17098
3	TANK 1(P)	29.0	5.1	12.5	147.7	362.0	5.9	44	2	5	-36599.1	-83296.2	-119895
4	TANK 1(STRB)	29.0	5.1	12.5	147.7	362.0	5.9	44	2	5	-36599.1	-83296.2	-119895
5	TANK 2(P)	29.0	5.1	12.5	147.7	362.0	5.9	44	2	5	-36599.1	-83296.2	-119895
6	TANK 2(STRB)	29.0	5.1	12.5	147.7	362.0	5.9	44	2	5	-36599.1	-83296.2	-119895
7	TANK 3(P)	30.3	5.1	12.5	154.5	378.8	5.9	44	2	5	-38292.5	-87150.4	-125443
8	TANK 3(STRB)	30.3	5.1	12.5	154.5	378.8	5.9	44	2	5	-38292.5	-87150.4	-125443
9	TANK 4(P)	29.6	5.1	12.5	151.2	370.5	5.9	44	2	5	-37458.4	-85252.1	-122710
10	TANK 4(STRB)	29.6	5.1	12.5	151.2	370.5	5.9	44	2	5	-37458.4	-85252.1	-122710
11	TANK 5(P)	30.3	5.1	12.5	154.5	378.8	5.9	44	2	5	-38292.5	-87150.4	-125443
12	TANK 5(STRB)	30.3	5.1	12.5	154.5	378.8	5.9	44	2	5	-38292.5	-87150.4	-125443
13	TANK 6(P)	24.5	5.1	12.5	125.0	306.4	5.9	44	2	5	-30975.2	-70496.9	-101472
14	TANK 6(STRB)	24.5	5.1	12.5	125.0	306.4	5.9	44	2	5	-30975.2	-70496.9	-101472
												QT1[W]=	-1463915

Double bottom contact with sea water and other effects are neglected. As shown in Table 4.3, heat transfer losses for double bottom calculated by using fundamental equation of heat transfer rate. Consequently, the temperature of the crude oil is 44 ^{0}C in number 2 and heat transfer losses in this part is 1376668 W (1376 kW) for double bottom wall.

Table 4. 2: Shell winter conditions heat transfer losses at 44 ^{0}C for deck.

NBR	TANK NAMES	LENGTH [m]	BREADTH [m]	A_3 [m^2]	k [W/m^{2}C]	T_c [^{0}C]	T_a [^{0}C]	Q_{T1} [W]
1	SLOP TANK(P)	4.13	18.80	77.6	8.72	44	2	-28436
2	SLOPTANK(STRB)	4.13	18.80	77.6	8.72	44	2	-28436
3	TANK 1(P)	28.96	18.80	544.4	8.72	44	2	-199399
4	TANK 1(STRB)	28.96	18.80	544.4	8.72	44	2	-199399
5	TANK 2(P)	28.96	18.80	544.4	8.72	44	2	-199399
6	TANK 2(STRB)	28.96	18.80	544.4	8.72	44	2	-199399
7	TANK 3(P)	30.30	18.80	569.6	8.72	44	2	-208625
8	TANK 3(STRB)	30.30	18.80	569.6	8.72	44	2	-208625
9	TANK 4(P)	29.64	18.80	557.2	8.72	44	2	-204081
10	TANK 4(STRB)	29.64	18.80	557.2	8.72	44	2	-204081
11	TANK 5(P)	30.30	18.80	569.6	8.72	44	2	-208625
12	TANK 5(STRB)	30.30	18.80	569.6	8.72	44	2	-208625
13	TANK 6(P)	24.51	18.80	460.8	8.72	44	2	-168759
14	TANK 6(STRB)	24.51	18.80	460.8	8.72	44	2	-168759
						Q_{T1}[W]=		−2434646

Table 4. 3: Shell winter conditions heat transfer losses at 44 ^{0}C for double bottom.

NBR	TANK NAMES	LENGTH [m]	BREADTH [m]	A3 [m^2]	k [W/m^{20}C]	T_c [^{0}C]	T_w [^{0}C]	Q_{T1} [W]
1	SLOP TANK(P)	4.13	18.80	77.6	5.31	44	5	-16079
2	SLOPTANK(STR)	4.13	18.80	77.6	5.31	44	5	-16079
3	TANK 1(P)	28.96	18.80	544.4	5.31	44	5	-112750
4	TANK 1(STRB)	28.96	18.80	544.4	5.31	44	5	-112750
5	TANK 2(P)	28.96	18.80	544.4	5.31	44	5	-112750
6	TANK 2(STRB)	28.96	18.80	544.4	5.31	44	5	-112750
7	TANK 3(P)	30.30	18.80	569.6	5.31	44	5	-117967
8	TANK 3(STRB)	30.30	18.80	569.6	5.31	44	5	-117967
9	TANK 4(P)	29.64	18.80	557.2	5.31	44	5	-115397
10	TANK 4(STRB)	29.64	18.80	557.2	5.31	44	5	-115397
11	TANK 5(P)	30.30	18.80	569.6	5.31	44	5	-117967
12	TANK 5(STRB)	30.30	18.80	569.6	5.31	44	5	-117967
13	TANK 6(P)	24.51	18.80	460.8	5.31	44	5	-95425
14	TANK 6(STRB)	24.51	18.80	460.8	5.31	44	5	-95425
						Q_{T1}[W]		-1376668

In addition to this, Q_{T2} was calculated by the same procedure which is illustrated in Table 4.3. Heat transfer losses was calculated for each 1 ^{0}C increment between 44 ^{0}C to 66 ^{0}C and heat transfer losses in this interval (number 3) is calculated by averaging these values. Finally, total heat transfer losses for double bottom are determined by accumulating Q_{T1} and Q_{T2} and these value is 3141628 W (3142 kW).

Table 4. 4: Shell winter conditions total heat losses for cargo tanks.

	Q_{HL}[W]
Heat Losses For Double Side	-3331725
Heat Losses For Deck	-5506940
Heat Losses For Double Bottom	-3141628
Total Heat Losses[W]	-11980293

Total heat losses for shell winter conditions is the sum of all heat losses which are double side, deck and double bottom heat losses. Total heat loss is 11980295 W (11980 kW) which is shown in Table 4.4.

Shell summer condition heat losses for double side

T_a=Ambient air temperature= 40 ^{0}C

T_w=Sea water temperature=32 ^{0}C

Q_1= Double side total heat transfer losses above the sea water= -42559.3 W

Q_2= Double side total heat transfer losses under the sea water=-312936 W

Q_{T1}=Heat transfer losses for double side at 44 ^{0}C =Q_1+Q_2 = -355495 W

Q_{T2}=Heat transfer losses for double side between 44 ^{0}C to 66 ^{0}C=-759391W(-759 kW)

Q_T=Total heat transfer losses for double side=Q_{T1}+Q_{T2}= -1114886 W(-1115 kW)

As shown in Table 4.5, heat transfer losses for both parts calculated by using fundamental equation of heat transfer rate. Consequently, shell summer condition total heat transfer losses are 1114886 W (1115 kW) for double side wall.

Table 4. 5: Shell summer conditions heat transfer losses at 44 ^{0}C for double side wall.

NBR	TANK NAMES	LENGTH [m]	h_{crda} [m]	h_{crdw} [m]	A_1 [m^2]	A_2 [m^2]	k [$W/m^{20}C$]	T_c [^0C]	T_a [^0C]	T_w [^0C]	Q_1 [W]	Q_2 [W]	Q_{T1} [W]
1	SLOP TANK(P)	4.13	5.1	12.5	21.1	51.6	5.9	44	40	32	-497.1	-3655.1	-4152.1
2	SLOPTANK(STR)	4.13	5.1	12.5	21.1	51.6	5.9	44	40	32	-497.1	-3655.1	-4152.1
3	TANK 1(P)	28.96	5.1	12.5	147.7	362.0	5.9	44	40	32	-3485.6	-25629.6	-29115.2
4	TANK 1(STRB)	28.96	5.1	12.5	147.7	362.0	5.9	44	40	32	-3485.6	-25629.6	-29115.2
5	TANK 2(P)	28.96	5.1	12.5	147.7	362.0	5.9	44	40	32	-3485.6	-25629.6	-29115.2
6	TANK 2(STRB)	28.96	5.1	12.5	147.7	362.0	5.9	44	40	32	-3485.6	-25629.6	-29115.2
7	TANK 3(P)	30.30	5.1	12.5	154.5	378.8	5.9	44	40	32	-3646.9	-26815.5	-30462.4
8	TANK 3(STRB)	30.30	5.1	12.5	154.5	378.8	5.9	44	40	32	-3646.9	-26815.5	-30462.4
9	TANK 4(P)	29.64	5.1	12.5	151.2	370.5	5.9	44	40	32	-3567.5	-26231.4	-29798.9
10	TANK 4(STRB)	29.64	5.1	12.5	151.2	370.5	5.9	44	40	32	-3567.5	-26231.4	-29798.9
11	TANK 5(P)	30.30	5.1	12.5	154.5	378.8	5.9	44	40	32	-3646.9	-26815.5	-30462.4
12	TANK 5(STRB)	30.30	5.1	12.5	154.5	378.8	5.9	44	40	32	-3646.9	-26815.5	-30462.4
13	TANK 6(P)	24.51	5.1	12.5	125.0	306.4	5.9	44	40	32	-2950.0	-21691.4	-24641.4
14	TANK 6(STRB)	24.51	5.1	12.5	125.0	306.4	5.9	44	40	32	-2950.0	-21691.4	-24641.4
												Q_{T1}[W]=	-355495

Shell summer condition heat losses for deck

A_3=Deck surface area =6647.68 m^2

k=Heat transfer coefficients for deck=8.72 ($W/m^{2}\,{}^{0}C$)

T_a=Ambient air temperature=40 ${}^{0}C$

Q_{T1}=Heat transfer losses for deck at 44 ${}^{0}C$= -231871W (-232 kW)

Q_{T2}=Heat transfer losses for deck between 44 ${}^{0}C$ to 66 ${}^{0}C$=-869516W (-869 kW)

Q_T=Total heat transfer losses for deck=Q_{T1}+Q_{T2}= -1101387 W(-1101 kW)

As shown in Table 4.6, heat transfer losses in shell summer conditions for deck calculated by using fundamental equation of heat transfer rate. Consequently,total heat transfer losses are 1101387 W (1101 kW) for deck.

Table 4. 6: Shell summer conditions heat transfer losses at 44 ${}^{0}C$ for deck.

NBR	TANK NAMES	LENGTH [m]	BREADTH [m]	A_3 [m^2]	k [$W/m^{2}\,{}^{0}C$]	T_c [${}^{0}C$]	T_a [${}^{0}C$]	Q_{T1} [W]
1	SLOP TANK(P)	4.13	18.80	77.6	8.72	44	40	-2708
2	SLOPTANK(STR)	4.13	18.80	77.6	8.72	44	40	-2708
3	TANK 1(P)	28.96	18.80	544.4	8.72	44	40	-18990
4	TANK 1(STRB)	28.96	18.80	544.4	8.72	44	40	-18990
5	TANK 2(P)	28.96	18.80	544.4	8.72	44	40	-18990
6	TANK 2(STRB)	28.96	18.80	544.4	8.72	44	40	-18990
7	TANK 3(P)	30.30	18.80	569.6	8.72	44	40	-19869
8	TANK 3(STRB)	30.30	18.80	569.6	8.72	44	40	-19869
9	TANK 4(P)	29.64	18.80	557.2	8.72	44	40	-19436
10	TANK 4(STRB)	29.64	18.80	557.2	8.72	44	40	-19436
11	TANK 5(P)	30.30	18.80	569.6	8.72	44	40	-19869
12	TANK 5(STRB)	30.30	18.80	569.6	8.72	44	40	-19869
13	TANK 6(P)	24.51	18.80	460.8	8.72	44	40	-16072
14	TANK 6(STRB)	24.51	18.80	460.8	8.72	44	40	-16072
						Q_{T1}[W]=		-231871

Shell summer condition heat losses for double bottom

A_4=Deck surface area =6647.68 m^2

k=Heat transfer coefficients for double bottom=5.31 [$W/m^{2}\,{}^{0}C$]

T_w=Sea water temperature=32 ${}^{0}C$

Q_{T1}=Heat transfer losses for double bottom at 44 ${}^{0}C$= -423590 W (-423 kW)

Q_{T2}=Heat transfer losses for double bottom between 44 ${}^{0}C$ to 66 ${}^{0}C$=-811881W(-812 kW)

Q_T=Total heat transfer losses for double bottom=Q_{T1}+Q_{T2}= -1235471 W(-1235 kW)

As shown in Table 4.7, heat transfer losses for double bottom calculated by using fundamental equation of heat transfer rate. Consequently total heat transfer losses are 1235471 W (1235 kW) for double bottom.

Table 4. 7: Shell summer conditions heat transfer losses at 44 ^{0}C for double bottom.

NBR	TANK NAMES	LENGTH [m]	BREADTH [m]	A_3 [m^2]	k [$W/m^{2 0}C$]	T_c [^{0}C]	T_w [^{0}C]	Q_{T1} [W]
1	SLOP TANK(P)	4.13	18.80	77.6	5.31	44	32	-4947
2	SLOPTANK(STRB)	4.13	18.80	77.6	5.31	44	32	-4947
3	TANK 1(P)	28.96	18.80	544.4	5.31	44	32	-34692
4	TANK 1(STRB)	28.96	18.80	544.4	5.31	44	32	-34692
5	TANK 2(P)	28.96	18.80	544.4	5.31	44	32	-34692
6	TANK 2(STRB)	28.96	18.80	544.4	5.31	44	32	-34692
7	TANK 3(P)	30.30	18.80	569.6	5.31	44	32	-36297
8	TANK 3(STRB)	30.30	18.80	569.6	5.31	44	32	-36297
9	TANK 4(P)	29.64	18.80	557.2	5.31	44	32	-35507
10	TANK 4(STRB)	29.64	18.80	557.2	5.31	44	32	-35507
11	TANK 5(P)	30.30	18.80	569.6	5.31	44	32	-36297
12	TANK 5(STRB)	30.30	18.80	569.6	5.31	44	32	-36297
13	TANK 6(P)	24.51	18.80	460.8	5.31	44	32	-29361
14	TANK 6(STRB)	24.51	18.80	460.8	5.31	44	32	-29361
						Q_{T1}[W]		-423590

Table 4. 8: Shell summer conditions total heat losses for cargo tank.

	Q_{HL}[W]
Heat Losses For Double Side	-1114886
Heat Losses For Deck	-1101387
Heat Losses For Double Bottom	-1235471
Total Heat Losses[W]	-3451744

Total heat losses for shell summer conditions is the sum of all heat losses which are double side, deck and double bottom heat losses. Total heat loss is 3451744 W (3452 kW) which is shown in Table 4.8. As a result of all these calculation, shell winter heat loss is approximately 3.45 times more than shell summer heat loss.

4.1.1.2 Calculation of quantity of heat

- Calculation of quantity of heat needed to cargo preheating in a given period of time which is shown in equation (4.2) :

$$Q_P = \frac{G_k \cdot C_{p_t} \cdot \Delta T}{\tau} \qquad (4.2)$$

Where :

Q_P=Quantity of heat needed to cargo preheating (kW)

G_k=mass of cargo (kg)

C_{pt} =specific heat of cargo (kJ/kg ^{0}C)

ΔT=Difference of temperatures which we are heating cargo for ^{0}C

τ =Period of time (h)

As shown in Table 4.9, Shell quantity of heat needed to cargo preheating from 44 ^{0}C to 66 ^{0}C is calculated and as a result of this calculation both summer and winter conditions quantity of heat needed for preheating are the same which is (Q_p)14143 kW.

Table 4. 9: Calculation of Shell quantity of heat needed to cargo preheating.

NBR	TANK NAMES	Tank Capacity [m^3]	Density [kg/m^3]	Mass [kg]	Specific Heat [kJ/kg ^{0}C]	Δt [^{0}C]	Time [h]	Q_P [kW]
1	SLOP TANK(P)	1366.5	965	1318705.7	1.9678	22	96	165.2
2	SLOPTANK(STRB)	1366.5	965	1318705.7	1.9678	22	96	165.2
3	TANK 1(P)	9582.3	965	9246904.8	1.9678	22	96	1158.3
4	TANK 1(STRB)	9582.3	965	9246904.8	1.9678	22	96	1158.3
5	TANK 2(P)	9582.3	965	9246904.8	1.9678	22	96	1158.3
6	TANK 2(STRB)	9582.3	965	9246904.8	1.9678	22	96	1158.3
7	TANK 3(P)	10025.7	965	9674765.8	1.9678	22	96	1211.9
8	TANK 3(STRB)	10025.7	965	9674765.8	1.9678	22	96	1211.9
9	TANK 4(P)	9807.3	965	9464028.3	1.9678	22	96	1185.5
10	TANK 4(STRB)	9807.3	965	9464028.3	1.9678	22	96	1185.5
11	TANK 5(P)	10025.7	965	9674765.8	1.9678	22	96	1211.9
12	TANK 5(STRB)	10025.7	965	9674765.8	1.9678	22	96	1211.9
13	TANK 6(P)	8110.3	965	7826424.8	1.9678	22	96	980.4
14	TANK 6(STRB)	8110.3	965	7826424.8	1.9678	22	96	980.4
							Q_P[kW]=	14143.1

4.2 Cargo Heating System Spirax Sarco Solution

Solution of Spirax Sarco and its values which they accept quite different than solution of Shell. Spirax Sarco have another approach to calculate quantity of heat for preheating. In this solution, quantity of heat needed for preheating is resolved by using heating speed which is 2.5 ^{0}C/24h and cargo is heated starting from 43 ^{0}C [20]. Spirax Sarco solution takes into account of thermal losses at 43 ^{0}C in the heating process and thermal losses higher than 43 ^{0}C in the heating process are neglected by Spirax Sarco solution. Method of calculation of heat losses is same. The only difference is different heat transfer coefficients values for calculation of heat losses. The calculation of heat losses of the heated cargo carried out according to the following k values which are shown in Figure 4.2 [20] :

Double Side Contact With Sea Water	7.1 $W/m^2\,^0C$
Double Side Contact With Air	7.1 $W/m^2\,^0C$
Deck	8.5 $W/m^2\,^0C$
Double Bottom	7.1 $W/m^2\,^0C$

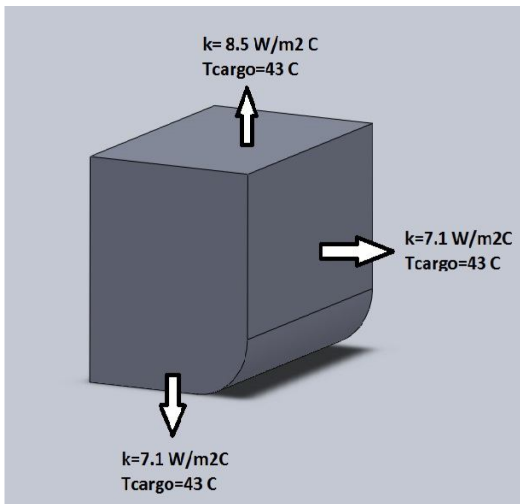

Figure 4. 2: Heat transfer coefficients for Spirax Sarco.

4.2.1 Spirax Sarco calculation procedure

4.2.1.1 Calculation of heat losses of the cargo (Q_s)

Calculation of heat losses procedure is same as Shell solution which is mentioned in part 4.1.1 . Winter and summer conditions sea water and air temperature are taken same values as Shell solutions.

Spirax Sarco winter conditions heat losses for double side

h_{crda}= crude oil height in contact with air= 5.1 m

h_{crdw}=crude oil height from double bottom until the sea water level=12.5 m

k_{ads}= heat transfer coefficients in contact with the air part for double side wall= 8.5 $W/m^2\,^0C$

k_{wds}= heat transfer coefficients in contact with the sea water part for double side wall= 7.1 $W/m^2\,^0C$

T_c=Crude oil temperature=43 ^{0}C

T_a=Ambient air temperature=2 ^{0}C

T_w=Sea water temperature=5 ^{0}C

Q_1= Double side total heat transfer losses above the sea water= -628471 W

Q_2= Double side total heat transfer losses under the sea water=-1192516 W

Q_{T1}=Total heat transfer losses for double side at 43 ^{0}C = Q_1+Q_2 = -1820987 W

As shown in Table 4.10, heat transfer losses for both parts calculated by using fundamental equation of heat transfer rate. Consequently total heat transfer losses are 1820987 W (1821 kW) for double side wall.

Spirax Sarco winter condition heat losses for deck

Table 4. 10: Spirax Sarco winter conditions heat transfer losses at 43 ^{0}C for deck.

NBR	TANK NAMES	LENGTH [m]	BREADTH [m]	A3 [m^2]	kad [W/m^{2}C]	Tc [^{0}C]	Ta [^{0}C]	QT1[W]
1	SLOP TANK(P)	4.13	18.80	77.6	8.5	43	2	-27058.9
2	SLOPTANK(STRB)	4.13	18.80	77.6	8.5	43	2	-27058.9
3	TANK 1(P)	28.96	18.80	544.4	8.5	43	2	-189740
4	TANK 1(STRB)	28.96	18.80	544.4	8.5	43	2	-189740
5	TANK 2(P)	28.96	18.80	544.4	8.5	43	2	-189740
6	TANK 2(STRB)	28.96	18.80	544.4	8.5	43	2	-189740
7	TANK 3(P)	30.30	18.80	569.6	8.5	43	2	-198520
8	TANK 3(STRB)	30.30	18.80	569.6	8.5	43	2	-198520
9	TANK 4(P)	29.64	18.80	557.2	8.5	43	2	-194195
10	TANK 4(STRB)	29.64	18.80	557.2	8.5	43	2	-194195
11	TANK 5(P)	30.30	18.80	569.6	8.5	43	2	-198520
12	TANK 5(STRB)	30.30	18.80	569.6	8.5	43	2	-198520
13	TANK 6(P)	24.51	18.80	460.8	8.5	43	2	-160585
14	TANK 6(STRB)	24.51	18.80	460.8	8.5	43	2	-160585
							QTHL[W]=	-2316716

A_3=Deck surface area =6647.68 m^2

k_{ad}=Heat transfer coefficients for deck=8.5 (W/m$^{2\,0}$C)

T_a=Ambient air temperature=2 ^{0}C

Q_{T1}= Total heat transfer losses for deck at 43 ^{0}C = -2316716 W (-2317 kW)

Neglected the effect of sea water collecting on the deck. Assumed that the only air contact with the deck. So, there is only air temperature on Table 4.11. As shown in Table 4.11, heat transfer losses for deck calculated by using fundamental equation of heat transfer rate. Consequently total heat transfer losses are 2316716 W (2316 kW) for deck.

Table 4. 11: Spirax Sarco winter conditions heat transfer losses at 43 ^{0}C for double side wall.

NBR	TANK NAMES	LENGTH [m]	h_{crda} [m]	h_{crdw} [m]	A_1 [m^2]	A_2 [m^2]	kwds [W/m^2C]	kads [W/m^2C]	Tc [^0C]	Ta [^0C]	Tw [^0C]	Q_1 [W]	Q_2 [W]	Q_{T1} [W]
1	SLOP TANK(P)	4.13	5.1	12.5	21.1	51.6	7.1	8.5	43	2	5	-7340.5	-13928.4	-21268.9
2	SLOP TANK(STRB)	4.13	5.1	12.5	21.1	51.6	7.1	8.5	43	2	5	-7340.5	-13928.4	-21268.9
3	TANK 1(P)	28.96	5.1	12.5	147.7	362.0	7.1	8.5	43	2	5	-51472.1	-97667.6	-149140
4	TANK 1(STRB)	28.96	5.1	12.5	147.7	362.0	7.1	8.5	43	2	5	-51472.1	-97667.6	-149140
5	TANK 2(P)	28.96	5.1	12.5	147.7	362.0	7.1	8.5	43	2	5	-51472.1	-97667.6	-149140
6	TANK 2(STRB)	28.96	5.1	12.5	147.7	362.0	7.1	8.5	43	2	5	-51472.1	-97667.6	-149140
7	TANK 3(P)	30.30	5.1	12.5	154.5	378.8	7.1	8.5	43	2	5	-53853.7	-102187	-156040
8	TANK 3(STRB)	30.30	5.1	12.5	154.5	378.8	7.1	8.5	43	2	5	-53853.7	-102187	-156040
9	TANK 4(P)	29.64	5.1	12.5	151.2	370.5	7.1	8.5	43	2	5	-52680.7	-99960.9	-152642
10	TANK 4(STRB)	29.64	5.1	12.5	151.2	370.5	7.1	8.5	43	2	5	-52680.7	-99960.9	-152642
11	TANK 5(P)	30.30	5.1	12.5	154.5	378.8	7.1	8.5	43	2	5	-53853.7	-102187	-156040
12	TANK 5(STRB)	30.30	5.1	12.5	154.5	378.8	7.1	8.5	43	2	5	-53853.7	-102187	-156040
13	TANK 6(P)	24.51	5.1	12.5	125.0	306.4	7.1	8.5	43	2	5	-43562.8	-82660	-126223
14	TANK 6(STRB)	24.51	5.1	12.5	125.0	306.4	7.1	8.5	43	2	5	-43562.8	-82660	-126223
													Q_{T1}[W]=	-1820987

Spirax Sarco winter condition heat losses for double bottom

A_3= Double bottom surface area =6647.68 m^2

k_{db}= Heat transfer coefficients for double bottom=7.1 ($W/m^{2\,0}C$)

T_w= Sea water temperature=5 ^0C

Q_{T1}=Total heat transfer losses for double bottom at 43 ^0C = -1793544 W (-1794 kW)

Double bottom contact with sea water and other effects are neglected. As shown in Table 4.12, heat transfer losses for double bottom calculated by using fundamental equation of heat transfer rate. Consequently total heat transfer losses are 1793544 W (1794 kW) for double bottom.

Table 4. 12: Spirax Sarco winter conditions heat transfer losses at 43 ^0C for double bottom.

NBR	TANK NAMES	LENGTH [m]	BREADTH [m]	A_3 [m^2]	kwdb [W/m^2C]	Tc [^0C]	Tw [^0C]	Q_{T1}[W]
1	SLOP TANK(P)	4.13	18.80	77.6	7.1	43	5	-20948.4
2	SLOPTANK(STRB)	4.13	18.80	77.6	7.1	43	5	-20948.4
3	TANK 1(P)	28.96	18.80	544.4	7.1	43	5	-146892
4	TANK 1(STRB)	28.96	18.80	544.4	7.1	43	5	-146892
5	TANK 2(P)	28.96	18.80	544.4	7.1	43	5	-146892
6	TANK 2(STRB)	28.96	18.80	544.4	7.1	43	5	-146892
7	TANK 3(P)	30.30	18.80	569.6	7.1	43	5	-153689
8	TANK 3(STRB)	30.30	18.80	569.6	7.1	43	5	-153689
9	TANK 4(P)	29.64	18.80	557.2	7.1	43	5	-150341
10	TANK 4(STRB)	29.64	18.80	557.2	7.1	43	5	-150341
11	TANK 5(P)	30.30	18.80	569.6	7.1	43	5	-153689
12	TANK 5(STRB)	30.30	18.80	569.6	7.1	43	5	-153689
13	TANK 6(P)	24.51	18.80	460.8	7.1	43	5	-124321
14	TANK 6(STRB)	24.51	18.80	460.8	7.1	43	5	-124321
						QT1[W]		-1793544

Table 4. 13: Spirax Sarco winter conditions total heat losses for cargo tank.

	Q_{HL}**[W]**
Heat Losses For Double Side	-1820987
Heat Losses For Deck	-2316716
Heat Losses For Double Bottom	-1793544
Total Heat Losses[W]	-5931247

Total heat losses for spirax sarco winter conditions is the sum of all heat losses which are double side, deck and double bottom heat losses. Total heat loss is 5931247 W (5931 kW) which is shown in Table 4.13.

Spirax Sarco summer conditions heat losses for double side

T_a=Ambient air temperature=40^0C

T_w=Sea water temperature=32 ^{0}C

Q_1= Double side total heat transfer losses above the sea water= - 38500W

Q_2= Double side total heat transfer losses under the sea water=- 345202W

Q_{T1}=Total heat transfer losses at 43 ^{0}C for double side=Q_1+Q_2 = -383702 W

As shown in Table 4.14, heat transfer losses for both parts calculated by using fundamental equation of heat transfer rate. Consequently total heat transfer losses are 383702 W (384 kW) for double side wall.

Spirax Sarco summer conditions heat losses for deck

Table 4. 14: Spirax Sarco summer conditions heat transfer losses at 43 ^{0}C for deck.

NBR	TANK NAMES	LENGTH [m]	BREADTH [m]	A_3 [m^2]	k_d [W/m^2C]	T_c [C]	T_a [C]	Q_{T1} [W]
1	SLOP TANK(P)	4.13	18.80	77.6	8.5	43	40	-1979.9
2	SLOPTANK(STRB)	4.13	18.80	77.6	8.5	43	40	-1979.9
3	TANK 1(P)	28.96	18.80	544.4	8.5	43	40	-13883.4
4	TANK 1(STRB)	28.96	18.80	544.4	8.5	43	40	-13883.4
5	TANK 2(P)	28.96	18.80	544.4	8.5	43	40	-13883.4
6	TANK 2(STRB)	28.96	18.80	544.4	8.5	43	40	-13883.4
7	TANK 3(P)	30.30	18.80	569.6	8.5	43	40	-14525.8
8	TANK 3(STRB)	30.30	18.80	569.6	8.5	43	40	-14525.8
9	TANK 4(P)	29.64	18.80	557.2	8.5	43	40	-14209.4
10	TANK 4(STRB)	29.64	18.80	557.2	8.5	43	40	-14209.4
11	TANK 5(P)	30.30	18.80	569.6	8.5	43	40	-14525.8
12	TANK 5(STRB)	30.30	18.80	569.6	8.5	43	40	-14525.8
13	TANK 6(P)	24.51	18.80	460.8	8.5	43	40	-11750.1
14	TANK 6(STRB)	24.51	18.80	460.8	8.5	43	40	-11750.1
							Q_{T1}[W]=	-169516

k_d=Heat transfer coefficients for deck=8.5 [W/m^{2} ^{0}C]

T_a=Ambient air temperature=40 ^{0}C

Q_{T1}=Heat transfer losses at 43 ^{0}C for deck= -169516 W (-169 kW)

Neglected the effect of sea water collecting on the deck. Assumed that the only air contact with the deck. So, there is only air temperature on Table 4.15. As shown in Table 4.15, heat transfer losses for deck calculated by using fundamental equation of heat transfer rate. Consequently total heat transfer losses are 169516 W (169 kW) for deck.

Table 4. 15: Spirax Sarco summer conditions heat transfer losses at 43 ^{0}C for double side.

NBR	TANK NAMES	LENGTH [m]	hcrda [m]	hcrdw [m]	A_1 [m^2]	A_2 [m^2]	kwds [W/m^2C]	kads [W/m^2C]	Tc [^0C]	Ta [^0C]	Tw [^0C]	Q_1 [W]	Q_2 [W]	Q_1 [W]
1	SLOP TANK(P)	4.13	5.1	12.5	21.1	51.6	7.1	8.5	43	40	32	-537.1	-4031.9	-4569.0
2	SLOPTANK(STRB)	4.13	5.1	12.5	21.1	51.6	7.1	8.5	43	40	32	-448.6	-4031.9	-4480.6
3	TANK 1(P)	28.96	5.1	12.5	147.7	362.0	7.1	8.5	43	40	32	-3145.9	-28272.2	-31418.1
4	TANK 1(STRB)	28.96	5.1	12.5	147.7	362.0	7.1	8.5	43	40	32	-3145.9	-28272.2	-31418.1
5	TANK 2(P)	28.96	5.1	12.5	147.7	362.0	7.1	8.5	43	40	32	-3145.9	-28272.2	-31418.1
6	TANK 2(STRB)	28.96	5.1	12.5	147.7	362.0	7.1	8.5	43	40	32	-3145.9	-28272.2	-31418.1
7	TANK 3(P)	30.30	5.1	12.5	154.5	378.8	7.1	8.5	43	40	32	-3291.5	-29580.4	-32871.9
8	TANK 3(STRB)	30.30	5.1	12.5	154.5	378.8	7.1	8.5	43	40	32	-3291.5	-29580.4	-32871.9
9	TANK 4(P)	29.64	5.1	12.5	151.2	370.5	7.1	8.5	43	40	32	-3219.8	-28936.1	-32155.8
10	TANK 4(STRB)	29.64	5.1	12.5	151.2	370.5	7.1	8.5	43	40	32	-3219.8	-28936.1	-32155.8
11	TANK 5(P)	30.30	5.1	12.5	154.5	378.8	7.1	8.5	43	40	32	-3291.5	-29580.4	-32871.9
12	TANK 5(STRB)	30.30	5.1	12.5	154.5	378.8	7.1	8.5	43	40	32	-3291.5	-29580.4	-32871.9
13	TANK 6(P)	24.51	5.1	12.5	125.0	306.4	7.1	8.5	43	40	32	-2662.5	-23927.9	-26590.4
14	TANK 6(STRB)	24.51	5.1	12.5	125.0	306.4	7.1	8.5	43	40	32	-2662.5	-23927.9	-26590.4
													Q_{T1}[W]=	-383702

Spirax Sarco summer conditions heat losses for double bottom

A_3=Deck surface area =6647.68 m^2

k_{db}=Heat transfer coefficients for double bottom=7.1 [$W/m^2\,^0C$]

T_w=Sea water temperature=32 ^0C

Q_{T1}=Heat transfer losses at 43 ^0C for double bottom = -519184 W (-519 kW)

As shown in Table 4.16, heat transfer losses for double bottom calculated by using fundamental equation of heat transfer rate. Consequently total heat transfer losses are 519184 W (519 kW) for double bottom.

Table 4. 16: Spirax Sarco summer conditions heat losses at 43 ^0C for double bottom.

NBR	TANK NAMES	LENGTH [m]	BREADTH [m]	A_3 [m^2]	k_{db} [W/m^2C]	Tc [^0C]	Tw [^0C]	Q_{T1} [W]
1	SLOP TANK(P)	4.13	18.80	77.6	7.1	43	32	-6064.0
2	SLOPTANK(STRB)	4.13	18.80	77.6	7.1	43	32	-6064.0
3	TANK 1(P)	28.96	18.80	544.4	7.1	43	32	-42521.4
4	TANK 1(STRB)	28.96	18.80	544.4	7.1	43	32	-42521.4
5	TANK 2(P)	28.96	18.80	544.4	7.1	43	32	-42521.4
6	TANK 2(STRB)	28.96	18.80	544.4	7.1	43	32	-42521.4
7	TANK 3(P)	30.30	18.80	569.6	7.1	43	32	-44488.9
8	TANK 3(STRB)	30.30	18.80	569.6	7.1	43	32	-44488.9
9	TANK 4(P)	29.64	18.80	557.2	7.1	43	32	-43519.8
10	TANK 4(STRB)	29.64	18.80	557.2	7.1	43	32	-43519.8
11	TANK 5(P)	30.30	18.80	569.6	7.1	43	32	-44488.9
12	TANK 5(STRB)	30.30	18.80	569.6	7.1	43	32	-44488.9
13	TANK 6(P)	24.51	18.80	460.8	7.1	43	32	-35987.5
14	TANK 6(STRB)	24.51	18.80	460.8	7.1	43	32	-35987.5
							Q_{T1}[W]	-519183.8

Table 4. 17: Spirax Sarco summer conditions heat losses at 43 ^0C for cargo tank

	Q_{HL}[W]
Heat Losses For Double Side	-383702
Heat Losses For Deck	-169516
Heat Losses For Double Bottom	-519184
Total Heat Losses[W]	-1072402

Total heat losses for spirax sarco summer conditions is the sum of all heat losses which are double side, deck and double bottom heat losses. Total heat loss is 1072402 W (1072 Kw) which is shown in Table 4.17.

As a result of all these calculation, spirax sarco winter heat loss is approximately 5.5 times more than spirax sarco summer heat loss.

4.2.1.2 Calculation of quantity of heat

- Calculation of quantity of heat needed to cargo preheating in a given period of time which is whown in equation (4.3) [20] :

$$Q_p = W \cdot S \cdot V_{heat} \tag{4.3}$$

W=Mass of cargo (kg)

S=Specific heat of cargo (kJ/kg ^{0}C)

V_{heat}=Heating Speed (1^{0}C/24h or 1^{0}C/24x3600s)

Q_P=Quantity of heat for preheating (kW)

Table 4. 18: Calculation of Spirax Sarco quantity of heat needed to cargo preheating.

NBR	TANK NAMES	Tank Capacity [m^3]	Density [kg/m^3]	Mass [kg]	S [kJ/kg^{0}C]	V_{heat} [^{0}C/24h]	V_{heat} [^{0}C/s]	Qp [kW]
1	SLOP TANK(P)	1348.82	965	1301616.1	2.1000	2.5	2.89352E-05	79.1
2	SLOPTANK(STR	1348.82	965	1301616.1	2.1000	2.5	2.89352E-05	79.1
3	TANK 1(P)	9458.10	965	9127070.7	2.1000	2.5	2.89352E-05	554.6
4	TANK 1(STRB)	9458.10	965	9127070.7	2.1000	2.5	2.89352E-05	554.6
5	TANK 2(P)	9458.10	965	9127070.7	2.1000	2.5	2.89352E-05	554.6
6	TANK 2(STRB)	9458.10	965	9127070.7	2.1000	2.5	2.89352E-05	554.6
7	TANK 3(P)	9895.74	965	9549386.8	2.1000	2.5	2.89352E-05	580.3
8	TANK 3(STRB)	9895.74	965	9549386.8	2.1000	2.5	2.89352E-05	580.3
9	TANK 4(P)	9680.19	965	9341380.3	2.1000	2.5	2.89352E-05	567.6
10	TANK 4(STRB)	9680.19	965	9341380.3	2.1000	2.5	2.89352E-05	567.6
11	TANK 5(P)	9895.74	965	9549386.8	2.1000	2.5	2.89352E-05	580.3
12	TANK 5(STRB)	9895.74	965	9549386.8	2.1000	2.5	2.89352E-05	580.3
13	TANK 6(P)	8763.30	965	8456584.5	2.1000	2.5	2.89352E-05	513.9
14	TANK 6(STRB)	8763.30	965	8456584.5	2.1000	2.5	2.89352E-05	513.9
							Qp[kW]=	6860.5

As shown in Table 4.18, Spirax Sarco quantity of heat needed to cargo preheating from 43 ^{0}C to adequate temperature to pump cargo out is calculated and as a result of this calculation both summer and winter conditions quantity of heat needed for preheating are the same which is (Q_p) 6860 kW.

4.3 Quantity of Heat Requirement Comparison For Shell and Spirax Sarco Solution

Referring to Table 4.19 and Table 4.20, Shell cargo heating system solution requires more quantity of heat than Spirax Sarco solution. In Shell solution, cargo is heated starting temperature 44 ^{0}C until the cargo temperature reach 66 ^{0}C in 96 hours before the journey finish whereas in Spirax Sarco solution, cargo is heated starting temperature 43 ^{0}C until the adequate temperature to pump cargo out. Spirax sarco solution requires more hours than Shell solution to heat up cargo due to the heat speed. In Spirax Sarco, temperature of the cargo is increased 2.5 ^{0}C in 24 hours thereby, it takes more time to heat up cargo. Heating power in Shell solution is much more than in Spirax Sarco solution but fuel consumption vary according to the length of the journey and this will be examined in following chapter.

Table 4. 19: Shell quantity of heat requirement for winter and summer conditions.

QUANTITY OF HEAT [kW]					
SHELL CONDITIONS			**SUMMER CONDITIONS**		
Cont. Heating 44 ^{0}C [kW]	**Preheating** 44 ^{0}C-66 ^{0}C [kW]	**Preheating Losses** (44-66 ^{0}C) [kW]	**Cont. Heating** 44 ^{0}C [kW]	**Preheating** 44 ^{0}C-66 ^{0}C [kW]	**Preheating Losses** (44-66 ^{0}C) [kW]
-5231.230	-14143.049	-6705.060	-1010.960	-14143.049	-2440.790
Qmax = -20848.109 kW			**Qmax**= -16583.839 kW		

Table 4. 20: Spirax Sarco quantity of heat requirement for winter and summer conditions.

QUANTITY OF HEAT [kW]			
SPIRAX SARCO CONDITIONS		**SUMMER CONDITIONS**	
Cont. Heating 43 ^{0}C [kW]	**Preheating** 2.5 ^{0}C/24h [kW]	**Cont. Heating** 43 ^{0}C [kW]	**Preheating** 2.5 ^{0}C/24h [kW]
-5931.250	-6860.546	-1072.400	-6860.546
Qmax = **-** 12791.796 kW		**Qmax**= -7932.946 kW	

4.4 Calculation of Steam Consumption

Quantity of heat requirement is necessary to calculate steam consumption for the cargo heating solutions. This heat requirements (Q_S, Q_P) are calculated in the previous part. Steam consumption is calculated by the following formula (4.4) and (4.5) :

$$G_{ps} = \frac{Q_S}{r} \tag{4.4}$$

$$G_{pg} = \frac{Q_p}{r} \tag{4.5}$$

$G_P=G_{ps}+G_{pg}$

Where;

G_{ps}=Quantity of steam needed to cover losses (kg/h)

G_{pg}=Quantity of steam needed for cargo preheating (kg/h)

G_P= Steam consumption (kg/h)

r= Steam evaporation heat (kJ/kg)

Q_S= Quantity of heat needed to cover heat losses (kW)

Q_P= Quantity of heat needed to cargo preheating (kW)

4.4.1 Shell solution steam consumption

Shell solution steam consumption in phase 2 is shown in Table 4.21.

Table 4. 21 Shell solution steam consumption in phase 2

SHELL CONDITIONS	Cont.Heating 44 ^{0}C [kW]	Steam Evoparation Heat [kJ/kg]	G_{ps} [kg/h]	G_{pg} [kg/h]	G_p [kg/h]
Shell Conditions	5231.23	1933.19	9741.63	0	9741.63
Shell Summer Cond.	1010.96	1933.19	1882.62	0	1882.62

Steam evaporation heat is calculated in the following formula according to the saturated steam table :

$h_{fg}=h_g-h_f$ (kJ/kg)

h_g=specific enthalpy of saturated steam at 16 bar (2791.73 kJ /kg)

h_f=specific enthalpy of liquid water at 16 bar (858.54 kJ /kg)

h_{fg}=latent heat of evaporation (energy required to transform saturated water into dry saturated steam) (kJ/kg)

h_{fg}=2791.73-858.54= 1933.19 kJ/kg

Q_s=5231.23 kW (Quantity of heat to cover heat losses at 44 ^{0}C in shell winter conditions)

$$G_{ps} = \frac{Q_S}{r} = \frac{5231.23 * 3600}{1933.19} = 9741.63 \frac{kg}{h}$$

$$G_{pg} = \frac{Q_p}{r} = \frac{0 * 3600}{1933.19} = 0 \frac{kg}{h}$$

G_P=G_{ps}+G_{pg}=9741.63+0= 9741.63 (kg/h)

This is the steam consumption for covering heat looses from cargo to the atmosphere, water and for keeping the temperature 44 ^{0}C in shell winter conditions.

Q_s= 1010.96 kW (Quantity of heat to cover heat losses at 44 ^{0}C in shell summer conditions)

$$G_{ps} = \frac{Q_S}{r} = \frac{1010.96 * 3600}{1933.19} = 1882.62 \frac{kg}{h}$$

$$G_{pg} = \frac{Q_p}{r} = \frac{0 * 3600}{1933.19} = 0 \frac{kg}{h}$$

G_P=G_{ps}+G_{pg}=1882.62+0= 1882.62 (kg/h)

This is the steam consumption for covering heat looses from cargo to the atmosphere, water and for keeping the temperature 44 ^{0}C in shell summer conditions.

Shell solution steam consumption in phase 3 is shown in Table 4.22.

Table 4. 22: Shell solution steam consumption in phase 3.

SHELL CONDITIONS	Preheating 44-66 ^{0}C [kW]	Preheating Losses Mean (44-66 ^{0}C) [kW]	Steam Evoparation Heat [kJ/kg]	G_{ps} [kg/h]	G_{pg} [kg/h]	G_p [kg/h]
Shell Conditions	14143.05	6705.06	1933.19	12486.21	26337.29	38823.50
Shell Summer Cond.	14143.05	2440.79	1933.19	4545.26	26337.29	30882.54

Q_s=6705.06 kW (Quantity of heat to cover heat losses between 44 ^{0}C to 66 ^{0}C in shell winter conditions)

Q_p= 14143.049 kW (Total quantity of heat needed to cargo preheating for shell winter conditions)

$$G_{ps} = \frac{Q_S}{r} = \frac{6705.06 * 3600}{1933.19} = 12486.21 \ \frac{kg}{h}$$

$$G_{pg} = \frac{Q_p}{r} = \frac{14143.049 * 3600}{1933.19} = 26337.29 \ \frac{kg}{h}$$

$G_P=G_{ps}+G_{pg}$=12486.21+26337.29= 38823.50 (kg/h)

This is the steam consumption for preheating the cargo from 44 ^{0}C till 66 ^{0}C and covering heat looses from cargo to the atmosphere and water in shell winter conditions.

Q_s= 2440.79 kW (Quantity of heat to cover heat losses between 44 ^{0}C to 66 ^{0}C in shell summer conditions)

Q_P=14143.049 kW (Total quantity of heat needed to cargo preheating for shell summer conditions)

$$G_{ps} = \frac{Q_S}{r} = \frac{2440.79 * 3600}{1933.19} = 4545.26 \ \frac{kg}{h}$$

$$G_{pg} = \frac{Q_p}{r} = \frac{14143.049 * 3600}{1933.19} = 26337.29 \ \frac{kg}{h}$$

$G_P=G_{ps}+G_{pg}$=4545.26+26337.29= 30882.54 (kg/h)

This is the steam consumption for preheating the cargo from 44 ^{0}C till 66 ^{0}C and covering heat looses from cargo to the atmosphere and water in shell summer conditions.

Consideration of the results, there is an absolute difference between shell winter conditions and summer condition steam consumption due to the difference of the ambient temperature. In summer condition heat losses occur less than winter condition , thereby it requires less steam consumption than winter conditions.

4.4.2 Spirax Sarco solution steam consumption

Spirax Sarco solution steam consumption in phase 2 is shown in Table 4.23

Table 4. 23: Spirax Sarco steam consumption in phase 2.

Spirax Sarco Conditions	Cont.Heating 43 ^{0}C [kW]	Steam Evoparation Heat [kJ/kg]	G_{ps} [kg/h]	G_{pg} [kg/h]	G_p [kg/h]
Winter Conditions	5931.25	1933.19	11045.22	0	11045.22
Summer Conditions	1072.40	1933.19	1997.03	0	1997.03

Q_s=5931.25 kW (Quantity of heat to cover heat losses at 43 ^{0}C in spirax sarco winter conditions)

$$G_{ps} = \frac{Q_S}{r} = \frac{5931.25 * 3600}{1933.19} = 11045.21 \ \frac{kg}{h}$$

$$G_{pg} = \frac{Q_p}{r} = \frac{0 * 3600}{1933.19} = 0 \ \frac{kg}{h}$$

G_P=G_{ps}+G_{pg}=11045.21+0= 11045.21 (kg/h)

This is the steam consumption for covering heat looses from cargo to the atmosphere, water and for keeping the temperature 43 ^{0}C in spirax sarco winter conditions.

Q_s=1072.40 kW (Quantity of heat to cover heat losses at 43 ^{0}C in spirax sarco summer conditions)

$$G_{ps} = \frac{Q_S}{r} = \frac{1072.40 * 3600}{1933.19} = 1997.03 \ \frac{kg}{h}$$

$$G_{pg} = \frac{Q_p}{r} = \frac{0 * 3600}{1933.19} = 0 \ \frac{kg}{h}$$

G_P=G_{ps}+G_{pg}=1997.03+0= 1997.03 (kg/h)

This is the steam consumption for covering heat looses from cargo to the atmosphere, water and for keeping the temperature 43 ^{0}C in spirax sarco summer conditions.

Spirax Sarco solution steam consumption in phase 3 is shown in Table 4.24

Table 4. 24: Spirax Sarco steam consumption in phase 3.

Spirax Sarco Conditions	Preheating Looses 43 ^{0}C [kW]	Preheating 2.5 C/24h [kW]	Steam Evoparation Heat [kj/kg]	G_{ps} [kg/h]	G_{pg} [kg/h]	Gp [kg/h]
Winter Conditions	5931.25	6860.54	1933.19	11045.22	12775.75	23820.96
Summer Conditions	1072.40	6860.54	1933.19	1997.03	12775.75	14772.78

Q_s=5931.25 kW (Quantity of heat to cover heat losses at 43 ^{0}C in spirax sarco winter conditions)

Q_p=6860.546 kW (Total quantity of heat needed to cargo preheating for spirax sarco winter conditions)

$$G_{ps} = \frac{Q_S}{r} = \frac{5931.25 * 3600}{1933.19} = 11045.21 \ \frac{kg}{h}$$

$$G_{pg} = \frac{Q_p}{r} = \frac{6860.546 * 3600}{1933.19} = 12775.76\ \frac{kg}{h}$$

$G_P = G_{ps} + G_{pg} = 11045.21 + 12775.76 = 23820.97$ (kg/h)

This is the steam consumption for preheating the cargo with the velocity 2.5 ^{0}C and covering heat looses from cargo to the atmosphere and water in spirax sarco winter conditions. Heat losses were taken into account for the cargo temperature 43 ^{0}C.

Q_s=1072.400 kW (Quantity of heat to cover heat losses at 43 ^{0}C in spirax sarco summer conditions)

Q_p= 6860.546 kW (Total quantity of heat needed to cargo preheating for spirax sarco summer conditions)

$$G_{ps} = \frac{Q_S}{r} = \frac{1072.4 * 3600}{1933.19} = 1997.03\frac{kg}{h}$$

$$G_{pg} = \frac{Q_p}{r} = \frac{6860.546 * 3600}{1933.19} = 12775.76\ \frac{kg}{h}$$

$G_P = G_{ps} + G_{pg} = 1997.03 + 12775.76 = 14772.79$ (kg/h)

This is the steam consumption for preheating the cargo with the velocity 2.5 ^{0}C and covering heat looses from cargo to the atmosphere and water in spirax sarco summer conditions. Heat losses were taken into account for the cargo temperature 43 ^{0}C.

Steam consumption for Spirax Sarco solution is also different for summer and winter conditions as Shell solution due to temperature differences between the cargo and environment. In summer condition heat losses occur less than winter condition ,thereby it requires less steam consumption than winter conditions.

4.4.3 Steam consumption comparison between Shell and Spirax Sarco solution

Table 4. 25: Steam consumptions for Shell and Spirax Sarco.

Cargo Heating Solution Method	Phase 2 [kg/h]	Phase 3 [kg/h]
Shell Winter Conditions	9741.63	38823.50
Shell Summer Cond.	1882.62	30882.54
Spirax Sarco Winter Cond.	11045.21	23820.97
Spirax Sarco Summer Cond.	1997.03	14772.79

Refering to the Table 4.25, there is immediately visible and obvious differences for steam consumptions between Shell and Spirax Sarco solutions both winter and summer conditions. Winter and summer conditions Shell steam consumptions required for per hour are bigger than Spirax Sarco required steam consumption due to the their difference solution methods. Cargo preheating according to Shell should be fast so preheating speed is 5.4 ^{0}C/24h. Preheating speed according to Spirax Sarco is lower, only 2.5 ^{0}C/24 h, therefore cargo is heated in Spirax Sarco more longer days than Shell condition. In addition to this, Shell solution also takes into account heat losses during preheating for average temperature between 44 ^{0}C and 66 ^{0}C. Spirax Sarco doesn't take into account that the heat losses will be bigger when the temperature of cargo will be higher than 43 ^{0}C. Because of this reasons, daily steam consumption for Spirax Sarco is less than Shell solution steam consumption. Although, fuel consumption vary considerably according to the length of the journey for both cargo heating solutions. In the following part ,fuel consumption will compared between Spirax Sarco and Shell solution to determine to suitable cargo heating solution depending on journey length.

Steam boiler capacity should be determined according to the most diffucult situation which is winter conditions for both cargo heating solutions.

According to Shell heating solution, boiler should be capable of producing 9741.63 kg steam per hour in phase 2 and boiler should be capable of providing 38823.49 kg steam per hour in phase 3 which require more steam than phase 2. Thus, steam boilers with the total capacity of 38823.49 kg steam per hour should be installed for proposed design ship according to Shell solution. This required steam can be obtained with a different number of boilers. 1 unit of steam boiler with capacity of 10 tons steam per hour and 1 unit of steam boiler with capacity of 30 tons steam per hour are selected for proposed design ship according to Shell solution. While small capacity boiler will work in phase 2 and phase 3, large capacity boiler will only work in phase 3.

According to the Spirax Sarco solution, boiler should be capable of producing 11045.22 kg steam per hour in phase 2 and boiler should be capable of providing 23820.05 kg steam per hour in phase 3 which require more steam than phase 2. Thus, steam boilers with the total capacity of 23820.05 kg steam per hour should be installed for proposed design ship according to Spirax Sarco solution. This required steam can be obtained with a different number of boilers. 1 unit of steam boiler with capacity of 10 tons steam per hour and 1 unit of steam boiler with capacity of 15 tons steam per hour are selected for proposed design ship according to Spirax Sarco solution. While large capacity boiler will work in phase 2 and 3, small capacity boiler will only work in phase 3. Steam boilers which are selected by considering phase 2 and 3 seperately are working efficiently in terms of fuel consumption for both cargo heating solution.

4.5 Comparison of Boiler Fuel Consumption

Boiler fuel consumption vary considerably according to the journey lenght. Some routes generally used by Aframax tankers are shown in Figure 4.3 and voyage lenght and time are shown in Table 4.26. Average cruising speed of the ship has been accepted 12 knot to determine voyage time.

Boiler fuel consumption is calculated according to the this formula (4.6) :

$$FC = \frac{M_s(i' - i_w)}{\eta_b . W} \tag{4.6}$$

M_s= Mass of steam produced by boiler (kg/h)

i'= specific entalpy of steam leaving the boiler (kJ/kg)

i_w= specific entalpy of feeding water to boiler (kJ/kg)

η_b= thermal efficiency of boiler

W= calorific value of heavy fuel (kJ/kg)

Table 4. 26: Aframax tanker routes lenght and voyage time [Url-14].

ROUTES	Lenght (Miles)	Haul Lenght	Average Ship Speed (Knot)	Voyage Time (h)
1-Caribbean-US	2300	Medium	12	191.67
2-Baltic-North West Europe	1300	Medium	12	108.33
3-Cross-Mediterranean	2050	Medium	12	170.83
4-Middle East-South East Asia	4450	Long	12	370.83

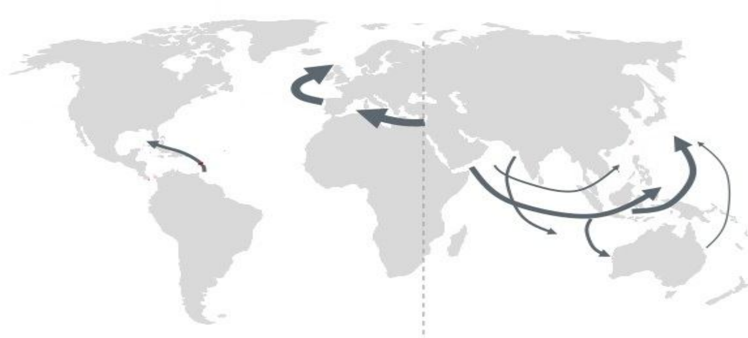

Figure 4. 3: Aframax tanker existing trade routes [Url-15].

Specific entalphy of steam leaving the boiler is taken as 2792.8 kJ /kg according to saturated steam pressure. Calorific value of heavy fuel is selected as 40000 kJ/kg and thermal efficiency of boiler is determined as 0.85. In addition to these, feeding water temperature was accepted as 70 ^{0}C and specific entalphy of feeding water to boiler was determined in the following :

$i_w = c_p \times t_w = 4.19\ (kJ/kg\ ^0C) \times 70\ (^0C) = 293.3\ kJ/kg$

According to equation 4.6, boiler hourly fuel consumption in phase 2 and phase 3 is calculated and shown in Table 4.27 and Table 4.28.

Table 4. 27: Boiler hourly fuel consumption in phase 2.

Cargo Heating Solution	M_s [kg/h]	i' [kj/kg]	i_w [kj/kg]	η_b	W [kj/kg]	FC [kg/h]
Shell Winter Conditions	9741.63	2792.8	293.3	0.85	40000	716.1531
Shell Summer Conditions	1882.62	2792.8	293.3	0.85	40000	138.4003
Spirax Sarco Winter Cond.	11045.21	2792.8	293.3	0.85	40000	811.9854
Spirax Sarco Summer Cond.	1997.03	2792.8	293.3	0.85	40000	146.8111

Table 4. 28: Boiler hourly fuel consumption in phase 3.

Cargo Heating Solution	M_s [kg/h]	i' [kj/kg]	i_w [kj/kg]	η_b	W [kj/kg]	FC [kg/h]
Shell Winter Conditions	38823.5	2792.8	293.3	0.85	40000	2854.098
Shell Summer Conditions	30882.54	2792.8	293.3	0.85	40000	2270.321
Spirax Sarco Winter Cond.	23820.97	2792.8	293.3	0.85	40000	1751.192
Spirax Sarco Summer Cond.	14772.79	2792.8	293.3	0.85	40000	1086.017

Shell and Spirax Sarco voyage times in phase 2 and 3 are shown in Table 4.29.

Table 4. 29: Shell and Spirax Sarco voyage times in phase 2 and 3.

ROUTES	Total Voyage Time (h)	Shell Solution		Spirax Sarco	
		In Phase 2 Voyage Time (h)	In Phase 3 Voyage Time (h)	In Phase 2 Voyage Time (h)	In Phase 3 Voyage Time (h)
Caribbean-US	191.67	95.67	96	0.00	220.8
Baltic-North West Europe	108.33	12.33	96	0.00	220.8
Cross-Mediterranean	170.83	74.83	96	0.00	220.8
Middle East-South East Asia	370.83	274.83	96	150.03	220.8

According to the voyage times for Shell and Spirax Sarco solution, total fuel consumptions during the ship journey for each of the different routes are calculated and shown in Table 4.30 and Table 4.31.

Table 4. 30: Total fuel consumption during the Caribbean-US and Baltic-North West Europe routes.

Cargo Heating Solution	Caribbean-Us			Baltic-North West Europe		
	Phase 2 [ton]	Phase 3 [ton]	Total FC [ton]	Phase 2 [ton]	Phase 3 [ton]	Total FC [ton]
Shell Winter Cond.	68.51	273.99	**342.5**	8.83	273.99	**282.82**
Shell Summer Cond.	13.24	217.95	**231.2**	1.71	217.95	**219.66**
Spirax Sarco Winter Cond.	0	386.66	**386.66**	0	386.66	**386.66**
Spirax Sarco Summer Cond.	0	239.79	**239.8**	0	239.79	**239.79**

Table 4. 31: Total fuel consumption during the Cross-Mediterranean and Middle East-East Asia routes.

Cargo Heating Solution	Cross-Mediterranean			Middle East-South East Asia		
	Phase 2 [ton]	Phase 3 [ton]	Total FC [ton]	Phase 2 [ton]	Phase 3 [ton]	Total FC [ton]
Shell Winter Cond.	53.58	273.99	**327.57**	196.82	273.99	**470.81**
Shell Summer Cond.	10.36	217.95	**228.31**	38.04	217.95	**255.99**
Spirax Sarco Winter Cond.	0	386.66	**386.66**	121.82	386.66	**508.48**
Spirax Sarco Summer Cond.	0	239.79	**239.79**	22.02	239.79	**261.81**

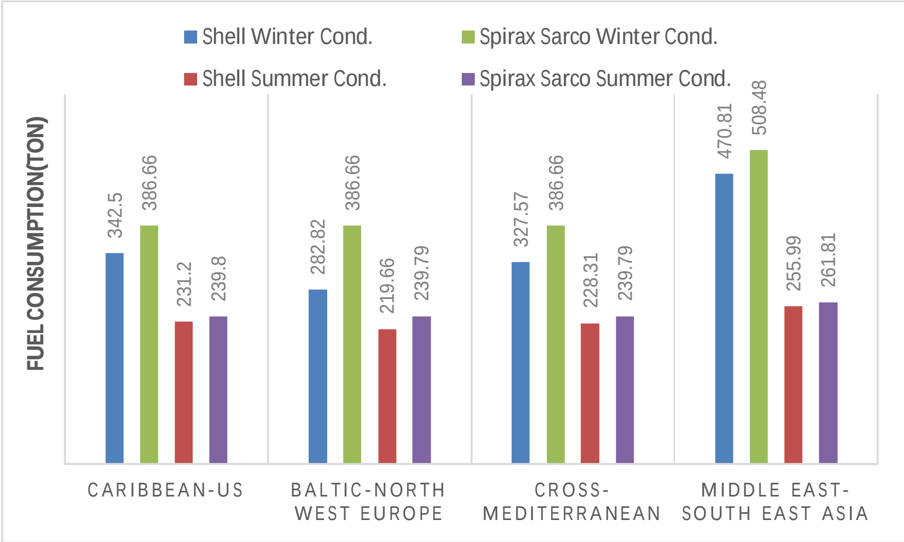

Figure 4. 4: Different routes total fuel consumption for Shell and Spirax Sarco solution.

In Table 4.27 and Table 4.28, it was shown that hourly fuel consumption in Shell solution is bigger than Spirax Sarco hourly fuel consumption. Although, total fuel consumption vary considerably according to the length of the journey for both cargo heating solutions. According to the Figure 4.4, total fuel consumption during the journey in Spirax Sarco is bigger than Shell solution for all selected routes. Voyage time is significantly important to determine suitable cargo heating solution method.

5. DETERMINATION OF HEAT TRANSFER COEFFICIENTS IN CARGO TANK

There are several different overall heat transfer coefficients defined for specific parts of the ship structure surfaces. Each part of the tank has a different physical state and conditions. Therefore, each part has diverse heat transfer coefficients and these heat transfer coefficients are calculated by separately for double side, deck and double bottom. These heat transfer coefficients are shown in Figure 5.1 and they represent the heat transfer from cargo tanks through ship structure to the sea water or air. For each of the overall heat transfer coefficients k_i , a corresponding surface F_i is calculated.

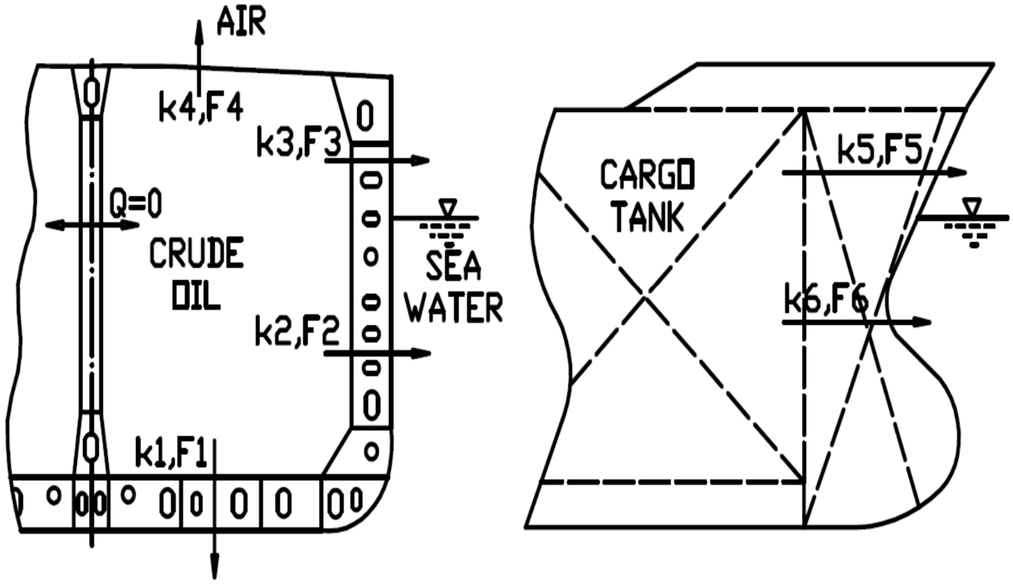

Figure 5. 1: Overall heat transfer coefficients on ship hull cross sections [25].

5.1 Calculating Heat Transfer Coefficients For Double Side

The first approach of our system is composed of 3 parts which is showed in Figure 5.2 as number 1,2 and 3 in terms of heat transfer. In the first part which is number 1 there is quiescent crude oil at 44 ^{0}C and this quiescent crude oil is contact with the steel plate. Crude oil temperature drop occurs in the portion in contact with steel and natural convection takes place in this section due to motionless of the crude oil. For the second part there is an air at 22 ^{0}C that temperature is accepted. Calculating the exact temperature of the air in the number 2 explained in the following section. In this part, natural convection takes place in this section as the first part due to the motionless of the air.

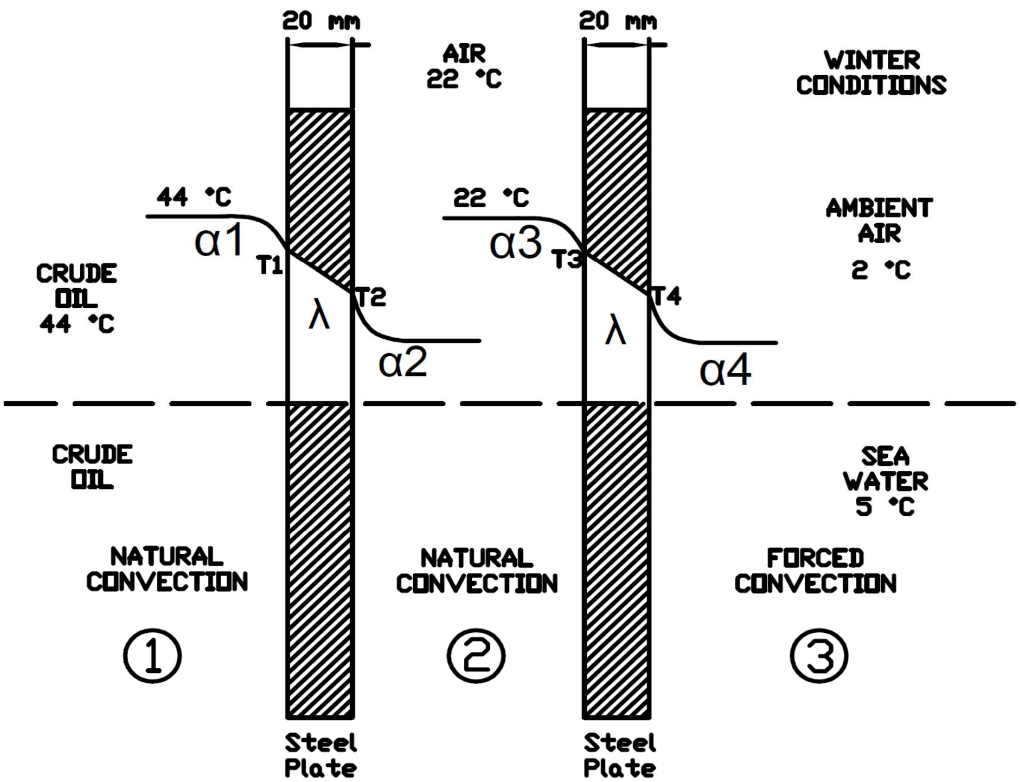

Figure 5. 2: Cargo tank double side part state and conditions.

Lastly, there are moving ambient air at 2 ^{0}C and sea water at 5 ^{0}C in winter conditions in number 3 and steel plate contact with moving air and sea water. Forced convection takes place in this section because of air and sea water speed. The system is divided into two parts to calculate heat transfer coefficient. Changes that have occurred in steel plates are examined separately to find total heat transfer coefficients for this approach. Heat transfer coefficient for the first plate will be calculated for the heavier crude oil than the Bachequero crude oil with properties which is shown below :[1]

Determination of heat transfer coefficient for the first plate

[1] Lack of information about properties of density, viscosity, thermal conductivity, specific heat capacity depending on temperature for Bachequero crude oil, crude oil which has close values to Bachequero crude oil is used to find accurate solution.

Crude oil specifications at 44 ^{0}C are taken as following Table 5.1 :

Table 5. 1: Crude oil properties at 44 ^{0}C [21].

Cp=	1848	J/kg·K	**λ=**	0.116	W/m·K
ρ=	972	kg/m^3	**μ=**	0.881604	Pa.s
ν=	0.000907	m^2/s	**β=**	0.00057	1/K

Acceleration of gravity (g) and characteristic length (l) is taken as 9.81 (m/s^2) and 1(m) respectively. In addition to this, steel thermal conductivity is taken 58 (W/m·K). Air specifications at 22 ^{0}C are taken as following Table 5.2 :

Table 5. 2: Air properties at 22 ^{0}C [21].

Cp=	1020	J/kg·K	**μ=**	0.000017565	Pa.s
ρ=	1.171	kg/m^3	**λ=**	0.026	W/m·K
ν=	0.000015	m^2/s	**β=**	0.00345	1/K

According to the Figure 5.3 and equations 5.3, 5.4 ; steel plate temperatures T_1 and T_2 are calculated by numbers of iterations using overall heat transfer equation (3.12) and heat flux equality equation. As a result, steel temperatures in both sides are as follows:

T_1=38.52 ^{0}C

T_2=38.49 ^{0}C

Firstly, heat transfer coefficient (α1) for natural convection in number 1 is calculated as follows :

$$Pr = \frac{c_p \cdot \mu}{\lambda} = \frac{1848 \cdot 0.881604}{0.116} = 14044.86$$

$$Gr = \frac{g \cdot \beta \cdot L_C^3 \cdot \Delta T}{\nu^2} = \frac{9.81 \cdot 0.00057 \cdot 1^3 \cdot (44 - 38.51651)}{0.000907^2} = 37272.31302$$

Gr.Pr=523484557

According to the 3.2.1.1 , if the multiplication of Grashof and Pradtl number is in this interval $20.10^6 < (Gr.Pr) < 10^{13}$,constants c and n are in the following :

c=0.135

n=0.333

$$Nu_L = c(Gr.Pr)^n = \frac{\alpha 1 \, x L_C}{\lambda} = 0.135.(523484557)^{0.333} = 108.728$$

As a result of this equation, heat transfer coefficient (α1) is determined as 12.612 ($W/m^2 \cdot K$)

Secondly, heat transfer coefficient (α2) for natural convection in number 2 was calculated as follows :

$$\mathrm{Pr} = \frac{c_p \cdot \mu}{\lambda} = \frac{1020 \cdot 0.000017565}{0.026} = 0.689$$

$$\mathrm{Gr} = \frac{g \cdot \beta \cdot L_C^3 \cdot \Delta T}{\nu^2} = \frac{9.81 \cdot 0.00345 \cdot 1^3 \cdot (38.49266 - 22)}{0.000015^2} = 2480825917$$

Gr.Pr=1709508515

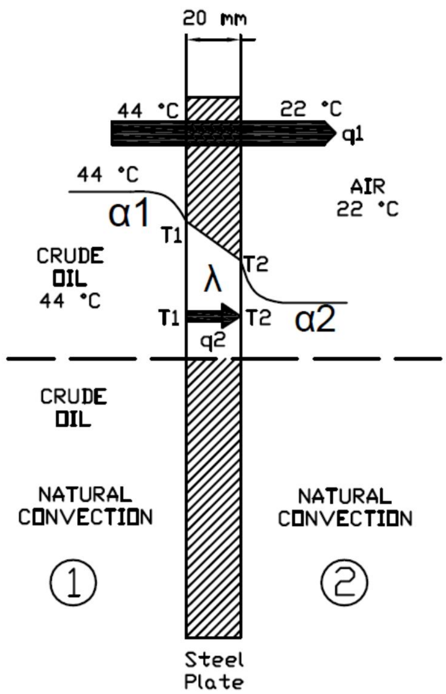

Heat flux has been assumed as a constant in the system. Therefore, heat fluxes which are showed as q1 and q2 in Figure 5.3 that are equal each other .

$q1=k(T_{crude}-T_{air})$ [heat exchanges from crude oil to air] **(5.1)**

$q2=\lambda/\delta(T_1-T_2)$ [heat exchanges from one plate side to the other side] **(5.2)**

q1=q2 must be equal. As a result of this ,temperatures of the plate can be written in the following :

$T_1=T_{crude}-k(T_{crude}-T_{air})/\alpha 1$ **(5.3)**

$T_2=T_{air}+ k(T_{crude}-T_{air})/\alpha 2$ **(5.4)**

Figure 5. 3: Double side inside plate.

$$\mathrm{Nu_L} = c(\mathrm{Gr.Pr})^n = \frac{\alpha 2 \cdot L_C}{\lambda} = 0.135.(1709508515)^{0.333} = 161.305$$

As a result of this equation ,heat transfer coefficient (α2) is determined as 4.1939 ($W/m^2 \cdot K$)

According to the thermal resistance topic (3.1.2) , overall heat transfer coefficients (k_1) can be written in the following :

δ=0.02 (m)-steel plate thickness

λ=58 (W/m·K)- steel plate thermal conductivity.

$$k_1 = \frac{1}{\frac{1}{\alpha 1} + \frac{\delta}{\lambda} + \frac{1}{\alpha 2}} = \frac{1}{\frac{1}{12.612} + \frac{0.02}{58} + \frac{1}{4.1939}} = 3.1439\ W/m^2 \cdot K$$

Determination of heat transfer coefficient for the second plate

a) Calculation heat transfer coefficients for part that is contact with the air

Air specifications at 22 ^{0}C are taken same values which showed in Table 5.2

Acceleration of gravity (g) and characteristic length (l) and steel thermal conductivity (λ) are taken the same values which explained in previous part.

Air specifications at 2 ^{0}C are taken as following Table 5.3 :

Table 5. 3: Air properties at 2 ^{0}C [21].

Cp=	1019	J/kg·K	**μ=**	0.000016855	Pa.s
ρ=	1.256	kg/m^3	**λ=**	0.02454	W/mK
ν=	0.00001342	m^2/s	**β=**	0.00354	1/K

Steel plate temperatures T_3 and T_4 are calculated by numbers of iterations on using overall heat transfer coefficient equation (3.12) and heat flux equality equation. As a result, steel temperatures in both sides are as follows :

T_3=3.13 ^{0}C

T_4=3.10 ^{0}C

Firstly, heat transfer coefficient (α3) for natural convection in number 2 is calculated as follows :

$$Pr = \frac{c_p \cdot \mu}{\lambda} = \frac{1020 \cdot 0.000017565}{0.026} = 0.689$$

$$Gr = \frac{g \cdot \beta \cdot L_C^3 \cdot \Delta T}{\nu^2} = \frac{9.81 \cdot 0.00345 \cdot 1^3 \cdot (22 - 3.13)}{0.00001342^2} = 2837583048$$

Gr.Pr=1955345737

According to the 3.2.1.1 , if the multiplication of Grashof and Pradtl number is in this interval $20.10^6 < (Gr.Pr) < 10^{13}$,constants c and n are in the following :

c=0.135

n=0.333

$$Nu_L = c(Gr.Pr)^n = \frac{\alpha 3 \cdot L_C}{\lambda} = 0.135.(1955345737)^{0.333} = 168.69$$

As a result of this equation, heat transfer coefficient (α3) is determined as 4.386 (W/m^{2}K)

Secondly, heat transfer coefficient (α4) for forced convection in number 3 is calculated as follows :

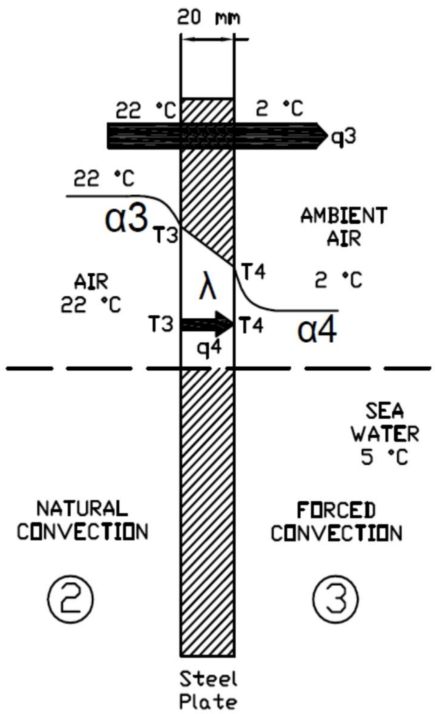

Heat flux has been assumed as a constant in the system. Therefore, heat fluxes which are showed as q3 and q4 in Figure 5.4 that are equal each other .

$q3=k(T_{air}-T_{ambientair})$ [heat exchanges from air which is between two plates to ambient air]

$q4=\lambda/\delta(T_3-T_4)$ [heat exchanges from one plate side to the other side]

q3=q4 must be equal. As a result of this ,temperatures of the plate can be written in the following :

$T_3=T_{air}-k(T_{air}-T_{ambientair})/\alpha3$

$T_4=T_{ambient}+ k(T_{air}-T_{ambientair})/\alpha4$

Figure 5. 4: Double side outside plate.

Ship speed (knot) and wind speed (knot) around the steel plate are determined as in the following :

It is assumed that proposed design ship generally expose strong breeze during the journey. Table 5.4 shows winds specifications and equivalent speeds, wind speed is selected according to the this table.

Table 5. 4: Beaufort scale [22].

Beaufort Number	Wind Descriptive Terms	Vwind [knot]
0	Calm	Vwind< 1
1	Light Air	1<Vwind<3
2	Light Breeze	4<Vwind<6
3	Gentle Breeze	7<Vwind<10
4	Moderate Breeze	11<Vwind<16
5	Fresh Breeze	17<Vwind<21
6	Strong Breeze	22<Vwind<27
7	Near Gale	28<Vwind<33
8	Gale	34<Vwind<40
9	Strong Gale	41<Vwind<47
10	Storm	48<Vwind<55
11	Violent Storm	56<Vwind<63
12	Hurricane	Vwind>64

Sea state in winds of strong breeze is showed in Figure 5.5.

Figure 5. 5: Sea appearance in winds of strong breeze [22].

Proposed design ship cruising speed is selected according to the similar vessels which is more closer to our design criterias.

V_{ship}=15.2 knot=0.5144x15.2=7.8188 (m/s)

V_{wind}=27 knot=0.5144x27=13.88 (m/s)

$V_{total\ air}$=42.2 knot=0.5144x42.2= 21.70 (m/s)

$$Re_L = \frac{\text{inertia forces}}{\text{viscous forces}} = \frac{\rho VL}{\mu} = \frac{VL}{\nu} = \frac{21.70x1}{0.00001342} = 1617562$$

Re=1617562 >5.10^5 (Flow is turbulent)

$$Pr = \frac{c_p \cdot \mu}{\lambda} = \frac{1019 \cdot 0.000016855}{0.02454} = 0.6999$$

$$\overline{Nu_L} = 0.037Re_L^{4/5}Pr^{1/3} = \frac{\alpha 4\ xL_C}{\lambda} \quad 0.6 \le Pr \le 50$$

$$\overline{Nu_L} = 0.037 \cdot 1617562^{4/5} \cdot 0.699^{1/3} = 3045.39$$

As a result of this equation ,heat transfer coefficient (α4) was determined as 74.73 (W/m^2K).

According to the thermal resistance topic (3.1.2) , overall heat transfer coefficients (k_2) can be written in the following :

$$k_2 = \frac{1}{\frac{1}{\alpha 3} + \frac{\delta}{\lambda} + \frac{1}{\alpha 4}} = \frac{1}{\frac{1}{4.386} + \frac{0.02}{58} + \frac{1}{74.73}} = 4.13\ W/m^2 \cdot K$$

Heat transfer coefficient (k_2) changes according to the wind speeds are showed in the following Table 5.5.

Table 5. 5: Heat transfer coefficient (k_2) changes depending on wind speeds.

Beaufort Number	Wind Descriptive Terms	V_{wind} [knot]	V_{wind}(max) [knot]	Vwind [m/s]	k_2 [W/m^{2}K]
0	Calm	Vwind< 1	1	0.5144	3.82
1	Light Air	1<Vwind<3	3	1.5432	3.86
2	Light Breeze	4<Vwind<6	6	3.0864	3.92
3	Gentle Breeze	7<Vwind<10	10	5.144	3.99
4	Moderate Breeze	11<Vwind<16	16	8.2304	4.05
5	Fresh Breeze	17<Vwind<21	21	10.8024	4.09
6	Strong Breeze	22<Vwind<27	27	13.8888	4.13
7	Near Gale	28<Vwind<33	33	16.9752	4.16
8	Gale	34<Vwind<40	40	20.576	4.19
9	Strong Gale	41<Vwind<47	47	24.1768	4.21
10	Storm	48<Vwind<55	55	28.292	4.23
11	Violent Storm	56<Vwind<63	63	32.4072	4.25
12	Hurricane	Vwind>64	80	41.152	4.28

Heat transfer coefficient for outside plate of double side is increasing logarithmically in terms of wind speed as shown in the Figure 5.6.

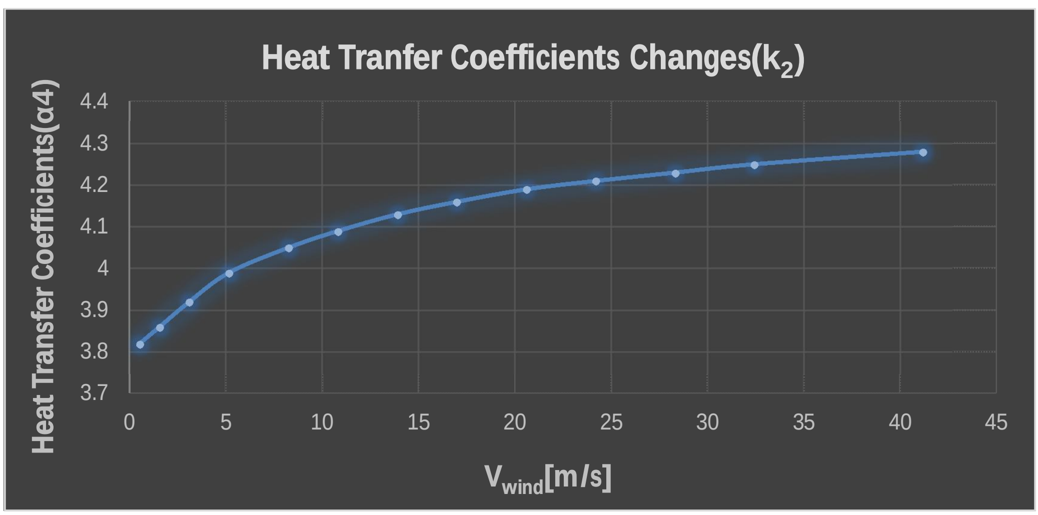

Figure 5. 6: Heat tranfer coefficient (k_2) changes according to the wind speeds.

b) Calculation heat transfer coefficients for part that is contact with the sea water

Air specifications at 22 ^{0}C are taken as same values which showed in Table 5.2.

It is assumed that salinity of the sea water is 30 ‰. Based on this information, sea water specifications at 5 ^{0}C are taken as following Table 5.6 :

Table 5. 6: Sea water properties at 5 ^{0}C [21].

C_p=	4021.45	J/kgK	**μ=**	0.00163453	Pa.s
ρ=	1023.5	kg/m^3	**λ=**	0.578	W/m·K
ν=	0.000001597	m^2/s	**β=**	0.0000785	1/K

Steel plate temperatures T_3' and T_4' are calculated by numbers of iterations using overall heat transfer coefficient equation (3.1.2) and heat flux equality equation. As a result, steel temperatures in both sides are as follows :

T_3'=5.03 ^{0}C

T_4'=5.00 ^{0}C

Firstly, heat transfer coefficient (α3') for natural convection in number 2 was calculated as follows :

$$\mathrm{Pr} = \frac{c_p \cdot \mu}{\lambda} = \frac{1020\mathrm{x}0.000017565}{0.026} = 0.689$$

$$\mathrm{Gr} = \frac{g \cdot \beta \cdot L_C^3 \cdot \Delta T}{\nu^2} = \frac{9.81 \cdot 0.00345 \cdot 1^3 \cdot (22 - 5.031)}{0.00001342^2} = 2552476980$$

Gr.Pr=1758882435

According to the 3.2.1.1 , if the multiplication of Grashof and Pradtl number is in this interval $20.10^6 < (\mathrm{Gr.Pr}) < 10^{13}$,constants c and n are in the following :

c=0.135

n=0.333

$$\mathrm{Nu_L} = c(\mathrm{Gr.Pr})^n = \frac{\alpha 3' \cdot L_C}{\lambda} = 0.135.(1758882435)^{0.333} = 162.843$$

As a result of this equation ,heat transfer coefficient (α3') is determined as 4.233 (W/m^{2}K)

Sea water speed was considered to be equal to the vessel speed.

$V_{seawater}$=15.2 knot=15.2·0.5144= 7.8188 (m/s)

$$\mathrm{Re_L} = \frac{\text{inertia forces}}{\text{viscous forces}} = \frac{\rho VL}{\mu} = \frac{VL}{\nu} = \frac{7.8188x1}{0.000001597} = 4895979.962$$

Re=4895979.962 >5.10^5 (Flow is turbulent)

$$\mathrm{Pr} = \frac{c_p \cdot \mu}{\lambda} = \frac{4021.45\mathrm{x}0.0163453}{0.578} = 11.372$$

$$\overline{\mathrm{Nu_L}} = 0.037\mathrm{Re_L^{4/5}}\mathrm{Pr}^{1/3} = \frac{\alpha 4' \cdot L_C}{\lambda} \qquad [\mathrm{Rex,c} = 0\, , 0.6 \le \mathrm{Pr} \le 50\,]$$

Prandtl number is suitable for nusselt number formulation conditions.

$$\overline{Nu_L} = 0.037 \cdot 4895979.962^{4/5} \cdot 11.372^{1/3} = 18706.28$$

As a result of this equation , heat transfer coefficient ($\alpha 4'$) is determined as 10812.22 (W/m^2K)

According to the themal resistance topic (3.1.2) ,overall heat transfer coefficients (k_2') can be written in the following :

$$k_2' = \frac{1}{\frac{1}{\alpha 3'} + \frac{\delta}{\lambda} + \frac{1}{\alpha 4'}} = \frac{1}{\frac{1}{4.233} + \frac{0.02}{58} + \frac{1}{10812.22}} = 4.226\ W/m^2 \cdot K$$

Air temperature and heat transfer coefficients correction

Firstly, air temperature between two plates is accepted as 22 ^0C to calculate heat transfer coefficients but this temperature of the air is not a real value. So, this temperature is corrected depending on the heat transfer rate equality for two steel plates.

After many iterations, new heat transfer coefficients (k_1, k_2, k_2') and air temperature (T_x,T_x') are in the following:

$Q_1=k_1 \cdot A \cdot (T_{crude}-T_x)= Q_2=k_2 \cdot A \cdot (T_x-T_{ambientair})$

$Q_1=3.1439 \cdot 1 \cdot (44-T_x)=Q_2=4.136 \cdot 1 \cdot (T_x-2)$

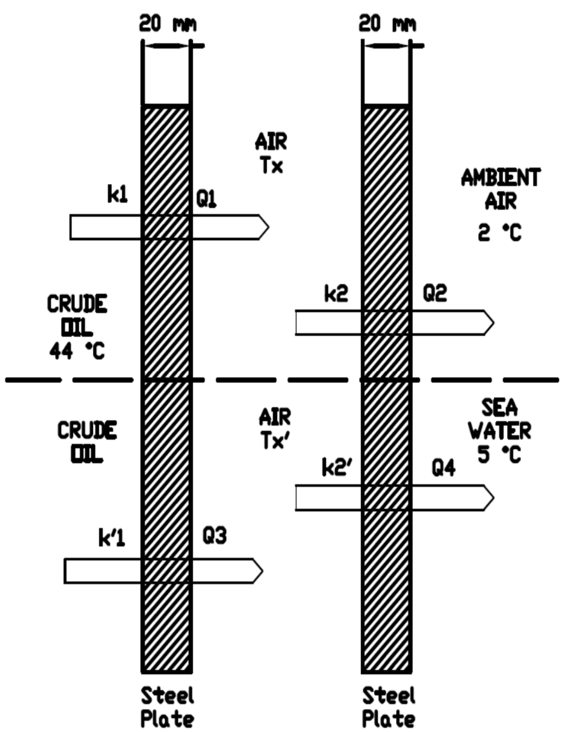

$\mathbf{Q_1=k_1 \cdot A \cdot (T_{crude}-T_x)}$

$\mathbf{Q_2=k_2 \cdot A \cdot (T_x-T_{ambientair})}$

$\mathbf{Q_3=k_1' \cdot A \cdot (T_{crude} -T_x')}$

$\mathbf{Q_4=k_2' \cdot A \cdot (T_x'-T_{seawater})}$

Heat transfer rate in the first plate is equal to the second plate heat transfer rate. For this reason, it can be written following equations :

$Q_1=Q_2$ and $Q_3=Q_4$

$k_1=3.1439\ W/m^2K$

$k_2=4.136\ W/m^2K$

$k_2'=4.226\ W/m^2K$

$A=1\ m^2$

Figure 5. 7: Steel plates heat tranfer rate equality.

Double side steel plates heat transfer rate equality is shown in Figure 5.7.

$T_x(1)=20.135$ (First iteration)

$T_x(2)=20.72$ (Second iteration)

$T_x(3)=20.54$ (Third iteration)

$T_x(4)=20.59$ (Fourth iteration)

Each temperature value for T_x produced new heat transfer coefficients. Number of iterations are maintened until the heat transfer rates are equal ($Q_1=Q_2$) and ($Q_1= Q_3$). After many iterations , corrected heat transfer coefficients and air temperature results are as follows :

k_1(corr.)=3.2096 (W/m^{2}K) $k_1^{'}$(corr.)=3.402 (W/m^{2}K)

k_2(corr.)=4.0446 (W/m^{2}K) $k_2^{'}$(corr.)=4.503 (W/m^{2}K)

T_x(corr.)=20.59 ^{0}C $T_x^{'}$(corr.)=21.75 ^{0}C

Average air temperature between the plates is 21.17 ^{0}C.

5.2 Calculating Heat Transfer Coefficient For Double Bottom

The first approach of our system is composed of 3 parts which is showed in Figure 5.8 as number 1, 2 and 3 in terms of heat transfer. In the first part which is number 1 there is quiescent crude oil at 44 ^{0}C and this quiescent crude oil is contact with the steel plate. Crude oil temperature drop occurs in the portion in contact with steel and natural convection takes place in this section due to motionless of the crude oil. For the second part there is an air at 25 ^{0}C that temperature is accepted. Calculating the exact temperature of the air in the number 2 explained in the following section. In this part, natural convection takes place in this section as the first part due to the motionless of the air. Lastly, there are moving sea water at 5 ^{0}C in winter conditions in number 3 and steel plate contact with moving sea water. Forced convection takes place in this section because of sea water speed. The system is divided into two parts to calculate heat transfer coefficient. Changes that have occurred in steel plates are examined separately to find total heat transfer coefficients for this approach. Heat transfer coefficient for the first plate was calculated as shown below :

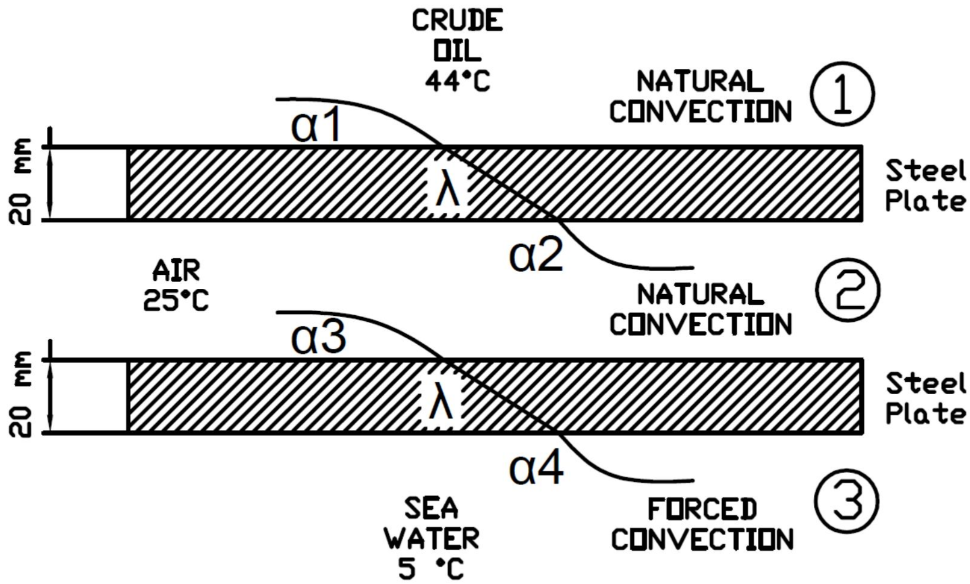

Figure 5. 8: Cargo tank double bottom part state and conditions.

Determination of heat transfer coefficient for the first plate

Crude oil properties at 44 ^{0}C is taken same values (Table 5.1) which mentioned and showed in previous part.

Air specifications at 25 ^{0}C are taken as following Table 5.7 :

Table 5. 7: Air properties at 25 ^{0}C [21].

C_p=	1020	J/kgK	**μ=**	0.000017883	Pa.s
ρ=	1.159	kg/m^3	**λ=**	0.02625	W/m·K
ν=	0.00001543	m^2/s	**β=**	0.00345	1/K

Heat flux has been assumed as a constant in the system. Therefore, heat fluxes which are showed as q1 and q2 in Figure 5.9 that are equal each other.

$q1=k(T_{crude}-T_{air})$ [heat exchanges from crude oil to air]

$q2=\lambda/\delta(T_1-T_2)$ [heat exchanges from one plate side to the other side]

q1=q2 must be equal. As a result of this , temperatures of the plate can be written in the following :

$T_1=T_{crude}-k(T_{crude}-T_{air})/\alpha 1$

$T_2=T_{air}+ k(T_{crude}-T_{air})/\alpha 2$

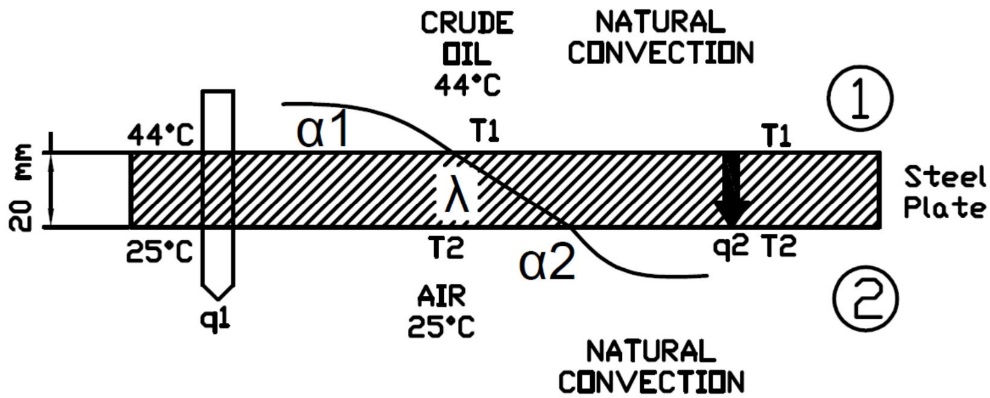

Figure 5. 9: First plate (tank top) conditions for double bottom.

Steel plate temperatures T_1 and T_2 are calculated by numbers of iterations using overall heat coefficient equation (3.12) and heat flux equality equation. As a result, steel temperatures in both sides are as follows :

T_1= 39.28^{0}C

T_2= 39.26 ^{0}C

Natural convection in a horizontal plates is calculated in a different way than vertical plates.

Firstly, heat transfer coefficient (α1) for natural convection in number 1 is calculated as follows :

$$\mathrm{Pr} = \frac{c_p \cdot \mu}{\lambda} = \frac{1848 \cdot 0.881604}{0.116} = 14044.86$$

Characteristic length for finding Grashoff number(Gr) and Nusselt Number(Nu) should be taken maximum 0.6 (3.2.1.2)

$$\mathrm{Gr} = \frac{g \cdot \beta \cdot L_C^3 \cdot \Delta T}{\nu^2} = \frac{9.81 \cdot 0.00057 \cdot (0.6)^3 \cdot (44 - 39.281)}{0.000907^2} = 19243.23377$$

Gr.Pr=270268595.9

According to the 3.2.1.1 , if the multiplication of Grashof and Pradtl number is in this interval $20.10^6 <$ (Gr.Pr) $<10^{13}$,constants c and n are in the following :

c=0.135

n=0.333

$$\mathrm{Nu_L} = c(\mathrm{Gr.Pr})^n = \frac{\alpha 1 \cdot L_C}{\lambda} = 0.135.(270268595.9)^{0.333} = 87.227$$

In the first plate, plate temperature (T_1) inside of the tank is less than crude oil temperature, this cold steel plate can not help natural convection positively, thereby

Nusselt number is reduced by 30 % due to surface of the plate is cold comparing to the crude oil.

Nu_L(corr.)=87.227-26.16812=61.058

As a result of this Nu_L(corr.) ,heat transfer coefficient (α1) is determined as 11.804 (W/m^2K)

Secondly, heat transfer coefficient (α2) for natural convection in number 2 is calculated as follows :

$$Pr = \frac{c_p \cdot \mu}{\lambda} = \frac{1020x0.000017883}{0.02625} = 0.694$$

$$Gr = \frac{g \cdot \beta \cdot L_C^3 \cdot \Delta T}{\nu^2} = \frac{9.81 \cdot 0.00345 \cdot (0.6)^3 \cdot (44 - 39.262)}{0.00001543^2} = 1216462975$$

Gr.Pr=845316062

$$Nu_L = c(Gr.Pr)^n = \frac{\alpha 2 \cdot L_C}{\lambda} = 0.135.(845316062)^{0.333} = 127.558$$

In the first plate, plate temperature (T_2) outside of the tank is higher than air temperature between two steel plates, this hot plate does not help natural convection positively, thereby Nusselt number was reduced by 30 % due to facing hot surface downward.

Nu_L(corr.)=127.558-38.267= 89.29

As a result of this Nu_L (corr.) ,heat transfer coefficient (α2) is determined as 3.906 (W/m^2K)

According to the thermal resistance topic (3.1.2) , overall heat transfer coefficients (k_1) can be written in the following :

$$k_1 = \frac{1}{\frac{1}{\alpha 1} + \frac{\delta}{\lambda} + \frac{1}{\alpha 2}} = \frac{1}{\frac{1}{11.804} + \frac{0.02}{58} + \frac{1}{3.906}} = 2.932\ W/m^2 \cdot K$$

Determination of heat transfer coefficient for the second plate

Steel plate temperatures T_3 and T_4 are calculated by numbers of iterations using overall heat transfer coefficient equation and heat flux equality equation. As a result, steel temperatures in both sides are as follows :

T_3=5.02 ^{0}C

T_4=5.00 ^{0}C

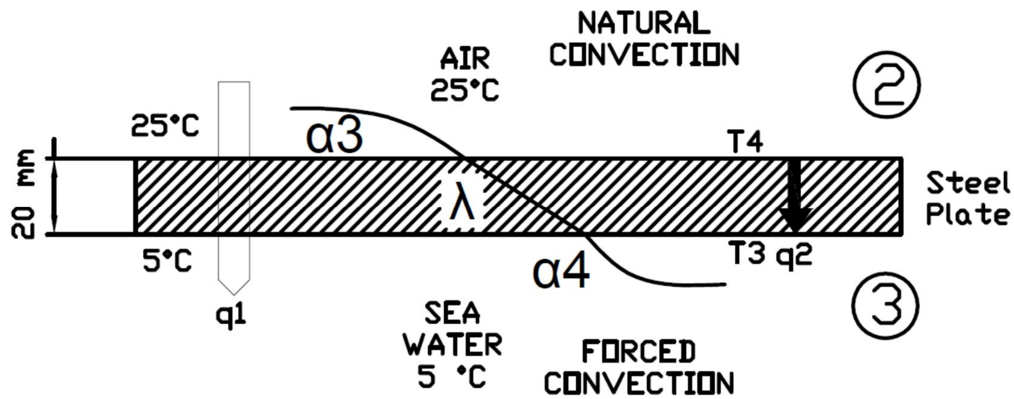

Figure 5. 10: Second plate (bottom plate) conditions for double bottom.

Firstly, heat transfer coefficient (α3) for natural convection in number 2 is calculated as follows :

Pr=0.694 (air at 25 ^{0}C)

$$Gr = \frac{g \cdot \beta \cdot L_C^3 \cdot \Delta T}{\nu^2} = \frac{9.81 \cdot 0.00345 \cdot (0.6)^3 \cdot (25 - 5.02)}{0.00001543^2} = 613487171$$

Gr.Pr=426310187.8

$$Nu_L = c(Gr.Pr)^n = \frac{\alpha 3 \cdot L_C}{\lambda} = 0.135.(426310187.8)^{0.333} = 101.536$$

In the second plate, plate temperature (T_3) is less than air temperature between two plates, hot air contact with the cold steel but cold steel can not help natural convection for this situation ,thereby Nusselt number is reduced by 30 % due to facing cold surface upward and effect natural convection negatively.

Nu_L(corr.)=101.536-30.460= 71.075

As a result of this Nu_L(corr.) ,heat transfer coefficient (α3) is determined as 3.109 (W/m^{2}K)

Sea water speed is considered to be equal to the vessel speed.

$V_{seawater}$=15.2 knot=15.2x0.5144=7.8188 (m/s)

$$Re_L = \frac{\text{inertia forces}}{\text{viscous forces}} = \frac{\rho VL}{\mu} = \frac{VL}{\nu} = \frac{7.8188x1}{0.000001597} = 4895979.962$$

Re=4895979.962 >5.10^5 (Flow is turbulent)

$$Pr = \frac{c_p \cdot \mu}{\lambda} = \frac{4021.45x0.0163453}{0.578} = 11.372$$

$$\overline{Nu_L} = 0.037Re_L^{4/5}Pr^{1/3} = \frac{\alpha 4 \cdot L_C}{\lambda} \qquad [\,Rex,c = 0\,, 0.6 \leq Pr \leq 50\,]$$

Prandtl number is suitable for Nusselt number formulation conditions.

$$\overline{Nu_L} = 0.037 \cdot 4895979.962^{4/5} \cdot 11.372^{1/3} = 18706.28$$

As a result of this equation , heat transfer coefficient (α4) is determined as 10812.22 (W/m^2K)

According to the thermal resistance topic (3.1.2) ,overall heat transfer coefficients (k_2) can be written in the following :

$$k_2 = \frac{1}{\frac{1}{\alpha 3} + \frac{\delta}{\lambda} + \frac{1}{\alpha 4}} = \frac{1}{\frac{1}{3.109} + \frac{0.02}{58} + \frac{1}{10812.22}} = 3.105\, W/m^2 \cdot K$$

Air temperature and heat transfer coefficients correction

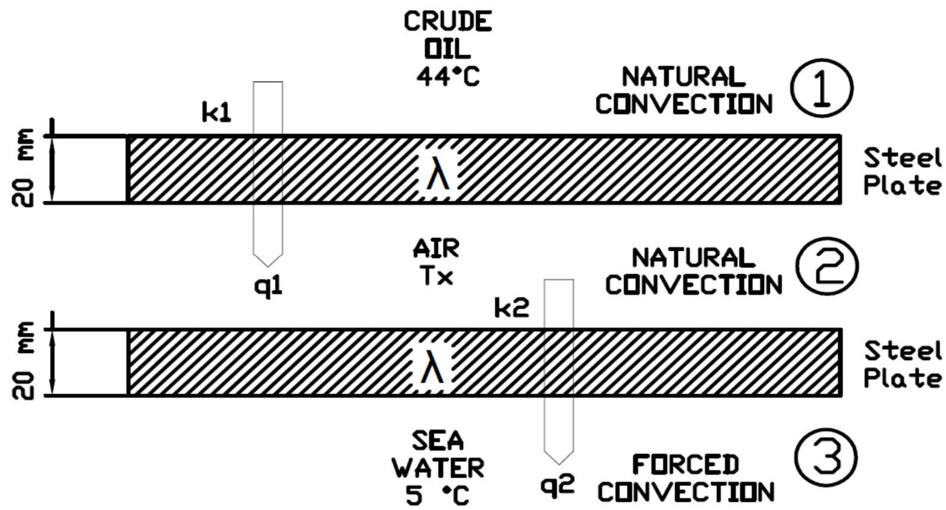

Figure 5. 11: Steel plates heat tranfer rate equality.

Firstly, air temperature between two plates is accepted as 25 ^{0}C to calculate heat transfer coefficients. But, this temperature of the air is not a real value. So, this temperature is corrected depending on the heat transfer rate equality for two steel plates.

$Q_1=k_1 \cdot A \cdot (T_{crude}-T_x)$

$Q_2=k_2 \cdot A \cdot (T_x-T_{seawater})$

Heat transfer rate in the first plate is equal to the second plate heat transfer rate which is shown in Figure 5.11. For this reason, following equations can be written:

$Q_1=Q_2$

k_1=2.9321 W/m^2K

k_2=3.1053 W/m^2K

A=1 m^2

After many iterations, new heat transfer coefficients (k_1, k_2) and air temperature (T_x) are in the following:

$Q_1=k_1 \cdot A \cdot (T_{crude}-T_x)= Q_2=k_2 \cdot A \cdot (T_x-T_{seawater})$

$Q_1=2.9321 \cdot 1 \cdot (44-T_x)=Q_2=3.1053 \cdot 1 \cdot (T_x-5)$

Table 5. 8: Iteration results of air temperature and heat transfer coefficients.

k_1	k_2	T_x	T_x(Corr.)
2.9321	3.1053	25	23.94
2.9856	3.0494	23.94	24.29
2.9682	3.0681	24.29	24.17
2.9742	3.0617	24.17	24.21
2.9722	3.0639	24.21	24.21

Each temperature value for T_x produced new heat transfer coefficients. Number of iterations are maintened until the heat transfer rates are equal ($Q_1=Q_2$). After many iterations which is shown in Table 5.8 , corrected heat transfer coefficients and air temperature results are as follows :

k_1(corr.)= 2.9722 (W/m^{2}K)

k_2(corr.)= 3.0639 (W/m^{2}K)

T_x(corr.)= 24.21 ^{0}C

5.3 Calculation Heat Transfer Coefficients For Deck

Storage tanks of crude oil marine tankers are produced volatile organic compounds (VOCs) due to hot crude oil evaporation. Emitted vapor is comprised of volatile organic compounds including methane, ethane, propane, butane, pentane, hexane and a small amount of heavier components. According to the emitted gas analysis, gas is composed of 13 % hydrocarbons, 70 % nitrogen, 10 % carbon dioxide, 5 % oxygen and 2 % other compounds such as hydrogen sulfide [23]. Emitted gas is a mixture of gas in the storage tanks and it is very difficult to determine physical properties of the mixture, thereby heat transfer coefficient is determined using the air physical properties at required temperature.

The first approach of our system is composed of 2 parts which is showed in Figure 5.12 as number 1, 2 in terms of heat transfer. In the first part which is number 1 there is crude oil vapour and air mixture at 44 ^{0}C and this mixture is contact with the steel plate. In this part, natural convection takes place due to the motionless of the mixture. In the second part which is number 2, there are moving ambient air at 2 ^{0}C in winter conditions and steel plate contact with moving air. Forced convection takes place in this section because of air speed. Heat transfer coefficient is calculated as shown below.

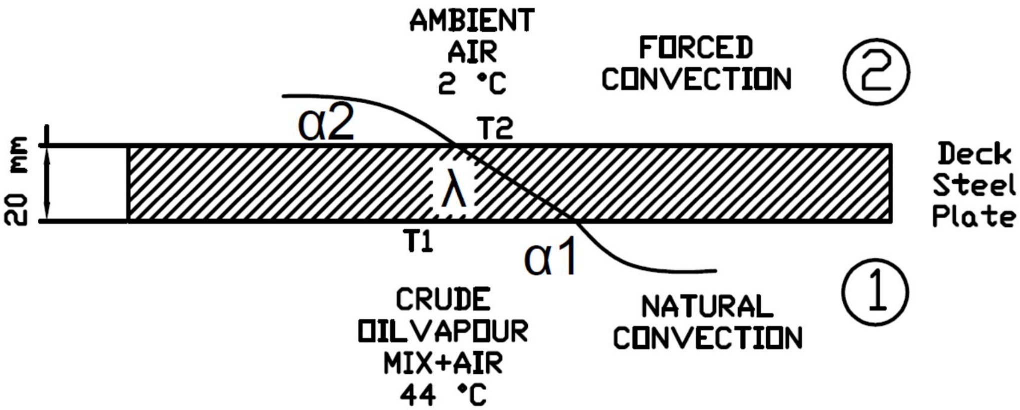

Figure 5. 12: Cargo tank deck part state and conditions.

Air specifications at 44 ^{0}C are taken as following Table 5.9 :

Table 5. 9: Air specifications at 44 ^{0}C [21].

C_p=	1021	J/kgK	**μ=**	0.000018776	Pa.s
ρ=	1.086	kg/m^3	**λ=**	0.02771	W/m·K
ν=	0.00001729	m^2/s	**β=**	0.003131	1/K

Air specifications at 2 ^{0}C were mentioned in previous part.(Table 5.3)

Steel plate temperatures T_1 and T_2 were calculated by numbers of iterations using overall heat transfer coefficient equation (3.1.2) and heat flux equality equation. As a result, steel temperatures in both sides are as follows :

T_1=5.58 ^{0}C

T_2=5.49 ^{0}C

Firstly, heat transfer coefficient (α1) for natural convection in number 1 was calculated as follows :

Characteristic length for finding Grashoff number(Gr) and Nusselt Number(Nu) should be taken maximum 0.6 m for horizontal plate natural convection.(3.2.1.2)

$$Pr = \frac{c_p \cdot \mu}{\lambda} = \frac{1021 \cdot 0.00018776}{0.02771} = 0.691$$

$$Gr = \frac{g \cdot \beta \cdot L_C^3 \cdot \Delta T}{\nu^2} = \frac{9.81 \cdot 0.003131 \cdot (0.6)^3 \cdot (44 - 5.58)}{0.00001729^2} = 852577043.8$$

Gr.Pr=589858265.8

c=0.135

n=0.333

$$Nu_L = c(Gr.Pr)^n = \frac{\alpha 1 \cdot L_C}{\lambda} = 0.135.(589858265.8)^{0.333} = 113.14$$

Plate temperature (T_1) is less than mixture temperature , thereby Nusselt number is increased by 30 % due to facing cold surface downward to help natural convection positively.

Nu_L(corr.)=113.14.653+33.94 = 147.084

As a result of this Nu_L(corr.) ,heat transfer coefficient (α1) is determined as 6.79 (W/m^2K)

Ship speed (knot) and wind speed (knot) around the steel plate are determined as in the following :

It is assumed that proposed design ship generally expose strong breeze during the journey. Proposed design ship cruising speed is selected according to the similar vessels which is more closer to our design criterias.

V_{ship}=15.2 knot=0.5144x15.2=7.8188 (m/s)

V_{wind}=27 knot=0.5144x27=13.88 (m/s)

$V_{total\ air}$=42.2 knot=0.5144x42.2=21.70 (m/s)

$$Re_L = \frac{\text{inertia forces}}{\text{viscous forces}} = \frac{\rho VL}{\mu} = \frac{VL}{\nu} = \frac{21.70 \cdot 1}{0.00001342} = 1617562$$

Re=965937.4 >5.10^5 (Flow is turbulent)

$$Pr = \frac{c_p \cdot \mu}{\lambda} = \frac{1019x0.000016855}{0.02454} = 0.6999$$

$$\overline{Nu_L} = 0.037 Re_L^{4/5} Pr^{1/3} = \frac{\alpha 4 \cdot L_C}{\lambda} \; [\, Rex, c = 0 \,, 0.6 \leq Pr \leq 50 \,]$$

$$\overline{Nu_L} = 0.037 \cdot 1617562^{4/5} \cdot 0.699^{1/3} = 3045.05$$

As a result of this equation ,heat transfer coefficient (α2) is determined as 74.72 (W/m^2K)

According to the thermal resistance topic , overall heat transfer coefficients (k)for deck can be written in the following :

$$k = \frac{1}{\frac{1}{\alpha 1} + \frac{\delta}{\lambda} + \frac{1}{\alpha 2}} = \frac{1}{\frac{1}{6.79} + \frac{0.02}{58} + \frac{1}{74.72}} = 6.21\, W/m^2 \cdot K$$

Heat transfer coefficient (k_{deck}) changes according to the wind speeds are showed in the following Table 5.10.

Table 5. 10: Heat transfer coefficient (k_{deck}) changes depending on wind speeds.

Beaufort Number	Wind Descriptive Terms	V_{wind} [knot]	Vwind(max) [knot]	Vwind [m/s]	k_{deck} [W/m^{2}K]
0	Calm	Vwind< 1	1	0.5144	5.53
1	Light Air	1<Vwind<3	3	1.5432	5.63
2	Light Breeze	4<Vwind<6	6	3.0864	5.76
3	Gentle Breeze	7<Vwind<10	10	5.144	5.89
4	ModerateBreeze	11<Vwind<16	16	8.2304	6.03
5	Fresh Breeze	17<Vwind<21	21	10.8024	6.12
6	Strong Breeze	22<Vwind<27	27	13.8888	6.21
7	Near Gale	28<Vwind<33	33	16.9752	6.28
8	Gale	34<Vwind<40	40	20.576	6.34
9	Strong Gale	41<Vwind<47	47	24.1768	6.39
10	Storm	48<Vwind<55	55	28.292	6.44
11	Violent Storm	56<Vwind<63	63	32.4072	6.48
12	Hurricane	Vwind>64	80	41.152	6.55

Heat transfer coefficient for outside plate of double side is increasing logarithmically in terms of wind speed as shown in the Figure 5.13.

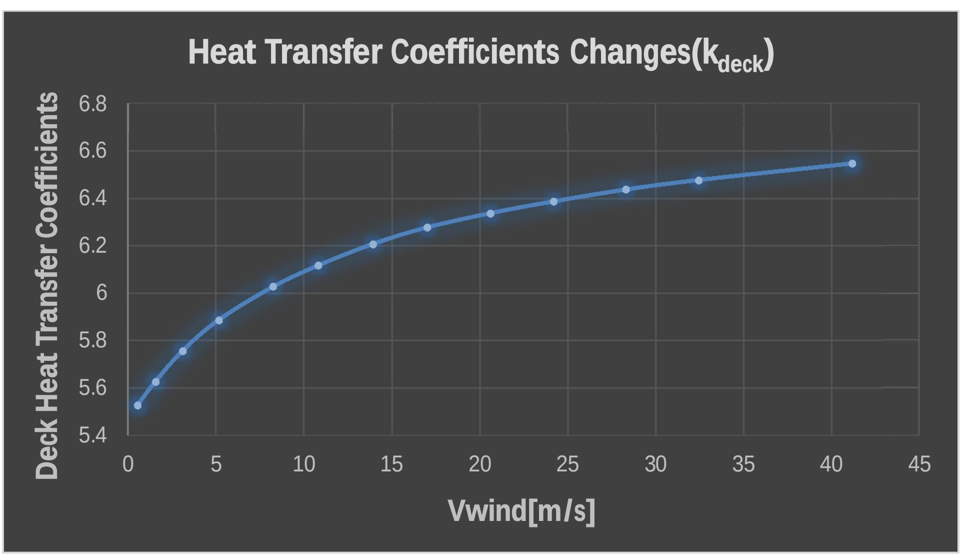

Figure 5. 13: Deck heat tranfer coefficient changes according to the wind speeds.

5.4 Comparison of Heat Transfer Coefficients

The comparison between obtained results and referential values of the heat transfer coefficients for similar type of ship [24] is shown in Figure 5.14. Labels k_1, k_2, k_3, k_4

on the x-axis are in accordance with same labels for overall heat transfer coefficients in Figure 5.1.

Table 5. 11: Heat transfer coefficients values for different parts of the tank.

CARGO HEATING SOLUTION METHOD	HEAT TRANSFER COEFFICIENT VALUES			
	Double Bottom [W/m²K] k_1	Double Side (SeaWater) [W/m²K] k_2	Double Side (Air) [W/m²K] k_3	Deck [W/m²K] k_4
Reference Values	3	3.3	3.2	4.3
Obtained Results	2.97	3.4	3.2	6.21
Shell Values	5.31	5.9	5.9	8.72
Spirax Sarco Values	7.1	7.1	7.1	8.5

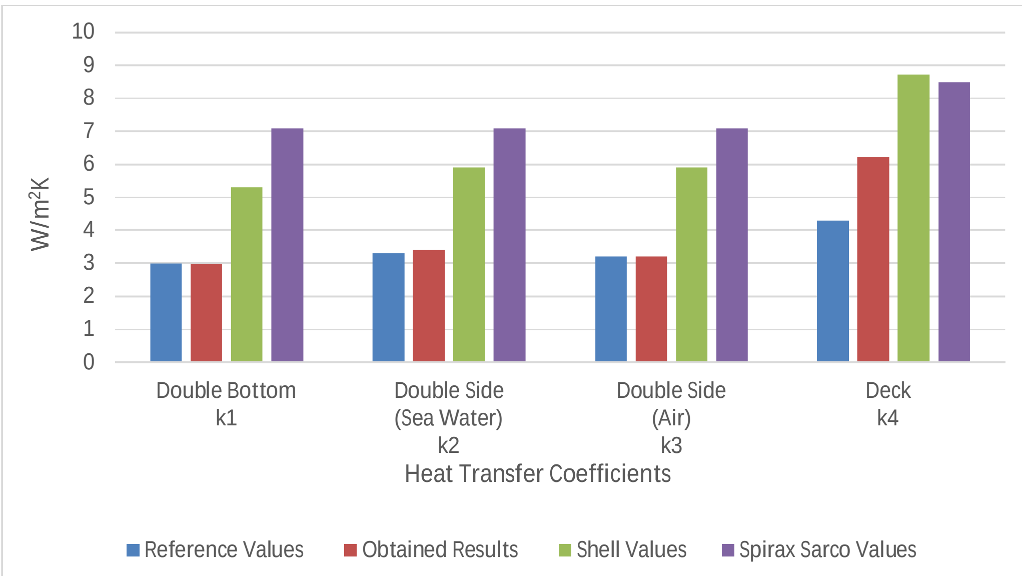

Figure 5. 14: Heat transfer coefficients comparison.

Referring to the Table 5.11, there are differences in heat transfer coefficients which these values are the most important values to determine accurate heat transfer rates. Referencial values shown in Figure 5.14 are determined by several measurements on similar ships and by relevant calculations. Our obtained result are satisfactory compatible with suggested values and they are acceptable limits. Small deviations between results can be explained by considerable influence of distrubition and spacing between ship hull frames, speed of the wind and water on heat transfer intensity. On the other hand, there are significant differences between obtained results and Shell, Spirax heat transfer coefficients values. Shell and Spirax Sarco heat transfer coefficients are higher than obtained results and reference values. Because, they are given these values for making projects and have a safe margin according to the authors' opinion but obtained results are more realistic which is shown in the example of reference values [24].

5.5 Calculation Quantity of Heat Requirement and Steam Consumption Using Independent Solution Heat Transfer Coefficients

Calculation quantity of heat requirement and steam consumption for Shell and Spirax Sarco solution is calculeted seperately by using independent solution heat transfer coefficients. Procedures which explained in previous part are used to calculate heat requirement.

Table 5. 12: Independent solution Shell quantity of heat requirement for winter and summer conditions.

QUANTITY OF HEAT [kW]					
SHELL CONDITIONS			**SUMMER CONDITIONS**		
Cont. Heating 44 ^{0}C [kW]	**Preheating** 44-66 ^{0}C [kW]	**Preheating Losses** (44-66 ^{0}C) [kW]	**Cont. Heating** 44 ^{0}C [kW]	**Preheating** 44-66 ^{0}C [kW]	**Preheating Losses** (44-66 ^{0}C) [kW]
-3288.310	-14143.049	-4232.380	-605.471	-14143.049	-1505.540
Qmax = -18375.42 kW			**Qmax**= **-**15648.58 kW		

Table 5. 13: Independent solution Spirax Sarco quantity of heat requirement for winter and summer conditions.

QUANTITY OF HEAT [kW]			
SPIRAX SARCO CONDITIONS		**SUMMER CONDITIONS**	
Cont. Heating 43 ^{0}C [kW]	**Preheating** 2.5 ^{0}C/24h [kW]	**Cont. Heating** 43 ^{0}C [kW]	**Preheating** 2.5 ^{0}C/24h [kW]
-3250.488	-6860.546	-523.646	-6860.546
Qmax = **-** 10111.034kw		**Qmax**= -7384.192 kW	

Based on the Table 5.12 and 5.13, steam consumption is calculated and shown in Table 5.14 and Table 5.15.

Steam consumption is calculated according to the quantity of heat requirement and steam calculation procedure in section 4.4 is performed. Independent solution of Shell and Spirax Sarco steam consumption in phase 2 and 3 was calculated and shown in Table 5.14, 5.15, 5.16, 5.17.

Table 5. 14: Independent solution Shell steam consumption in phase 2.

SHELL CONDITIONS	Cont.Heating 44 ^{0}C [kW]	Steam Evoparation Heat [kJ/kg]	G_{ps} [kg/h]	G_{pg} [kg/h]	G_p [kg/h]
Shell Conditions	3288.31	1933.19	6123.51	0	6123.51
Shell Summer Cond.	605.471	1933.19	1127.51	0	1127.51

Table 5. 15: Independent solution Shell steam consumption in phase 3.

SHELL CONDITIONS	Preheating 44-66 ^{0}C [kW]	Preheating Losses Mean (44-66 ^{0}C) [kW]	Steam Evoparation Heat [kJ/kg]	G_{ps} [kg/h]	G_{pg} [kg/h]	G_p [kg/h]
Shell Conditions	14143.05	4232.380	1933.19	7882.34	26337.29	34219.63
Shell Summer Cond.	14143.05	1505.540	1933.19	2803.62	26337.29	29140.91

Table 5. 16: Independent solution Spirax Sarco steam consumption in phase 2.

Spirax Sarco Conditions	Cont.Heating 43 ^{0}C [kW]	Steam Evoparation Heat [kJ/kg]	G_{ps} [kg/h]	G_{pg} [kg/h]	G_p [kg/h]
Winter Conditions	3250.488	1933.19	6053.08	0	6053.08
Summer Conditions	523.646	1933.19	975.13	0	975.13

Table 5. 17: Independent solution Spirax Sarco steam consumption in phase 3.

Spirax Sarco Conditions	Preheating Looses 43 ^{0}C [kW]	Preheating 2.5 C/24h [kW]	Steam Evoparation Heat [kJ/kg]	G_{ps} [kg/h]	G_{pg} [kg/h]	Gp [kg/h]
Winter Conditions	3250.488	6860.54	1933.19	6053.08	12775.75	18828.83
Summer Conditions	523.646	6860.54	1933.19	975.13	12775.75	13750.88

5.6 Steam Consumption Comparison Between Independent Solution and Project Solution

Table 5. 18: Comparison of steam consumption.

Cargo Heating Solution	Independent Solution		Project Solution	
	Phase 2 [kg/h]	Phase 3 [kg/h]	Phase 2 [kg/h]	Phase 3 [kg/h]
Shell Conditions	6123.51	34219.63	9741.63	38823.5
Shell Summer Cond.	1127.51	29140.91	1882.62	30882.5
Spirax Sarco Winter Cond.	6053.08	18828.83	11045.2	23820.9
Spirax Sarco Summer Cond.	975.13	13750.88	1997.03	14772.8

When the phase 2 and phase 3 cases are examined seperately in Table 5.18, there is obvious differences between independent and project solution hourly steam consumption for both phases. Independent solution hourly steam consumption is less than project solution hourly steam consumption depending on the use of different heat transfer coefficients.

5.7 Comparison of Boiler Fuel Consumption Between Independent and Project Solution

Boiler fuel consumption procedure in section 4.5 was performed and boiler fuel consumption for independent solution in phase 2 and 3 is shown in Table 5.19 and Table 5.20.

Table 5. 19: Independent solution boiler fuel consumption in phase 2.

Cargo Heating Solution	M_s [kg/h]	i' [kJ/kg]	i_w [kJ/kg]	η_b	W [kJ/kg]	FC [kg/h]
Shell Winter Conditions	6123.51	2792.8	293.3	0.85	40000	450.17
Shell Summer Conditions	1127.51	2792.8	293.3	0.85	40000	82.89
Spirax Sarco Winter Cond.	6053.08	2792.8	293.3	0.85	40000	444.99
Spirax Sarco Summer Cond.	975.13	2792.8	293.3	0.85	40000	71.69

Table 5. 20: Independent solution boiler fuel consumption in phase 3.

Cargo Heating Solution	M_s [kg/h]	i' [kJ/kg]	iw [kJ/kg]	η_b	W [kJ/kg]	FC [kg/h]
Shell Winter Conditions	34219.63	2792.8	293.3	0.85	40000	2515.64
Shell Summer Conditions	29140.91	2792.8	293.3	0.85	40000	2142.28
Spirax Sarco Winter Cond.	18828.83	2792.8	293.3	0.85	40000	1384.19
Spirax Sarco Summer Cond.	13750.88	2792.8	293.3	0.85	40000	1010.89

Boiler hourly fuel consumption for independent solution is less than project solution boiler hourly fuel consumption as in steam consumption. Independent solution total fuel consumption during the journey for different routes is shown in Figure 5.15.

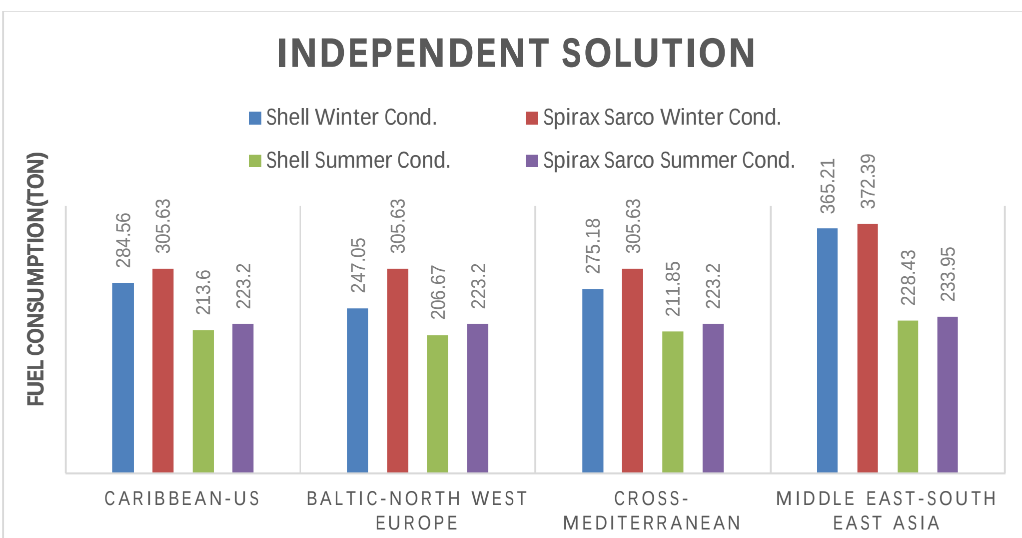

Figure 5. 15: Different routes total fuel consumption for independent solution.

In Shell method hourly fuel consumption is higher than Spirax Sarco. In Spirax Sarco, temperature of the cargo is increased 2.5 ^{0}C in 24 hours thereby, it takes more time to heat up cargo. So, in Spirax Sarco total fuel consumption during the journey is higher than Shell as shown in the Figure 5.15.

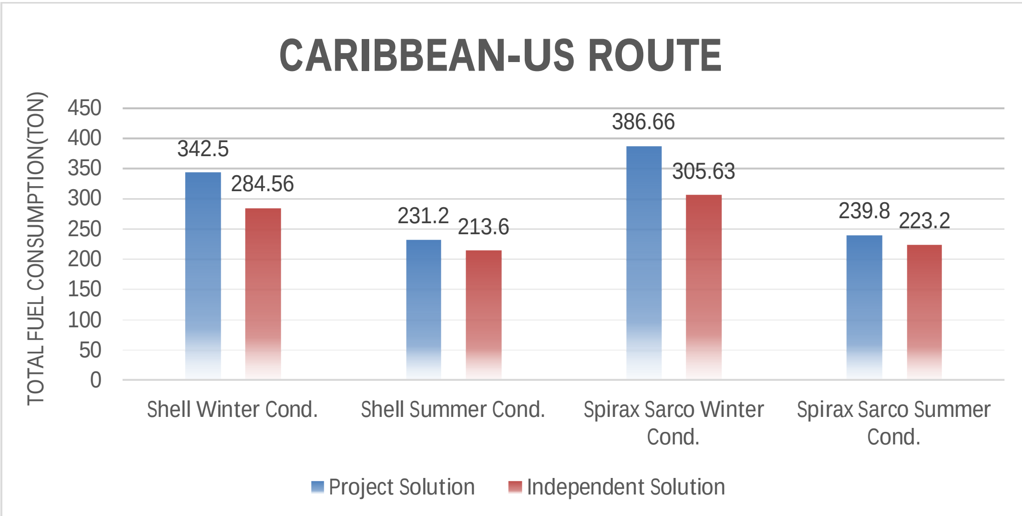

Figure 5. 16: Total fuel consumption comparison between project and independent solution for Caribbean-US route.

Caribbean-US route was selected to compare total fuel consumption values between project solution and independent solution. As shown in Figure 5.16 , the total fuel consumption values obtained from independent solution is less than project solution total fuel consumption which is calculated according to the their literature values for both winter and summer conditions. The same conclusion is observed in other routes.

6. SOLUTION OF HEAT TRANSFER FROM HEAT EQUIPMENT TO CARGO

6.1 Cargo Heating Methods

Heavy oils have very high pour points. They become very thick and sluggish when they are cold. It is necessary to keep them heated to load and discharge of these oils without delay and to avoid it is going to solid. Heavy oils are generally required to be kept at a temperature ranging between 40 ^{0}C and 70 ^{0}C. They are easy to handle within this temperature.

Nowadays, oil trade is wide spread and vast. Oil tankers can be trading in the tropics one voyage and after this voyage they can change their route to Artic. Therefore, oil tankers cargo heating system has to design to cope with this extreme conditions.

[Url-11]

Liquids cargo can be heated in a number of different ways. Indirect heating methods (conventional) is one of the them which heat is generated externally to the product and then is transferred to it through its external surface by conduction (the product is contact with the heat source) and then the product receives heat through steam, hot air or another intermediate heated fluid transferred to it by convection. The heat is transferred across a heat transfer surface in these methods. Indirect heating method include two different options to heat liquid cargo. One of them is using submerged heating coils which is common for heating system in cargo tanks. The second most frequently used method is using heat exchangers fitted on ships deck.

6.1.1 Heat exchanger method

In this method, heating is obtained with recirculation of the cargo by submerged pump through heat exchangers which mounted on deck. Cargo is always circulated which prevents stratifying and provides temperature distribution about the tank contents. Also, absence of heating coils simplify the tank washing in this method. Heat exchangers are not expose to the cargo when the cargo is not being heated and this results with less corrosion. The use of steam, hot pressurized water or thermal fluids is possible in this cargo heating system. Series of heat exchanger fitted on deck and layout of the heat exchanger cargo heating method are shown in Figure 6.1 and Figure 6.2 respectively [Url-11].

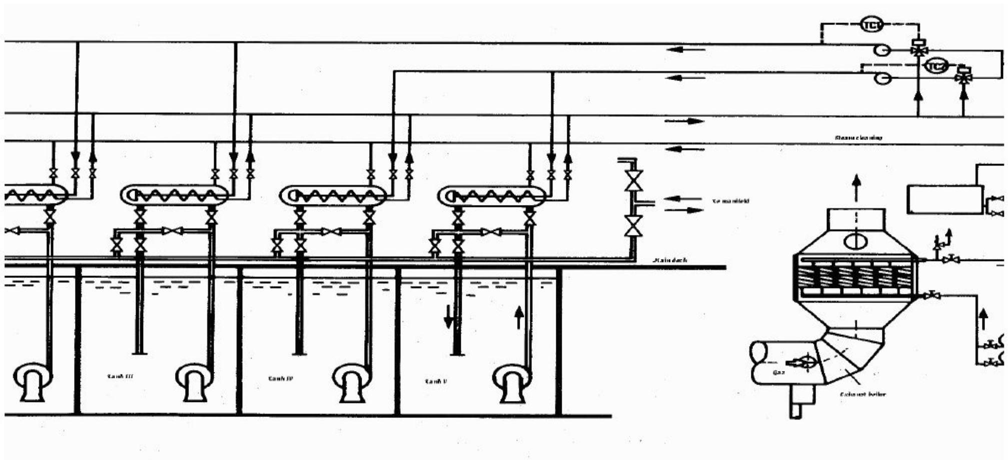

Figure 6. 1: Series of heat exchangers fitted on deck [Url-11].

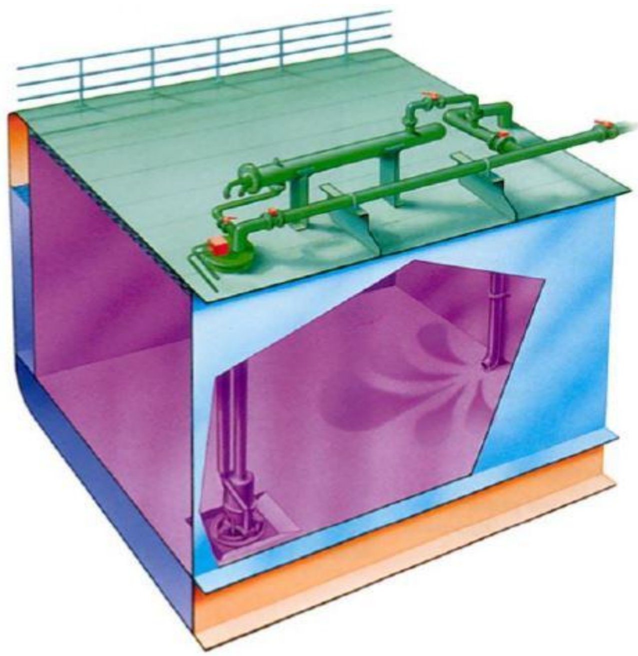

Figure 6. 2: Layout of the heat exchanger cargo heating method [25].

6.1.2 Submerged heating coils method

The use of heating coils is widely use in ships where the high viscosity cargoes are heated in deep tanks. These high viscosity cargoes are difficult to handle at cold temperature due to their high viscosity. Steam, hot pressurized water or thermal fluid (mixture of water and glycol) can use as working fluid in this cargo heating method [25]. Heated coils are used to increase the temperature of these viscous liquids to reduce their viscosity. After this process, they can handle and pump easily. Possible layout of heating coils in tank is shown in Figure 6.3.

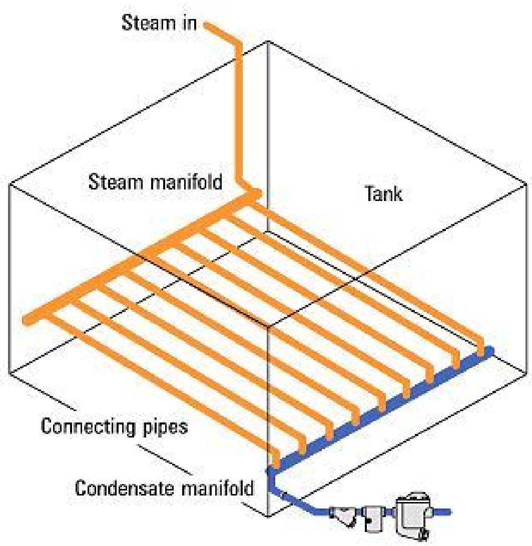

Figure 6. 3: Possible layout of heating coils in tank [Url-12].

6.2 Implementation of Submerged Heating Coils Method in Proposed Ship Design

Submerged heating coils method which is most commonly use of the two methods is selected to implement for the proposed ship cargo heating. Heating steam supplied by steam boiler and these heating steam flows passing through the main deck steam pipe and reach each cargo tanks. During this process, there is energy dissipation due to heat transfer along pipe wall. After steam enters the heating coil in the tank, heat transferred to the cargo oil through steam convection in the coil, heat conduction by coil wall and natural convection between cargo oil and outside coil wall which this description is shown in Figure 6.4.

Before calculation heat transfer coefficients of the heating coil system, it is necessary to determine some values. The first of these is determination of coil pipe wall thickness according to saturated steam pressure and DNV rules.

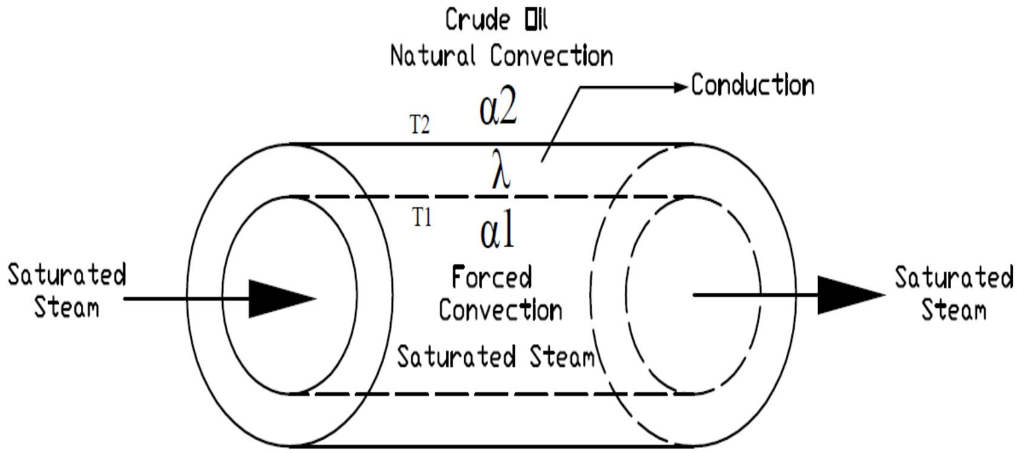

Figure 6. 4: Coil pipe heat transfer description.

6.2.1 Determination of pipe minimum wall thickness

Heavy lubricating oils which require heating and coils are generally chosen steel pipe. Crude oils which also have to be heated but coils are chosen cast iron or alloys. Heating surfaces of the coil are exposed to excessive corrosion from the lighter fractions in the crude. Ordinary steel pipes do not stand up this corrosion effect so well as cast iron, alloys, aluminum brass.

Therefore, it has been assumed that the heating coils are made of aluminized brass pipe due to its corrosion resistance and saturated steam of 16 bar will be used for heating. Pipe outer diameter is defined as 50 mm. Being subject to pipe outer diameter and internal pressure , wall thickness is determined according to the proposed ship design class notation DNV (DET NORSKE VERITAS)[26].

The minimum wall thickness (6.1) of a straight or bent pipe shall not be less than :

$$t=t_0+c \tag{6.1}$$

If to be bent, the minimum wall thickness (6.2) before bending shall not be less than :

$$t+b \tag{6.2}$$

The Strength thickness (t_0) shall not be less than calculated by the following formula (6.3) :

$$t_0 = \frac{pD}{20\sigma_t e+p} \tag{6.3}$$

p=design pressure (bar)

D=outer diameter of pipe (mm)

σ_t =permissible stress (N/mm^2)

e=strength ratio(efficiency factor)

e=1 for seamless pipe [26]

c=corrosion allowance (mm)

b=bending allowance (mm)

Design temperature was determined according to the saturated steam tables. This temperature according to 16 bar saturated steam was defined as 200 ^{0}C. After that, permissible stress for aluminum brass pipe is determined as 25 (N/ mm^2) based on design temperature from Table A.4 in DNV [26] machinery piping systems rules. Bending allowance shall not be less than in the following equation 6.4 :

$$b = \frac{1}{2.5}\frac{D}{R}to \qquad \textbf{(6.4)}$$

R=mean radius of the bend (mm)

D/R=bending ratio

This ratio will be taken 1/3 according to DNV rules [26]. Bending ratio is calculated as 0.2 mm according to the 6.4 equation.

Corrosion allowance value varies for different materials. This value for aluminum brass pipe is determined 0.5 mm according to the corrosion allowance tables [26].

Referring to the above equations , strength thickness (t_0), minimum required pipe thickness for straight part (t) and for bending part minimum wall thickness (t+b) are calculated as 1.55 mm, 2.05 mm and 2.25 mm respectively. As a result of this values, minimum wall thickness for aluminum brass pipe is determined as 2.25 mm according to the DNV piping system rules [26]. C68700 (ISO name CuZn22Al2) aluminum brass tube is selected from the existing pipes on the market [Url-13]. American Society Testing and Material (ASTM) specification code is B111, B 395 and American Society of Mechanical Engineering (ASME) specification code is SP 111, SB 395 for this pipe.

6.2.2 Determining steam coil sizing

After determination of the required energy with the knowledge of the steam pressure and temperature in the coil, the heat transfer surface can be determine using common heat transfer rate equation (6.5). Heat transfer surface is equivalent to the surface area of the coil. It is necessary to determine heat transfer coefficients accurately to define an appropriate coil size.

$$Q=k \cdot A \cdot \Delta T \qquad \textbf{(6.5)}$$

6.2.3 Determining overall heat transfer coefficient of the system

Overall heat transfer coefficient is vary considerably with thermal and transport properties of both fluids and range of other conditions.

6.2.3.1 Calculation of heat transfer coefficient (α_1) between saturated steam and pipe

Forced convection occurs between saturated steam and pipe according to steam velocity and temperature. Heat transfer coefficient between steam and pipe is calculated in the following formula (6.6) [19].

$$\alpha = C.\sqrt[4]{\frac{\lambda'^3 . \rho' . g}{\nu'}} . \frac{\sqrt[4]{\Delta i}}{\sqrt[4]{l.(t_s - t_w)}} \qquad (6.6)$$

For practical approach

C=1.15 and l= H for walls and vertical pipes (on their inner and outer surfaces)

C=0.725 and l= d for horizontal pipes (inner surface)

l= characteristic dimension (m)

Δi= saturated steam condensation heat (kJ/kg)

The physical properties of the fluid is taken at the average temperature (6.7) of the steam and pipe wall temperature [19].

$$t = t_{char.} = \frac{t_s + t_w}{2} \qquad (6.7)$$

t_s = steam saturation temperature (^{0}C)

t_w = pipe inside wall temperature (^{0}C)

As a first approach, pipe wall temperature value is determined as average value of cargo oil temperature and saturated steam temperature. After many iterations, wall temperature close the real value is calculated.

$$f(t) = \sqrt[4]{\frac{\lambda'^3 . \rho' . g}{\nu'}} \qquad (6.8)$$

f(t) which is shown in equation (6.8) is determined according to characteristic temperature(t_{char}) from the following Table 6.1.

Table 6. 1: f(t) values according to the temperature [19].

t[^{0}C]	f(t)	t[^{0}C]	f(t)	t[^{0}C]	f(t)
0	321.41	60	489.66	140	605.67
5	329.49	65	500.98	150	613.66
10	346.56	70	512.33	160	620.76
15	363.25	75	521.92	170	624.65
20	379.36	80	531.19	180	627.12
25	394.86	85	540.08	190	629.11
30	409.88	90	548.53	200	628.62
35	424.75	95	556.48	210	626.09
40	439.94	100	563.88	220	621.77
45	453.50	110	575.59	230	616.73
50	466.15	120	586.10	240	611.91
55	478.12	130	597.04	250	606.20

If the fluid is going outside of the pipes, heat transfer coefficient (α) is taken as the result value which is found from equation 6.6. If the fluid is going inside of the pipe, heat transfer coefficient (α1) is taken as 60 % of the value which is found in equation 6.6 [19].

t_s= steam saturation temperature =201.4 ^{0}C (from saturated steam table)

t_w= pipe wall temperature=(44+201.4)/2= 122.7 ^{0}C (estimated value)

t= characteristic temperature= (201.4+122.7)/2= 162.05 ^{0}C

According to the characteristic temperature, f (t) is found as 621.5 from Table 6.1.

Based on the above descriptions, heat transfer coefficient (α) is calculated as 2172 W/m$^{2\cdot}$K. Heat transfer coefficient (α1) between steam and pipe wall is 60 % of this value (α).

Heat transfer coefficient (α1) between steam and pipe wall is determined as 1303.2 W/m^{2}K due to steam is going inside of the pipe.

6.2.3.2. Calculation of heat transfer coefficient (α_2) between pipe wall and crude oil

Natural convection occurs between crude oil and outside surface of the pipe. Crude oil specifications are determined at characteristic temperature that is average value of the crude oil temperature and pipe wall temperature.

t_{char} =($t_{crudeoil}$+t_w)/2= 83 ^{0}C

Crude oil specifications at 83 ^{0}C are taken as following Table 6.2 :

Table 6. 2: Crude oil properties at 83 ^{0}C [21].

Cp=	1982	J/kg·K	λ=	0.1134	W/mK
ρ=	948.52	kg/m^3	μ=	0.095212	Pa.s
ν=	0.00010038	m^2/s	β=	0.000567	1/K

Acceleration of gravity (g) is taken as 9.81 (m/s^2) and characteristic length (l) is taken as pipe outside diameter (d_o) which is 0.05 (m). In addition to this, aluminum brass pipe thermal conductivity is taken 100 [W/m·K].

Heat transfer coefficient (α2) for natural convection part is calculated as follows :

$$\mathrm{Pr} = \frac{c_p \cdot \mu}{\lambda} = \frac{1982 \cdot 0.095212}{0.1134} = 1664.12$$

$$\mathrm{Gr} = \frac{g \cdot \beta \cdot L_C^3 \cdot \Delta T}{\nu^2} = \frac{9.81 \cdot 0.000567 \cdot 1^3 \cdot (122.7 - 44)}{0.00010038^2} = 5430.5326$$

Gr.Pr= 9037050

According to the 3.2.1.1 , if the multiplication of Grashof and Pradtl number is in this interval $500 < (\mathrm{Gr.Pr}) < 20.10^6$,constants c and n are in the following :

c=0.54

n=0.25

$$\mathrm{Nu_L} = c(\mathrm{Gr.Pr})^n = \frac{\alpha 2 \cdot L_C}{\lambda} = 0.54.(9037050)^{0.25} = 29.61$$

As a result of this equation, heat transfer coefficient (α2) is determined as 67.1 [W/m^{2}K]

Temperature values of the inside pipe wall and outside pipe wall are approximately equal to each other due to the pipe high conductivity of the material. Temperature of the pipe wall at high conduction systems can find in the following formula(6.9) [27] :

$T_{wo} \approx T_{wi} \approx T_w$

$$T_w = \frac{\alpha 1 . T_s + \alpha 2 . T_c}{\alpha 1 + \alpha 2} \qquad \mathbf{(6.9)}$$

As a result of first iteration, pipe wall temperature is determined as 193.6 ^{0}C. Difference between pipe inside wall temperature and outside wall temperature is assumed as 0.40 ^{0}C.

Overall heat transfer coefficients for pipes can be written in the following formula (6.10) :

$$k = \frac{1}{\frac{1}{\alpha 1 \frac{d_1}{d_0}} + \frac{\delta}{\lambda \frac{d_w}{d_0}} + \frac{1}{\alpha 2 \frac{d_2}{d_0}}} \qquad (6.10)$$

d_1= pipe inside diameter (m)

d_2= pipe outside diameter (m)

d_w= d_0= pipe average diameter (m)

At the end of first iteration, overall heat transfer coefficient is determined as 61.2 W/m^{2}K. Iterations are continued until reaches the correct pipe wall temperatures and heat transfer coefficient for the system. Pipe wall temperature changes in each iteration caused to the formation of the new value of the characteristic temperature. Therefore, steam properties and crude oil properties values changed depending on variation of the characteristic temperature. Finally, pipe inside and outside wall temperature is calculated as 194.2 ^{0}C and 193.8 ^{0}C respectively which are closer to the steam temperature. After many iterations, overall heat transfer coefficient is determined as 103.7 W/m^2 ·K. This heat transfer coefficient for the system is within acceptable limits (80-110 W/m^2·K) according to the reference values [Url-12].

6.2.4 Total length of coil calculation for the biggest tank

Pressure of condensate at outlet from heating coil is calculated according to the following formula (6.11) [20].

$$\mathbf{P_2}^2 = \mathbf{P_1}^2 - \frac{\lambda \mathbf{L_e}}{2\mathbf{d_i}}\left(\frac{\mathbf{L_e G_L}}{\mathbf{A}}\right)^2 \frac{\mathbf{P_1}}{\boldsymbol{\rho}_1''} \qquad (6.11)$$

P_1= Steam pressure at inlet to heating (Pa)= 1600000 Pa

P_2= Pressure of condensate at outlet from heating coil (Pa)

L_e=Effective coil length (m)

λ =Coefficient of steam frictional resistance = 0.05

d_i= Internal diameter of the coil(m)=0.0455 m

d_o= External diameter of the coil(m)=0.05 m

G_L=Mass of steam condensing on one meter length in the time of one second (kg/s.m)

A=Area of steam flow (m^2)

ρ_1''= Density of condensate (kg/m^3)

F= Area of the 1 meter length of the coil (m^2)

v_1''=Specific volume of the condensate for saturation temperature and pressure (m^3/kg)= 0.124 m^3/kg

$A = \pi . d_i^{\,2}/4 = 0.001625\ m^2$

$F = \pi . d_0 = 0.15707\ m^2$

k= Overall heat transfer coefficient= 0.1037 $kW/m^2 \cdot K$

ΔT=Temperature difference between steam and cargo= 157.4 ^0C

$Q_{1m} = k.\ F.\Delta T$ = 2.563 kW (per meter of the coil heat rate)

r=Condensation heat (kJ/kg)= 1933.2 kJ / kg

$G_L = Q_{1m}/r$ = 0.001326 kg/s·m

Effective length of coil (L_e) is selected as 120 m.

Based on the 6.11 equation, outlet pressure is calculated as 1560344.134 Pa.

Corresponding to the these pressure values, effective coil length is checked whether it is in allowable range or not and this check is performed by the following formula (6.12) [20] :

$$L_e = \frac{d_i}{2}\left\{\left[1-\left\{\frac{P_2}{P_1}\right\}^2\right]\frac{gr^2P_1d_i^{\,2}}{[kd_o(t_s-t_c)]^2 v_1" \lambda}\right\}^{\frac{1}{3}} \qquad \mathbf{(6.12)}$$

According to the this equation effective coil length is calculated and our selection of effective coil length is calculated to be within the allowable range.

Heating power and heating area is calculated in the following :

Largest tank of the proposed design tanker is determined. Quantity of heat requirement for preheating cargo inside of the this tank and quantity of heat to cover heat looses were calculated seperately for Shell and Spirax Sarco cargo heating solution in the previous section. Shell method which gives better results in terms of total fuel consumption during the voyage is used to calculate heating coil length and numbers. Shell calculation solution procedures for heat losses at 66 ^0C and quantity of heat requirements for preheating are shown in indicated pages. Shell procedures using the independent solution heat transfer coefficients are performed. It is calculated heat requirement for preheating and heat losses which is shown in the following table 6.3 :

$Q_{preheating}$= 1211.9 kW (Shell solution quantity of heat for preheating)[2]

---

[2] Table 4.9 in page number 59 shows quantity of heat for preheating.

Table 6. 3: Largest tank heat losses according to the Shell solution.

Tank Parts	**Heat Losses at 66 ^{0}C Q_{HL}(kW)**
Deck	226.398 [3]
Double Bottom	103.202 [3]
Double Side (Water)	78.552 [4]
Double Side (Air)	31.647 [4]
Total Looses(Q_{THL})	408.152

Q_{total}= $Q_{preheating}$ +Q_{THL}= 1620.05 kW (Heating power according to the Shell solution)

Coil lenght according to Shell solution

A=Q/ k ·ΔT= 99.3 m^2 (cargo temperature is selected 44 ^{0}C)

115.4 m^2 (cargo temperature is selected 66 ^{0}C)

Total lengths of the coil :

L_{tot} = A/π.d_a = 770 m

d_a=average diameter of the coil =0.0477 m

Effective length of coil is chosen as 120 m. So, number of coils are calculated as follows :

Number of coils =Total Length of the coil/ Effective Length of the Coil = 6

Layout of heating coils in biggest tank according to Shell solution is drawn and shown in Figure 6.5.

[3] Table 4.2 and Table 4.3 in page number 54 shows heat losses at 44 ^{0}C for deck and double bottom respectively.The same procedures was performed considering the cargo temperature 66 ^{0}C and obtained this values.

[4] Table 4.1 in page number 53 shows heat losses at 44 ^{0}C for double side contact with air and sea water seperately. The same procedures was performed considering the cargo temperature 66 ^{0}C and obtained this values.

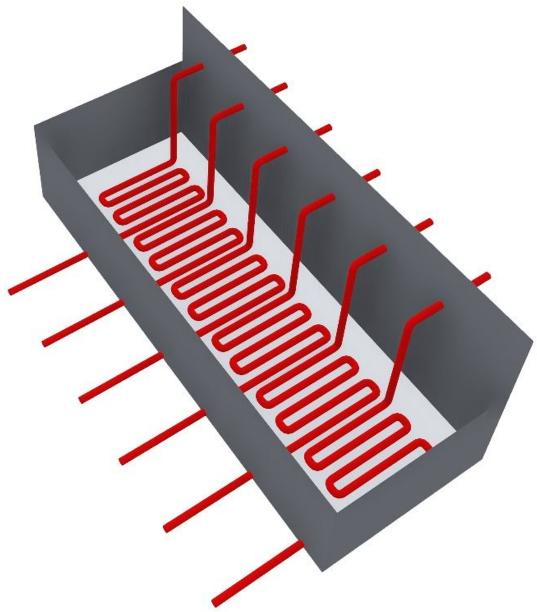

Figure 6. 5: Layout of heating coils in biggest tank according to Shell solution.

Schematic diagram of proposed design ship cargo heating system is drawn and heating equipments is shown in detail in the following Figure 6.6.

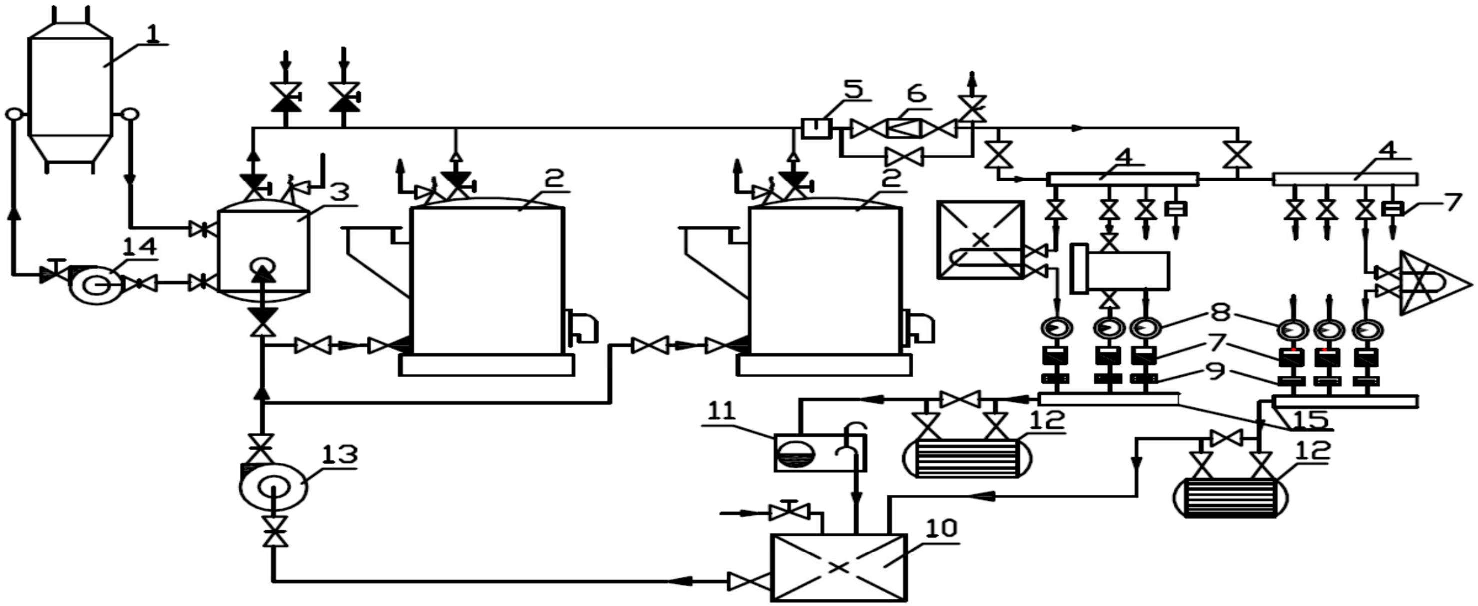

1-Exhaust Gas Heated Boiler
2-Oil Fired Boilers
3-Steam/Water Tank
4-Inlet Steam Main Pipelines
5-Dryer
6-Steam Pressure Reductor
7-Steam Traps
8-Vaposcope
9-Non-Return Plate Valves
10-Condensate Tank
11-Observation Tank of Condensate
12-Condensate Cooler
13-Feeding Pump For Oil Fired Boilers
14-Circulating Pump For Exhaust Gas Heated Boiler
15-Condensate Main Pipelines

Figure 6. 6: Schematic diagram of cargo heating equipments.

7. CONCLUSIONS AND RECOMMENDATIONS

In this study, analysis of possible solutions of the cargo heating systems which are Shell and Spirax Sarco is performed. Quantity of heat requirements for Shell and Spirax Sarco are calculated and then these heat requirements for both solutions are compared with each other. Steam consumptions for this cargo heating solutions are determined and compared. According to the results, it has been shown hourly steam consumption in Shell solution is higher than Spirax Sarco solution steam consumption. Additionally, these two solutions and our independent solution's boiler fuel consumption onboard crude oil tanker is compared with each other. According to the results, Spirax Sarco total fuel consumption is higher than Shell solution total fuel consumption during the journey in contrast to hourly fuel consumption. Total fuel consumption obtained from these two methods and our result are quite a significant differences. According to our results, total fuel consumption obtained by using heat transfer coefficients which we find our own is much less than these two cargo heating methods's total fuel consumption due to the difference in heat transfer coefficients.

The 100.000 dwt crude oil tanker with double bottom and double hull is taken as an example of calculation. Crude oil tanker main dimensions and its cargo tanks capacities are determined to calculate heat transfer rate and coefficients properly.

The classic approach to determination of heat loss from filled tanks is based on use of predefined overall heat transfer coefficients. But, heat transfer coefficients defined for specific parts of the ship structure are calculated independently and heat requirements are determined using these coefficients in this study. Heat losses occur in crude oil tankers' specific parts of the cargo tanks which are defined as double side, double bottom and deck. It is accepted that there is no thermal losses in the other parts of the tank based on the fact that tanks have cargo at same temperature. Heat transfer coefficient for double bottom (k_1), double side part which in contact with sea water (k_2), double side part which in contact with air (k_3) and deck (k_4) are calculated by using similarity theory with several interpolations and calculation process. They are calculated as 2.97 $W/m^2 \cdot K$, 3.4 $W/m^2 \cdot K$, 3.2 $W/m^2 \cdot K$, 6.21 $W/m^2 \cdot K$ respectively.

Obtained results of heat transfer coefficients and referential values of heat transfer coefficients for similar type of ship are compared. Consequently, it is shown that results obtained by our solution are satisfactory compatible with suggested values and they are within acceptable limits.

In the last part, modeling of heat transfer from heat equipment to the cargo is performed. Cargo heating methods are explained and appropriate one which is called submerged heating coil is implemented to proposed design ship. Overall heat transfer coefficient of the coil system are calculated using several interpolations and it is calculated as 103.7 $W/m^2 \cdot K$. It is shown that this heat transfer coefficient value is within acceptable limits. After calculating overall heat transfer coefficient of the system, coil size is determined. Possible layout of the coils in the tank and schematic diagram of proposed design ship cargo heating system and heating equipment's are shown in details.

Cargo quality and quantity; loading, carriage and discharge temperature ,air and sea temperature, weather conditions, type of vessel, tank capacity and arrangement, boiler operation, performance and efficiency, fuel oil characteristics, statistical cargo and voyage data are main factors affecting the efficiency of the cargo heating operation. There is no 'one size fits all' option, due to the vast variations in vessel type, size, cargo properties and quantity, voyage and weather conditions. Further research shall be focused on development of special software which includes all these factors to devise a comprehensive voyage specific cargo heating plan. The software can take into account the various factors affecting the efficiency of the cargo heating operation such as heat losses, expected drop in cargo temperature in prevailing weather, climatic, regional and seasonal conditions, cargo and fuel characteristics, vessel type and freeboard during the voyage. This special software can provide several outputs which are cargo heating plan, daily fuel consumption, cargo temperature projections, cargo heating operation schedule ,alerts and troubleshooting ,fuel oil consumption, cargo heating log, cargo heating performance indicator and post voyage analysis, monthly, quarterly and annual reporting of all cargo heating voyages. This kind of special software can greatly enhance operating profits of various tanker owners and operators and contributed significantly towards saving emissions.

REFERENCES

[1] **Abarasi Hart** (22.10.2013).Review Paper, University of Birmingham, School of Chemical Engineering”. Review of technologies for transporting heavy crude oil and bitumen via pipelines”

[2] **Rafael Martínez-Palou, María de Lourdes Mosqueira, Beatriz Zapata-Rendón, Elizabeth Mar-Juárez, César Bernal-Huicochea, Juan de la Cruz Clavel-López, Jorge Aburto** (26.11.2010).” Transportation of heavy and extra-heavy crude oil by pipeline”

[3] **Francis S.Maning, Richard E.Thompson, William P.Manning, Paul Buthod, Kelly L.** (n.d.) “Oilfilled processing Volume 2: Crude Oil”, Pennwell publishing company Tulsa/Oklahoma.

[4] **Sulzer Pumps Ltd.Winterthurt** (2010) Centrifugal Pumps Handbook, third edition

[5] **Danting Yue, Hui XING, Zhanhua WU,Yanwu XU** (2010) “Development of Cargo Oil Heating System on Oil Tanker “,ICLEM :Logistics for Sustained Economic Development.

[6] **Significant Ships**(2013). ISBN:978 1 909024 19 9. A publication of the royal institution of naval architects, data retrieved from page 62

[7] **Significant Ships**(2012). ISBN:978 1 909024 01 4. A publication of the royal institution of naval architects, data retrieved from page 50,80

[8] **Significant Ships**(2010). ISBN:978 1 905040 82 7. A publication of the royal institution of naval architects, data retrieved from page 12,34,74

[9] **Significant Ships**(2009). ISBN:978 1 905040 41 4. A publication of the royal institution of naval architects, data retrieved from page 109

[10] **Significant Ships**(2008). ISBN:978 1 905040 51 3. A publication of the royal institution of naval architects data retrieved from page 46

[11] **Significant Ships**(2006). ISBN:0 905040 30 X. A publication of the royal institution of naval architects data retrieved from page 77,109

[12] **Significant Ships**(2005). ISBN:1 905040 18 0. A publication of the royal institution of naval architects data retrieved from page 32,118

[13] **Significant Ships**(2004). ISBN:1 905040 06 7. A publication of the royal institution of naval architects, data retrieved from page 82

[14] **Significant Ships**(2003). ISBN:0 903055 95 3. A publication of the royal institution of naval architects data retrieved from page 79

[15] **Det Norske Veritas** (2008).Common structural rules for double hull oil tankers with length 150 metres and above, data retrieved from page 71

[16] **Volker Bertram, H.Schneekluth** (1998).Ship Design For Efficiency and Economy, Second edition, data retrieved from page 184,185

[17] **Michael J. Moran, Howard N. Shapiro, Bruce R. Munson, David P. DeWitt** (2012) Introduction Thermal Systems Engineering: Thermodynamics, Fluid Mechanics, and Heat Transfer John Wiley & Sons Inc.

[18] **Frank P. Incropera, David P. Dewitt, Theodere L. Bergman, Adrienne S. Lavine** (10.05.2012). Fundamentals of Heat and Mass Transfer, seventh edition.

[19] **Roman Kazimierczak, Zdzislaw Puhaczewski, Czeslaw Buraczewski** (2012) ZdWIESŁAW PUDLIK-Podręcznik dla studentów wydziałów mechanicznych specjalizujących się w technikach cieplnych i chłodniczych " Gdansk Politechnika Manual for Students Mechanical Departments Specializing in the Heating and Cooling Techniques 2012",data retrieved from page 156,157

[20] **Office Project** "Oil tanker 90000 dwt cargo tanks heating calculation" Komuni Paris Construction Shipyard in Gdyni

[21] **Tadeusz Wieszczeczynski,Andrzej Dilling**(1983).Charakterystyka i wlasnosci okretowych paliw i olejow smarowych "Physical Properties of Ship Fuels and Lubricating Oils"Gdansk

[22] National Meteorological Library and Archive Fact Sheet 6-The Beaufort Scale Met Office, data retrieved from< library.metoffice.gov.uk>

[23] **Maryam Tamaddoni, Rahmat Sotudeh-Gharebagh, Shunji Nario, Mehdi Hajihosseinzadeh**, **Navid Mostoufi** (2013)."Experimental study of the VOC emitted from crude oil tankers"

[24] **Heeden, D.J.Van Der, Mulder, L.L**.(n.d). Heat-transfer in cargo tanks of a 50000 dwt tanker, International shipbuilding Progress, Volume 12, pp.309-328

[25] **Bojan Jandrijevic,Tomislav Mrakovcic,Nikola Racic** (2006)."Numerical Simulation of Heat Loss From Ships' Cargo Tanks"

[26] **Det Norske Veritas** (2011) Rules for Classification of Ships Piping Systems Part 4 Chapter 6, data retrieved from page 26,27,28

[27] **Zdzislaw Kawala, Makymilian Pajak, Jan Szust**(1987).Zbior zadan z podstawowych Procesow Inzynierii Chemicznej-"A Set of Tasks From Basic Processes of Chemical Engineering Heat Transfer" Wroslaw

Url-1 < http://www.shipfinance.dk >,data retrieved 01.10.2014

Url-2 < http://en.wikipedia.org/wiki/Oil_tanker >,data retrieved 01.10.2014

Url-3 <http://www.eia.gov >,data retrieved 02.10.2014

Url-4 < http://maritime-connector.com >,data retrieved 03.10.2014

Url-5 <http://www.generalmaritimecorp.com >,data retrieved 04.10.2014

Url-6 <http://en.wikipedia.org/wiki/Tanker_(ship) >,data retrieved 05.10.2014

Url-7 <http://marine.man.eu >, data retrieved 17.10.2014

Url-8 <http://www.wartsila.com/en/products/netGTD>, data retrieved 17.10.2014

Url-9 <http://www.dieselserviceandsupply.com >, data retrieved 17.10.2014

Url-10 <https://www.mhi-mme.com/products/boilerturbine/auxiliary_boilers.html>, data retrieved 17.10.2014[24]

Url-11 <http://tankerfleet.ru/info/OIL_TANKER_DESIGN_EQUIPMENT.pdf >, data retrieved 08.05.2015

Url-12 <http://www2.spiraxsarco.com/resources/steam-engineering-tutorials/steam-engineering-principles-and-heat-transfer/heating-with-coils-and-jackets.asp>, data retrieved 15.05.2015

Url-13 <http://www.admiraltyindustries.com/c68700/ > data retrieved 29.05.2015

Url-14 < http://www.sec.gov/Archives/edgar/data/ 1627482/000119312515056485/d836806df1a.htm >data retrieved 15.06.2015

Url-15 < http://www.slideshare.net/teekaytankers/tnk-investor-day-presentation **>**data retrieved 15.06.2015

CURRICULUM VITAE

Name Surname: Koray Şahin

Place and Date of Birth: Dinar/AFYON 04.09.1988

E-Mail: sahinko@itu.edu.tr

EDUCATION:

B.Sc.: Yıldız Technical University (2006-1011)